POLITECNICO DI TORINO

Master's degree in Biomedical Engineering

Academic year 2023/2024

Development of a photoresponsive hydrogel based on azo compound

Supervisor:
Dott. Ignazio Roppolo

Candidate:
Miriana Imberti
Matricola 318940

ABSTRACT

Hydrogels are materials composed of hydrophilic polymeric chains which retain a huge amount of water. They are extremely advantageous in the biomedical field because such synthetic materials may mimic the characteristics of extracellular matrix (ECM) in terms of physical/chemical properties, and additionally for their biodegradability and biocompatibility. Moreover, it is possible to define their composition from scratch based on wide range of available starting materials, promoting different properties such as cell adhesion and proliferation, tissue regeneration, waste removal ability as well as tailor the mechanical properties or the diffusivity characteristic. Nowadays hydrogels are well established for a plethora of applications, nevertheless there is an urgent need to expand their capabilities, going into the direction of making these hydrogels active and able to respond to stimuli such as pressure, temperature, pH or light. Such materials are commonly known as smart hydrogels.

The aim of this thesis project was to obtain a smart hydrogel based on the incorporation of an azo compound in the structure. Such chemical moieties are well-known for exhibiting light/thermal activated properties of isomerization. A specific azo compound, named AzoPEGMA, was employed. It consists of a azobenzene unit linked to a short hydrophilic methacrylate oligoethylene chain. Interestingly, azobenzene is hydrophobic in its stable E isomerization, while it becomes more hydrophilic in the Z form. Therefore, such compounds are amphiphilic structures in the stable form and capable of spontaneously forming micelles in aqueous solutions. It has also been methacrylated to make it polymerizable and possibly capable of forming physical crosslinks. Therefore, in this study we aimed at assessing the possibility to fabricate a smart hydrogel with light controllable micelles embedded.

The hydrogel was formed employing other photocurable hydrophilic polymers to create the macromolecular structure, in particular polyethylene glycol methyl ether methacrylate (PEGMEMA) as the main monomer and polyethylene glycol diacrylate (PEGDA) as crosslinker. The formulation was then polymerized activating a water soluble photoinitiator with 420nm light irradiation. The properties of the liquid formulation were studied through rheological tests. The successful polymerization of the hydrogel, as well as the choice of the optimal photoinitiator quantity, was analysed through photorheology. The hydrogel's mechanical properties were further investigated through compression tests. FT-IR spectroscopy was employed to further assess the polymerization process and the contribution of azoPEGMA to the hydrogel.

The E-to-Z isomerization of azoPEGMA within the hydrogel was achieved using 365nm light irradiation, while the Z-to-E isomerization was performed with 450nm light. In order to monitor and to study the occurred isomerization, UV-VIS spectroscopy was exploited. Subsequently, the presence of the micelles and their behaviour were analysed, first, as a function of the quantity of monomer by observing the turbidity of the formulation itself. Then, it was analysed following polymerization and ultraviolet and visible light irradiation both through optical microscopy and through fluorescence.

Then, a well-established colorant with solvatochromic behaviour, 9-diethylamino-5H-benzo[alpha]phenoxazine-5-one (Nile red), was used as a dye to assess the micelles' capabilities of encapsulation and release, with the aim of evaluating and mimicking a possible drug release. Swelling and evaporation tests were carried out to examine water uptake. To conclude, preliminary 3D printing tests of the formulation obtained were successfully performed.

This project evidenced promising results but also new scientific questions that need to be addressed, paving the way for the development of a photopolymerizable and physically cross-linkable smart hydrogel.

SUMMARY

1.INTRODUCTION

1.1.HYDROGEL

1.1.1.HYDROGEL CLASSIFICATION

Hydrogels are three dimensional (3D) hydrophilic polymeric networks capable of absorbing and retaining a significant amount of water, without undergoing alteration to their shape. (1) This property is due to the chemical and/or physical cross-linking of individual polymer chains. Hence, to be considered a hydrogel, a material has to be composed of water for at least 10 to 20% of its total weight (or volume) (2), even if water content is usually higher, and it can make it to 100% in the case of superabsorbent hydrogels (SAHs) (3). Hydrogels have many properties and characteristics, which will be better discussed in the following paragraphs, which make them particularly suitable for different applications in the biomedical field, in environmental engineering, in soft robotics and in wastewater treatment (4). Hydrogels use is growing in different application fields, including the biomedical sector, together with the know-how related to these materials. This is clearly demonstrated by the steady rise in publications concerning them over the years. (Fig. 1)
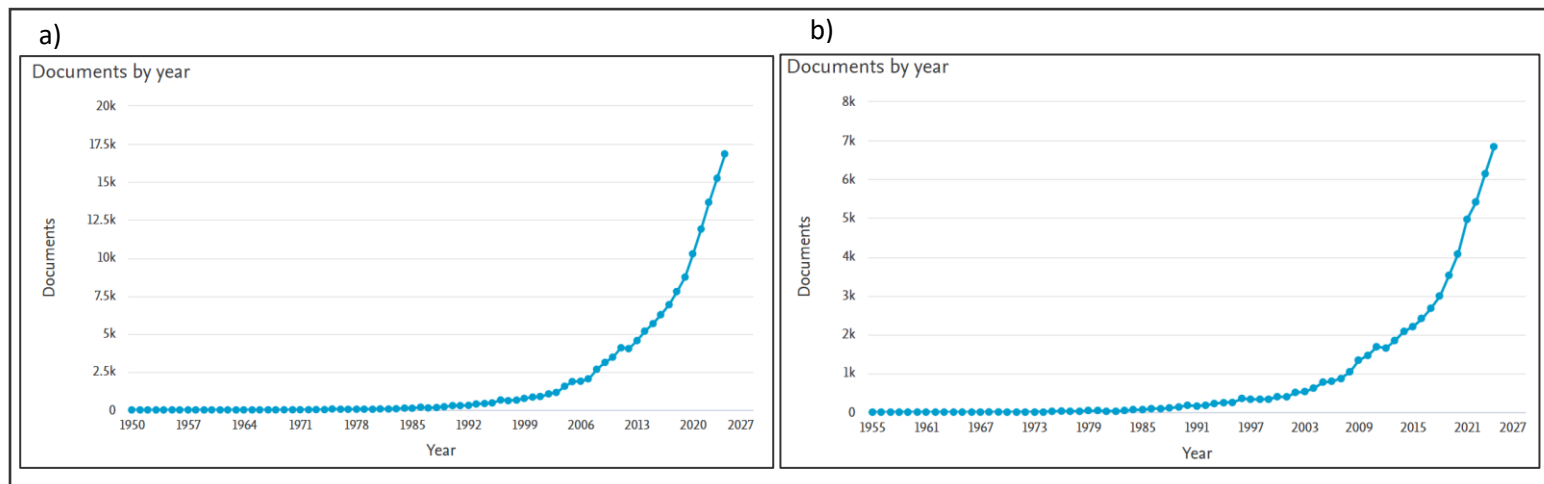
Figure 1 (a) Document by year from 1950 to 2024 on SCOPUS. Key word: "Hydrogel". (b) Document by year from 1950 to 2024 on SCOPUS. Key word: "Hydrogel" in the following subject areas: Biochemistry, Genetics and Molecular Biology, Medicine, Pharmacology, Toxicologicology and Pharmaceutics, Immunology and Microbiology, Neuroscience, Health Professions, Dentistry and Nursing. Update: 2024/11/17

Given the aforementioned vastness of studies regarding hydrogels, it is possible to classify them based on different characteristics, such as their cross linking method, their polymeric composition, the configuration, the ionic charge, the source, the preparation method and the response.(5)(2)(6)

1.1.1.1.CROSS LINKING METHOD

Based on the cross linking method, hydrogels can be classified as chemical or physical. In the biomedical field, this aspect is crucial because it is one of the main actors in the interactions with biological tissues.(5)

The chemical ones are also called permanent because of the formation of covalently-crosslinked networks, while when networks are bounded by molecular entanglements and secondary forces, hydrogels are known as physical. These secondary forces could be ionic, H-bonding or hydrophobic forces.

On the one hand, the chemical ones can be furthermore differentiated between preparation by free radical reactions (by polymerizing monomers in the presence of linking agents or by cross linking of functional groups present in the polymer backbone) or by condensation reactions (possible reactant groups are isocyanates and amines or alcohols to form urea, amines or thiols and vinyl groups to form amines, amines and active esters to for amides, acids or acid chlorides and alcohols to form esters and aldehydes and amines to form Schiff bases). A schematic of these methods is reported in Fig. 2.
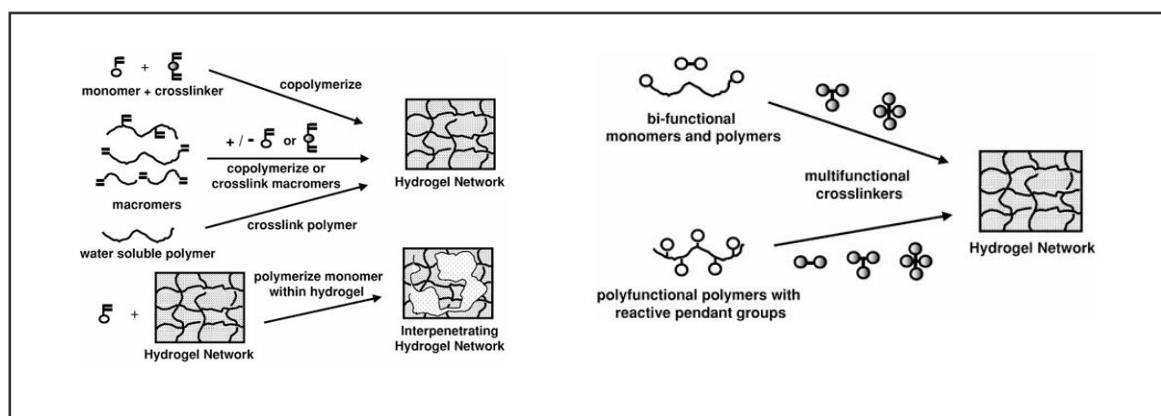
Figure 2 Schematic of methods for formation of crosslinked hydrogels (a) by free radical reactions, or (b) by condensation reactions of multifunctional reactants. (7)

On the other hand, physical hydrogels can be divided in ionic-crosslinked (which is the case of ionotropic hydrogels and polyion complex hydrogels), thermo-sensitive (LCGT or UCGT hydrogels) or supramolecular hydrogels (mainly based on self-assembly capacities). Usually, physical ones better show reversible response, mainly because the forces between the polymer chains are not strong. They are mechanically weak, and so fragile when external stimuli are applied.(5)

Both chemical and physical hydrogels present advantages and drawbacks, as outlined in Fig. 3.
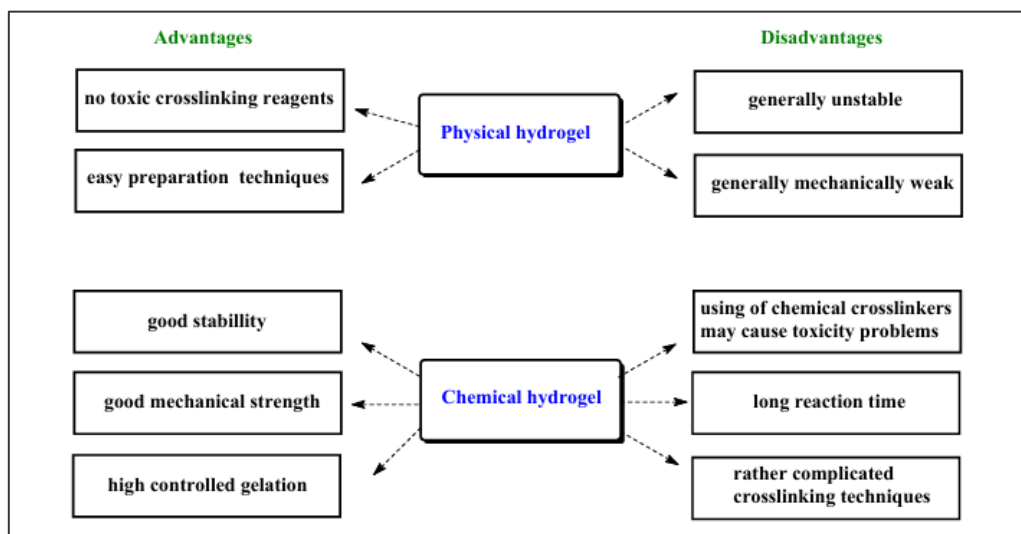
Figure 3 Advantages and disadvantages of chemical and physical hydrogels. (18)

In fact, physical hydrogels are usually safe for biomedical applications thanks to the absence of toxic crosslinking reagents, but they are lamentably unstable, mechanically weak and their lifetime is usually between a few days and a maximum of a month. (5) Chemicals ones present the opposite properties and they are useful because of their capacity to modulate the hydrogel behaviour, in particular the swelling one, the biodegradability and the mechanical strength.(5)

In order to mitigate these disadvantages without excessively reducing the benefits, scientists synthetize hydrogels with hybrid crosslinking. Finally, both physical and chemical crosslinking method can cause network defects, such as clusters, phase separation, voids, loops and entanglements.(7) Some of them are represented in Fig. 4.
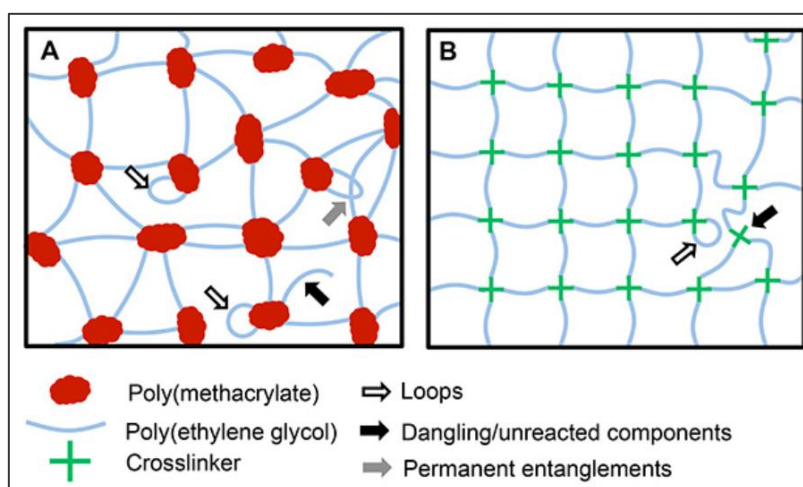
Figure 4 Network nonidealities such as loops, unreacted precursors, and permanent entanglements (8)

In light of these considerations, and if not considering the hybrid hydrogels, it is clear that the choice between a physical or chemical crosslinking is strongly related to the intended application. If high mechanical strength, stability and resistance is required, chemically crosslinking is better, otherwise physical one will be preferred when injectability or biodegradability are preferential properties.(9)

1.1.1.2.POLYMERIC COMPOSITION

The polymeric composition of hydrogels could be homopolymer, copolymer, interpenetrating network (IPN) or semi-interpenetrating networks (semi-IPN), as diagrammed in Fig 5. (6) (4).
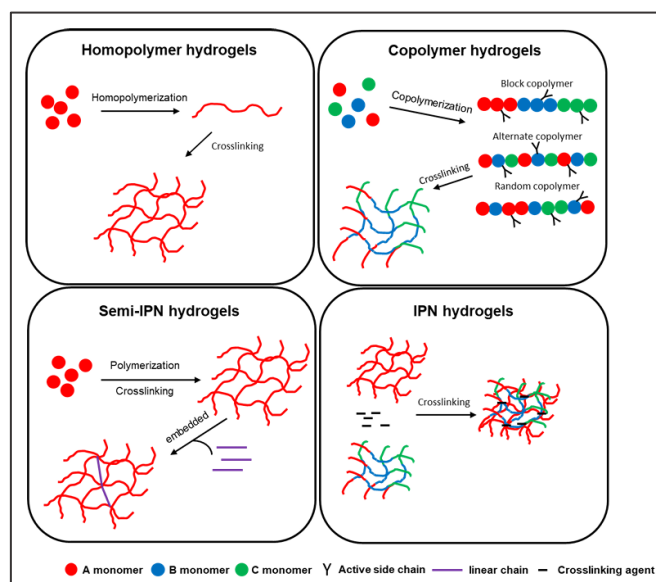
Figure 5 Diagram of homopolymer hydrogels, copolymers hydrogels, semi-IPNs, and IPN hydrogels (4)

When the polymerization concerns only one type of polymer, a hompolymeric hydrogel is formed, while the copolymerization of two or more polymers leads to a copolymeric hydrogel. In this latter case, we can distinguish between different shapes, such as alternating, random, or block, depending on the position order of monomers constituting the hydrogel. Homopolymeric and copolymeric hydrogels are united by the presence of just one type of polymer chains, standing out from IPN and semi-IPN ones, which have two or more types of polymer chain. In particular, IPN and semi-IPN hydrogels are differentiated by the presence or absence of crosslinking agents between the polymer network embedded in the linear polymeric chain characteristic of these particular types of hydrogels. IPN and semi-IPN hydrogels exhibit better properties as compared to homopolymeric and copolymeric ones, such as the mechanical strength and swelling abilities.(4)

4

1.1.1.3.CONFIGURATION AND IONIC CHARGE

Hydrogels can also be distinguished by their configuration at the molecular level: if they have a random network structure, they are defined amorphous, otherwise they are crystalline.(4) This hallmark is extremely important because crystallinity can affect different properties of hydrogels, like their strength, stiffness and swelling behaviour.

In addition, there is a particular advantageous class of hydrogel, known as semi-crystalline, which blend in their network the aforementioned amorphous and crystalline regions. The presence of both of them enhance the material, making it suitable for numerous applications ranging on different field. Moreover, benefits are tunable as it is possible to modulate the degree of crystallinity, by controlling the synthesis and processing conditions.(9)

A further classification of hydrogels is related to their ionic charge. Hydrogels can be neutral, ionic or ampholytic.

In neutral hydrogel, ionic charge is missing resulting in biocompatible and non-toxic materials. Usually, they are formed by polymers with hydrophilic groups, able to absorb and retain water.

On the opposite, ionic hydrogels present charged functional groups: positive for cationic hydrogels and negative for the anionic ones. This kind of hydrogel allows the interaction between itself and its surrounding environment, affecting its own properties. Their specific ability to selectively interact with oppositely charged species makes them particularly convenient in drug delivery field or in molecular recognition.

Finally, ampholytic hydrogels, also named zwitterionic, present both positive and negative charged groups, showing different attitude influenced by surrounding pH environment. They are notably useful when pH is able to trigger some particular response.(4,9)

1.1.1.4.SOURCE

Hydrogel can be based on components with natural or synthetic source. Natural polymers are mainly polysaccharides, proteins and bacteria, yeast or fungi, respectively extracted from plants, animals or microorganism.

These polymers are useful in biomedical field because of their biocompatibility, biodegradability and their particular similarity with the human extracellular matrix (ECM). Besides, they are non-toxic, economic and naturally abundant. (10)

The drawbacks are their fast degradation, the weak stability and a low mechanical strength. The most common natural materials are collagen, hyaluronic acid, fibrin, alginate, chitosan and decellularized matrices.(2,4)

As predictable, synthetic hydrogels own the opposite properties. Their main advantages are the easy protocol, cost effectiveness, and most of all, they have the possibility to have their properties tailored. (5)

Unfortunately, the waste produced by this kind of hydrogels can't be biologically degraded. The most common are PVA and PEG. (5)

In order to improve the hydrogels capabilities, semi-synthetic hydrogels, created by the combination of natural and synthetic polymers, were developed.(4,5)

1.1.1.5.PREPARATION METHODS

According to a recent review (6), hydrogel can also be differently classified if they are prepared by crosslinking by free radical polymerization, by crystallization or by radiation. The first one need of additional chemical crosslinkers and initiators and it is possible thanks to the generation of radical active sites. Its main advantage is the creation of stronger covalent bond. Alternatively, it is possible to introduce crystallization, resulting in an improvement in the hydrogel properties, as already noted. Finally, radiation can be used to polymerize the hydrogel. This method does not require the addition of multiple reagents and it involved the use of radiations such as electron or ion beams, or gamma rays. The convenience of this method is to be found not only in its possibility of modulating the dose of the irradiation, resulting in a variation in the hydrogel main properties, but also in its economic convenience, its absence of initiator and its simplicity.(6)

1.1.1.6.RESPONSE

One major feature of some hydrogels is their capability to respond to different external stimuli. Scientist defined and classified this kind of hydrogels as "smart". This kind of stimuli can be physical, chemical or biochemical, such as temperature, light, pH, electric and magnetic field, presence of particular enzymes, ionic strength, ultrasound and shear stress.(5,11)

This particular kind of hydrogel will be one main focus of the present work and for this reason will be further investigated in the following chapter. (1.2.)

1.1.2. HYDROGEL PROPERTIES

Hydrogels can be extremely versatile thanks to their multifaceted and tunable properties: swelling-deswelling rate, stiffness, degradability, mesh size (4), injectability, ease of handling, shape, capacity to be sterilized (7), self healing, stimuli sensitivity, antibacterial properties (1), mechanical strength, biocompatibility and biodegradability. (5)

It is important to highlight three aspects which influence the majority of the above-listed properties: the chain mobility, the water content and the character of water. (7) In particular, the free volume is strictly linked with the mesh size of the hydrogel: being the hydrogel a polymeric network made of crosslink points, the mesh size is by definition the average linear distance between two proximal point. The mesh size can be influenced by different parameters such as the polymers used, the cross linker concentration, and the external stimuli. In particular, a higher cross linking density results not only in a lower mesh size value, but also to a lower permeability and diffusivity. These ones bring, in turn, to better viscoelastic and mechanical properties. The mesh size can be measured both with labelled molecules (such as fluorescent dextrans) and rheological tests. Usually, it is between few nanometres and the microscale range.

Another similar and important feature of hydrogels is the average molecular weight between two cross linking point, which represents the aforementioned degree of cross-linking.

In hydrogels it is possible to evaluate the character of water, which can be free or bound water, in turn also divided in primary and secondary bound water.

The primary bound water is the first one to interact directly with the hydrophilic polymeric chains, then the hydrogel conformation starts to change, allowing a major exposure of the hydrophobic groups, which will be bounded by the secondary bound water.

Following the complete saturation of the ionic, polar and hydrophobic groups, additional water can enter the hydrogel, filling the remaining spaces between network chains. To distinguish bound and free water, probe molecules, different scanning calorimetry (DSC) or low field magnetic resonance spectroscopy (LF-NMR) are commonly used.

In order to evaluate the water absorption, it is possible to measure the swelling degree: the analysis can be carried out using the hydrogel both wet or dry. In biomedical application it is usually preferable to use the wet option to avoid cellular damages. It must be highlighted that, as the other properties, also the swelling rate can be modified by different external conditions, such as ionic strength, pH and temperature. (9,12). As predictable, also the water content can influence, in turn, other properties, like the mechanical, rheological and optical ones.

Mechanical properties are needed to be tuned in order to fully leverage the hydrogel across various field. As already pointed out, they can be improved by changing the cross linking density and the swelling ratio. In any case, it is important to find a balance between the strength and the elasticity, which are strictly and mutually influenced by each other. (5,13) Mechanical properties can be analysed with compression and tension tests, dynamic mechanical analysis and frequency-based tests.(5)

Usually these tests aim to investigate the tensile strength, the percent elongation to break, the toughness and the Young modulus of the tested hydrogel.(12)

Finally, biocompatibility and biodegradability are fundamental when hydrogels are applied in biomedical field. They respectively represent the ability to not induce a negative host response when injected in the human body and the capacity to degrade in physiological environment without generating products which could damage the host.(12)

1.1.3.HYDROGEL APPLICATIONS

Hydrogels, as already pointed out, can be employed in different fields due to their great and tunable properties. For example, they are used in different electrochemical applications, such as in electrolytes and batteries devices for energy conversion. They are also exploited as sensors such as, to name a few, those for strain, gas, humidity, pH and temperature. Their use can also be observed for electrophysiological signal detection, self-powered triboelectric active and finally also for energy harvesters. Hydrogels are well known also in waste water treatment and storage, in coatings, corrosion inhibitors, actuators and in food industry.

Regardless, the focus of this paragraph will be on their biomedical applications. In this field, hydrogels are extremely advantageous due to their similarity to the extracellular matrix (ECM), which is, amongst other things, soft and wet. These properties are consistent with those of hydrogels as they are able to absorb water,

due to their 3D structure composed of hydrophilic polymer network. (4) Hydrogels have other properties which make them a good solution in this field, like their biodegradability and biocompatibility.(1)

Moreover, it is possible to design them, in order to facilitate cell adhesion, proliferation, waste removal and tissue regeneration. Establishing their mesh size allows to tailor some mechanical properties, like the stretchability and flexibility, leading to the alteration of liquids absorption and release. (9) Thanks to this, hydrogels are excellent as wound dressing, because they maintain a moist environment. This characteristic provides the cooling of the wound surface, alleviating the pain and even assuring a faster wound healing. Moreover, it grants the removal of the excess of the typical exudate, leading to an isolation of bacteria, detritus and odour molecules, protecting the wound from infections.

Micropores, then, permit the exchange of nutrients and metabolites, adjusting the concentration of oxygen, to which hydrogel is permeable. (14) Hydrogels then, not only inherently have all these properties, but they can also be further endowed through functionalization, obtaining even the possibility to promote blood coagulation and regeneration. It is also possible to induce the elimination of death tissue. Moreover, their limited adhesion to the wound may reduce the pain and make it easier to take the hydrogel away. In addition, thanks to the aforementioned settable properties, it is possible to give further advantages as regard the biocompatibility, biodegradability and permeability.

Not to be underestimated the typical transparency of the material: wound healing process can be monitored without remove the shield given by the hydrogel.

Finally, yet importantly, hydrogels can be both sprayable and injectable: also wounds with particular and irregular borders can be protected.

All the properties described so far, with a specific emphasis on biocompatibility, resemblance to ECM, responsiveness and biodegradability, are crucial also in making hydrogels suitable for the production of scaffold for tissue engineering. (4) Biodegradability in particular is not only necessary to have the scaffold reabsorbed once the tissue has regenerated, but also to release an eventual encapsulated drug in a controlled manner over specific timeframes. Although all these properties are necessary, in tissue engineering field, mechanical once are the cornerstone: they are required to provide spatial support, preserving cellular functions and encouraging tissue formation. In fact, they are tailored to maintain loads and volume and transmit mechanical stimuli, in order to permit cell differentiation and tissue development. Moreover, cell

differentiation is impacted by the mechanosensing given by the stiffness of the microenvironment. Rigidity is essential, since the higher it is, the greater is cell proliferation. Finally, as regards the mechanical properties, one must consider the viscoelasticity, since it helps the hydrogel to mimic and interact with injured tissue. Hydrogels are then used to regenerate some tissues, like nerves, cardiac tissue, cartilage and bone, also considering the characteristic porosity which allows, among others things, the encapsulation of cells. (4) Finally, some biomedical specific applications which involve the hydrogel utilization are contact lenses, blood-contact, spinal cord regeneration, biosensors, anti-fungal, anti-bacterial materials and hygiene products.

1.1.3.1.HYDROGEL IN DRUG DELIVERY FIELD

One major branch of the biomedical applications in which hydrogels are involved is the one of drug delivery system (DDS). In Fig. 6, it is possible to notice how this field has kept growing in the last decades.
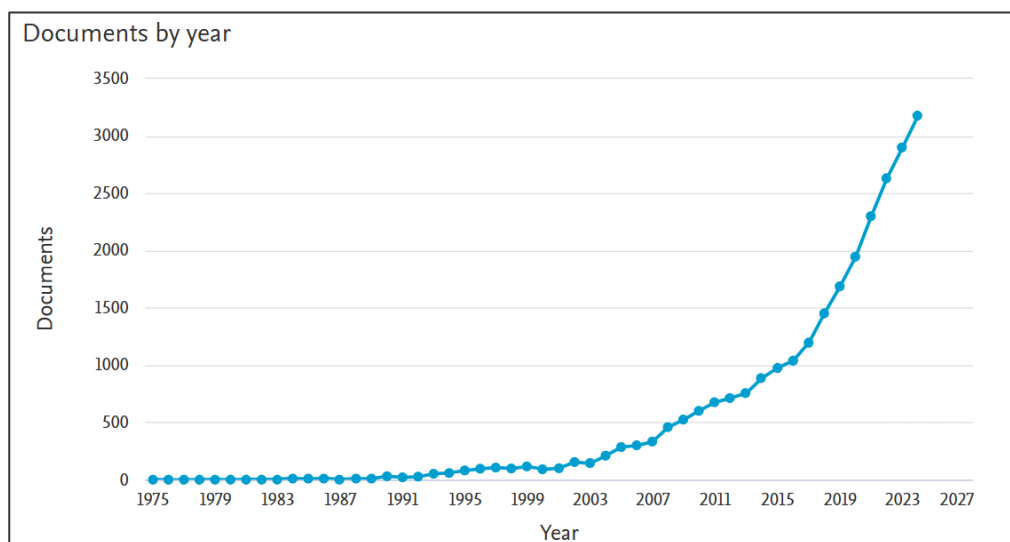
Figure 6 Documents by year from 1975 to 2024 on SCOPUS. Key words: "Hydrogel" AND "Drug Delivery". Update: 2024/11/17

This is mainly due to the ability of hydrogels to hold a considerable amount of water and biological fluids and to the chain mobility. (9) Thanks to these properties, it is possible for the hydrogel to be permeable and then to be loaded in with different drugs. (2) A factor to take into account is that hydrogels have good swelling rates, which, additionally, can be tailored. This helps to maintain the desired drug concentration, with no sudden increase or decrease and to extend the release duration. As already noticed, it is possible to design the mesh size of hydrogel, which is linked to capacity of drug encapsulation and release time. (4) Being able to manage the release is fundamental, because it helps to improve the drug bioavailability. This means a reduced frequency

of dose for the patient and then a better compliance and convenience for him. (9) These advantages, together with low toxicity and few side-effects, are what scientists are trying to obtain from DDS. (15)

The customizability of hydrogels can be exploited to adapt its characteristics, such as its size, shape or composition, according to the requirements of the drug needed. (11) The drug can be bonded to the hydrogels both in a physical and chemical way, by electrostatic interactions or covalent bonding (16), so that its release can be obtain by swelling/deswelling properties, by diffusion and/or by chemical mechanisms and degradation. (11,14,17)

In this area, the mesh size continues to be a leading influence, in fact it must be considered the dimension of the drug in relation to the free volume: if the drug is smaller than the mesh size, it will be released via diffusion-controlled mechanism, while if mesh size and drug sizes are similar, a swelling controlled mechanism is required. The resultant relaxation of the polymer chains will permit the drug to be released. Finally, the chemically controlled drug release is due to hydrolytic or enzymatic degradation of polymeric chains. (10)

Hydrogels also allow for targeted drug delivery (9), which have the convenience of reducing the systemic exposure of the patient to the drug and even of a fewer off-target side effects. (9) Not only this, hydrogels can protect the drug (7) and release it only in response to a specific stimulus. (16) , such as PH, temperature, light, ionic charge , enzyme and so on: this is the case of smart hydrogels (9,11,12).

Moreover, hydrogels are a good choice as DDS because they can be modified to improve their stability, integrity and functionality.(2)

First and foremost, it is necessary that the hydrogel possesses sufficient strength to be handled during fabrication, implantation, and drug release without breaking. (9) Researchers are looking for DDS which are easy to produce, Eport and storage, as well as comfortable to carry and take. (15) Then, it is advisable that the hydrogel exhibits good elasticity and flexibility in order to withstand mechanical stress and adhere to irregular wounds or be implantable in specific locations: this is important to maximise the drug delivery efficacy and minimize the drug leakage or migration.(9) Also the viscoelasticity affects the hydrogel ability to handle the aforementioned stresses without compromising its structural integrity.

DDS also need to have strict biological properties, such as the biocompatibility and the biodegradability before and after the drug release.(9) Being the DDS so tricky, hydrogels and their tunable properties result in an optimal solution. Even if only a few hydrogels have been approved by FDA in this field up to now, new systems

entered the preclinical phase, suggesting that more hydrogels will likely emerge in the future as DDS. (18)

Some interesting future perspectives arise from the development of smart materials and the emergence of 3D printing: complex and customized hydrogel for drug delivery could be produced. (9)

1.2. SMART HYDROGELS

1.2.1. SMART MATERIALS OVERVIEW

Smart materials, also known as intelligent materials, are those materials with the ability to respond to stimuli and environmental changes and then to activate their functions according to these alterations. (19)

For example, they could change shape or size because of heat, or undergo a phase Transition because of an external magnetic field. (20)

There are different typologies of smart materials, like piezoelectric ones, electrorheological fluids, magnetoactive elastomers, electrostrictive, magnetostrictive, shape memory alloys, optical fibres and finally smart polymers. (19,20)

In this paragraph, focus will be on smart polymers. They are able to change their physiochemical properties based on the variation of their environment. In particular, they can modify their structure or conformation when a stimulus is detected. The main stimuli are pH, temperature, solvent, salt ionic strength, magnetic/electric field and light. Normally, these modifications are reversible, which means that they return to their original properties once the stimulus is removed, even if exception are present. (21)

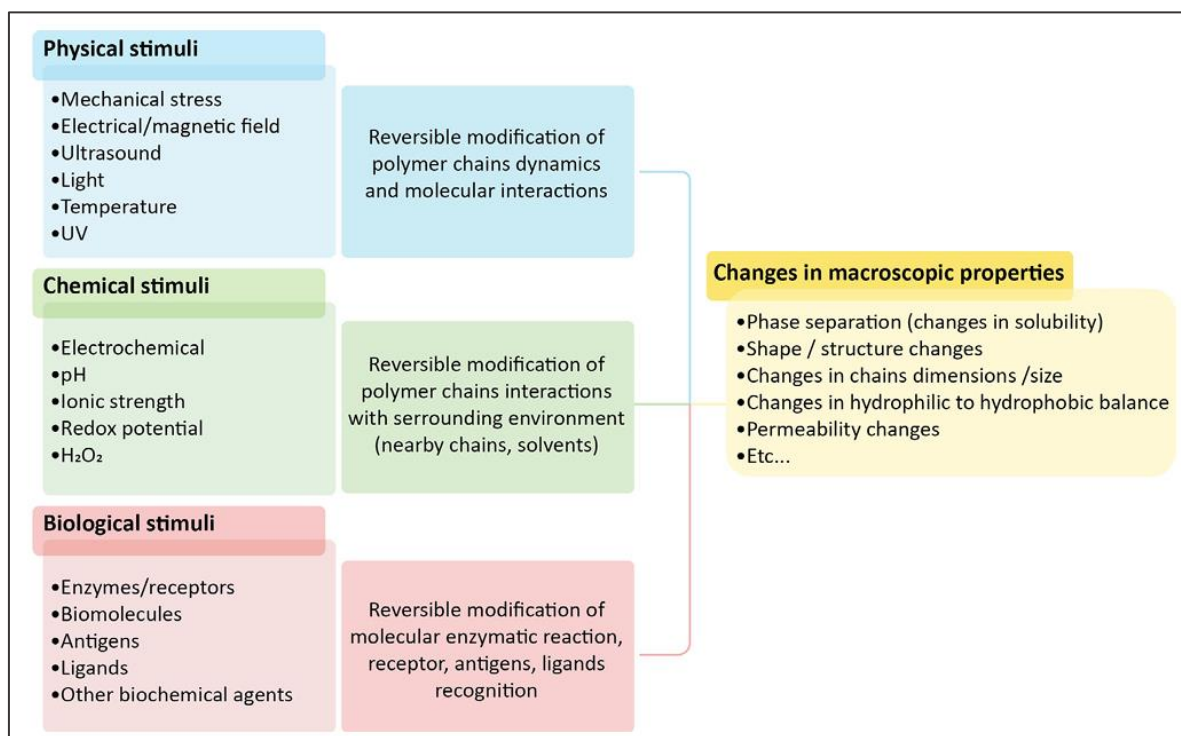An overview on the different typologies of stimuli is shown in Fig. 7. (21)

Physical stimuli

- Mechanical stress
- Electrical/magnetic field
- Ultrasound
- Light
- Temperature
- UV

Reversible modification of polymer chains dynamics and molecular interactions

Chemical stimuli

- Electrochemical
- pH
- Ionic strength
- Redox potential
- H_2O_2

Reversible modification of polymer chains interactions with serrounding environment (nearby chains, solvents)

Changes in macroscopic properties

- Phase separation (changes in solubility)
- Shape / structure changes
- Changes in chains dimensions /size
- Changes in hydrophilic to hydrophobic balance
- Permeability changes
- Etc...

Biological stimuli

- Enzymes/receptors
- Biomolecules
- Antigens
- Ligands
- Other biochemical agents

Reversible modification of molecular enzymatic reaction, receptor, antigens, ligands recognition

Figure 7 Classification of stimuli-responsive polymers with their induced modification. (21)

1.2.2. DEFINITION OF SMART AND RESPONSIVE HYDROGELS

Smart hydrogels, as the name itself suggests, are a specific category of hydrogels with the same properties as smart materials. Briefly, they can respond to different external stimuli (Fig. 8) and for this reason are further advantageous. In the biomedical field, scientists commonly leverage this category of hydrogels, mostly for controlled drug delivery, 3D bioprinting, 3D cell culture and self-healing process, as well as chemical sensors, soft actuators and robotics.(22,23)
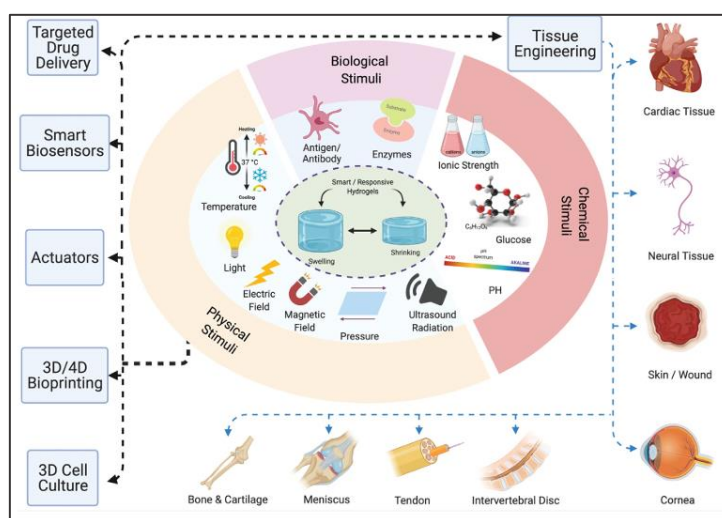

Figure 8 Schematic illustration of different smart/stimuli-responsive hydrogels employed for different biomedical applications. (22)

Stimuli can be chemical, biological or physical. This work thesis exploits a physical triggered hydrogel, for this reason this category will be better review.

Among hydrogels that respond to physical trigger, those that respond to temperature are the most prominent and studied. They exploit the Lower Critical Solution Temperature (LCST) and are therefore able to shrink when this temperature is exceeded. They are particularly harnessed in the biomedical field.

Light responsive hydrogels are also very common in this sphere due to several intrinsic advantages of light trigger. They will be further discussed in the following paragraph.

Considering the physical stimuli, also electric/magnetic responsive hydrogels are well known, as they can change their characteristics because of field alterations.

Finally, pressure/strain-responsive hydrogels and ultrasound-responsive ones are exploited in the biomedical field. The first ones because of their great flexibility and sensitivity that can be advantageous when cyclic analyses are needed. Ultrasound are extremely useful due to their self-healing capacity.

As already pointed out, smart hydrogels can also respond to chemical stimuli: pH, glucose and ionic strength are the most common. For what concern biological stimuli, the most useful are enzymes and antigen/antibody. (22)

1.2.3. PHOTORESPONSIVE HYDROGELS

Photoresponsive hydrogels were already investigated in the second half of the 1990s, and the first relevant one was reported in 1984.(24)

Photoresponsive hydrogels are composed of a polymeric chain with a functional photoreceptive moiety or with a NIR absorbing nanostructure. (22) , which give to the hydrogel itself the capability of actively responding to light irradiation. The most common are o-Nitrobenzyl ester, Coumarin, Thiol-ene, Trithiocarbonate, Disulfide, Allylsulfide, Spiropyran and Azobenzene.(23) Light exposure leads to physiochemical changes in the hydrogel, making it promising in the biomedical field. (22). Hydrogels are particularly suitable for this area, as water is almost transparent for light in the NIR-UV range, which is the photochemically relevant range. (23)

The most common photoreaction typologies are cleavage, addition, exchange and isomerization.

In particular, the main properties which can undergo modifications as a response of light triggers are the polarity, conformation, charge, optical chirality, amphiphilicity and conjugation properties. The direct

consequences are changes in hydrogel's solubility, wettability, adhesion, conductivity, gelation, shape and optical properties. These alterations can be reversible or irreversible. (25,26)

Among the external stimuli, light trigger is one of the most favorable due to several advantages. First of all, it has a high spatial and temporal resolution, and an extreme rapid, contactless and remote real-time control on it. (23,27)

Notably, light has the great merit to be extremely tailorable in its properties. For instance, wavelength can be chosen according to the specific necessities. For what concern the biomedical field and particularly when cells are present, it is advisable to prioritize irradiation in the visible spectrum rather than in the UV range mainly for safety reasons. (25,26)

Similarly, also intensity and irradiation time are adaptable to specific necessities, allowing then for control over dosage, which is evidently essential in the biomedical domain. Moreover, light trigger is versatile as it is possible to induce wavelength-selective photochemical reactions, which can differently modify the hydrogel properties.

Moreover, light can also be used as a heat source. It is possible to include in hydrogels both inorganic nanomaterials and organic compound as photothermal agents. Such compounds are able to generate heat after light exposure, triggering a reversible phase-Transition in thermoresponsive polymers. This particularly ability is extremely exploitable in the biomedical field, and in particular in photothermal therapy-based drug delivery. (23,26)

Light trigger can allow the photoresponsive hydrogel formation or degradation, (23) as well as the network contraction or expansion. Also, chemical properties can be sensitive to light.(23)

For instance, light trigger can be exploited for remote controlled actuators as it can work on hydrophilicity, and crosslinking density of the hydrogel, actually changing the swelling ratio and so its volume.

This photoinduced alteration of cross linking density can led to a variation in the hydrogel's stiffness, which is notably in the domain of dynamic cell microenvironments.

Scientists are relying on smart hydrogel based on light stimuli also to give self-healing properties to the hydrogel itself. It was discovered that light can exchange covalent bonds, as the ones in disulphide bridges or trithiocarbonates, in the presence of a photoinitiator that can be activated thanks to UV light. (23)

Among the field which can derive benefits from light, also the controlled drug delivery one is under investigation, as light-responsive hydrogels present significant potential for innovative application in this area. In particular, thanks to the aforementioned spatial and temporal control, it is possible to improve the therapeutic efficacy and minimizing adverse effects. (23,26) As well known, basic hydrogels can encapsulate different typologies of drug, but thanks to the photoresponsiveness, they can be released more easily. (23) Azobenzene is one of the key components for this purpose. (26) . Scientists are also working on producing hydrogels with embedded photoswitchable moieties able to form micelles, with the aim to encapsulate hydrophobic drugs and release them thanks to light triggers. (28,29)

In light of these briefly summarized considerations, it is evident why it is essential for new studies to be directed towards this direction.

1.3.AZOBENZENE

1.3.1.AZOBENZENE IN HYDROGELS

Azobenzene is a light responsive molecule composed of two phenyl rings interconnected by a N=N bond. (30) This compound can undergo a Transition from the planar and apolar E to non-planar polar Z configuration with a bent conformation when exposed to UV light (340-380nm) (Fig. 9).
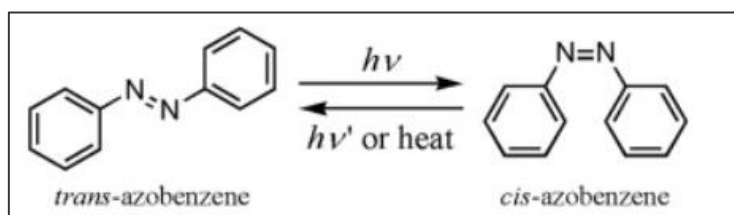

Figure 9 Photoisomerization of azobenzene.

Being the E configuration the thermally stable one, this Transition process is reversible by simply storing azobenzene in dark or by heating. (23,31,32) However, it is also possible to obtain the Z-to-E isomerization due to the n-π* Transition (32)

by irradiating the molecule with visible light (420-490nm). (30)

Azobenzene was discovered in 1834, but its isomerization properties weren't investigated upon the last century. Because of its properties, this molecule is exploited in different field and in particular in the biomedical area.

Azobenzene is extremely advantageous in drug delivery system, bioimaging, macromolecule regulation, photopharmacology, on demand cell adhesion and morphology regulation. Moreover, the isomerization of azobenzene is possible even when it is incorporated in polymeric materials.

When it comes to isomerization, the ratio of Z/E in the photostationary state is usually 80/20. Z-azobenzene has a half-life of about 2 days at room temperature. (31,32)

Photo-induced isomerization can be exploited in different ways. For instance, azobenzene is commonly used in hydrogel with host-guest interaction because the photo isomerization can modify the polarity of the compound and its spatial demand. Azobenzene is usually complexed with cyclodextrin (CD), whose stability depend on the Z or E state of azobenzene moiety. Several typologies of azobenzene-CD host-guest interaction were studied, with different purpose, such as drug delivery or swelling control. (23,24)

Isomerization of azobenzene can also be exploited to enhance hydrogels' swelling degree because the hydrophobic interactions are weakened by the E-to-Z isomerization, as the Z isomer is polar. This is advantageous in drug delivery, when an UV-irradiation could lead to a faster rate of a drug diffusion. Likewise, it has been demonstrated that irradiating with visible light leads to the shrinkage of the hydrogels. (23)

Azobenzene remains an intriguing subject of study, as it holds great potential for growth. There is still much to be discovered, considering that the structural changes of azobenzene are still really challenging. In particular, the rapid spatiotemporal control as well as the stability of the switch in vivo are still needed to be investigated. Moreover, it is also important to study absorption wavelength compatible with biological tissue optical windows in order to better integrate the azobenzene advantages in the biomedical area.(31)

1.3.2.AZOBENZENE MICELLE

Azobenzene capabilities have been predictably explored in the last decades, leading to the rise of new studies. In particular, Villa et al. (33) synthetized E-AzoPeg, a specific azobenzene-based amphiphile. With more specificity, it is a photo-switchable non-ionic amphphilic molecule composed of an azobenzene unit linked to a short hydrophilic methacrylate oligoethylene chain. It was obtained in high yield by alkylation of 4-hydroxyazobenzene with 2-[2-(2-chloroethoxy)ethoxy]ethanol.

The characteristic photoisomerization of azobenzene is maintained in AzoPeg, as the Z configuration is obtained through 365nm ultraviolet irradiation. This photoisomerization is reversible both leaving the

molecule in dark for 168 hours, and irradiating it with 450nm visible light. This process is shown in Fig. 10 on

a 30µm aqueous solution of E-AzoPeg (black line). Blue line represents the Z-AzoPeg isomer.
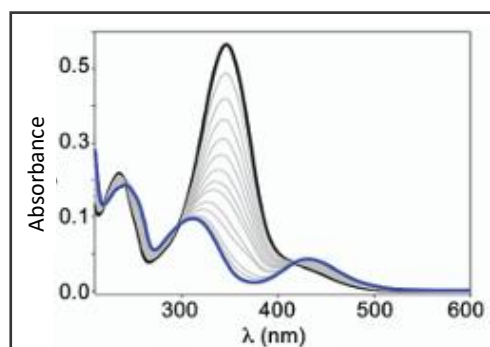

Figure 10 UV-Vis absorption spectra of a 30 mM aqueous solution of E-AzoPeg (black trace) and the photostationary state obtained upon irradiation at 365 nm (blue trace). Spectra taken at intermediate times during the irradiation are shown in light gray. (33)

Notably, it is of interest of this molecule its amphiphilic structure in the stable form, as the azobenzene is

hydrophobic while the PEG chain is hydrophilic. This brings to the capacity of spontaneously forming micelles

in aqueous solution. This spontaneous emulsification process is also known as ouzo effect. This is possible

only if the critical aggregation concentration (CAC) is at least 0,3mM. The mean diameter of these aggregates

is about 105nm. These properties enable for broader application of azobenzene in the drug delivery domain,

as a drug can be encapsulated while micelles are forming. Upon UV-irradiation, AzoPeg becomes hydrophilic,

consequently micelles are expected to unfold, releasing the encapsulated drug. Finally, upon visible irradiation,

micelles are destined to re-form.

Preliminary tests on encapsulation and release were successfully carried out using NileRed as a dye.

This interesting study has served as inspiration for this thesis project subject, with the aim of developing a

hydrogel which maintained the reported properties.

1.4.3D PRINTING

1.4.1.3D PRINTING OVERVIEW

3D printings techniques were first commercialised in 1980 by Charles Hull, with the purpose to produce objects

without the need for molds or machining.(34,35)

The most common are fused filament fabrication (FFF), direct ink writing (DIW), direct inject printing (DIP), selective laser sintering (SLS), stereolitography apparatus (SLA) and digital light processing (DLP). (36)

Nowadays 3D printing techniques are considered the most promising technologies for design to such an extent that they are often seen as a catalyst for a new industrial revolution. (37)

These versatile techniques of rapid prototyping are also known as additive manufacturing (AM) or layered manufacturing. (35) They actually represent the opposite of traditional subtractive fabrication techniques. The mechanism by which they operate is rather simple, as it is based on the subsequential 2D layer upon layer deposition of material, up to the formation of a 3D structure. (38,39)

The fabrication of a customized object with additive manufacturing can be divided in three steps: designing, printing and post processing. First of all, the desired 3D shape is created using a Computer Automated Design (CAD) software. Usually the most common are TinkerCAD, Fusion 360, SOLID WORKS and AutoCAD. Then, this geometry is converted in a Standard Tessellation Language (STL) file and sliced into 2D layers by a slicing software. The printer software generates a G-code, which is a file where every information required for printing are stored. In particular, G-codes contain the needed printable command sequence to obtain the object (on the X-Y plane), as well as the slices images, the exposure time, the temperature and so on.

As the printing proceeds, the 2D layers will form along the Z-axis, creating the so-called green body, which is supposed to undergo post-processing. Post-processing strictly depends on the AM techniques implemented but usually consists in the remove of the excess materials or in general in the final finishing. (34,38,39)

Several classes of materials can be exploited in 3D printings, such as metals, alloys, ceramics, polymers, composites, airy structures and even multi-phase materials. (34,37) However, in order to obtain a successful printing, it is fundamental to find a material able to rapidly fix in its predesigned structure. (39)

Nowadays, 3D printing technology is exploited in an enormous variety of field, from aviation (such as PGA rocket engine), to construction (i.e. steel bridge in Amsterdam), agriculture, jewellery collections, food industry, automobile, soft robotics and finally in healthcare. In particular, in the biomedical domain, 3D printing has been used for microfluidics devices, surgery, tissue engineering (i.e. artificial heart pump, 3D printed cornea) and drug delivery. (34,35,38)

The biomedical field will be further investigated in paragraph 2.3.

The great potential of this fabrication technique is evidently demonstrated by the exponential increasing of the number or research articles, as shown in Fig. 11.
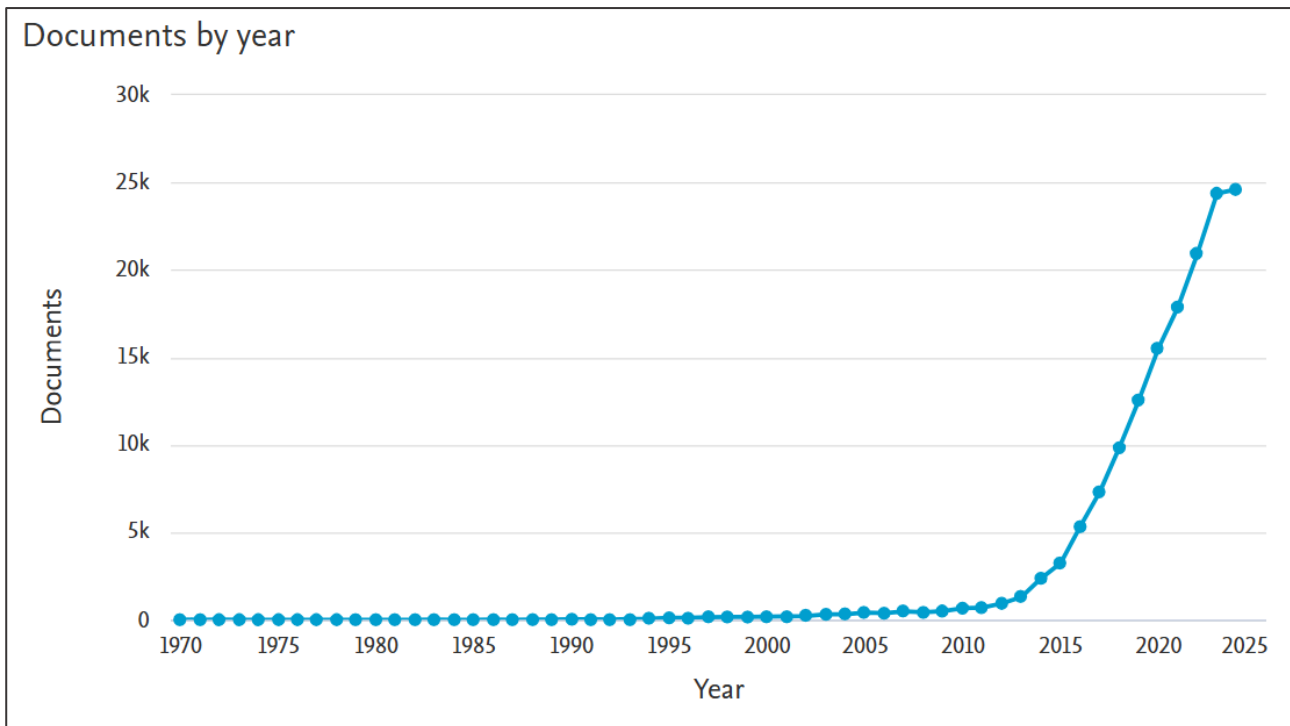

Figure 11 Documents related to 3D printing on SCOPUS from 1970 to 2024. Key words: "Selective laser sintering" OR "selective laser melting" OR "laser engineered net shaping" OR "prometal" OR "3DP binder jetting" OR "laminated object manufacturing" OR "fused deposition modelling" OR "polyjet technology" OR "stereolithography" OR "vat polymerization" OR "3D printing" OR "stereolithography" OR "Digital light processing" OR "Additive Manufacturing". Update: 2024/11/17

3D printing technology is advantageous because it allows to increase the production speed while reducing costs. Moreover, it permits to fabricate customised items which perfectly fit the customer's requests, thanks to open source designs. Compared to traditional manufacturing methods, 3D printing overcomes a lot of typical geometry limitations, producing more complex shapes. A higher resolution is also possible, even in the range of micrometers. Moreover, it is more environmental friendly, as it generates a lower quantity of wastes. This will also be due to the possibility to set the 3D printing facilities up closer to the consumer. (34,35,37,38) According to ASTM Standard F2792, 3D printing technologies can be divided in seven different groups: binding jetting, directed energy dissipation, material extrusion, material jetting, powered bed fusion, sheet lamination and vat photopolymerization. In the following paragraph (2.3), the vat photopolymerization will be further investigated. (34)

1.4.2.PHOTOPOLYMERIZATION PROCESS

3D Photopolymerization is one of the most common 3D printing techniques used, and it is otherwise known as photo-curing or photo cross-linking. In this technique, specific photopolymerizable monomers and oligomers in a liquid state are used. They are deposited on a vat and then polymerized, solidifying, on predetermined spots, where they are specifically irradiated by light through the vat. Photopolymerization is possible thanks to a photoinitiator which convert photons energy into reactive species, which drives a chain growth reaction. The photopolymerization reactions are usually radical, even if cationic photopolymerization can be also exploited.

In Fig. 12, a schematic of a photopolymerization process. The photopolymerization process occurs thanks to the activation of the photoinitiator, which generates reactive species when exposed to light. The polymerization starts when these reactive species interact with monomers, triggering a chain reaction. Photopolymerization goes on with propagation until termination. At the end of the process, the liquid photopolymer will be in a polymerized structure.
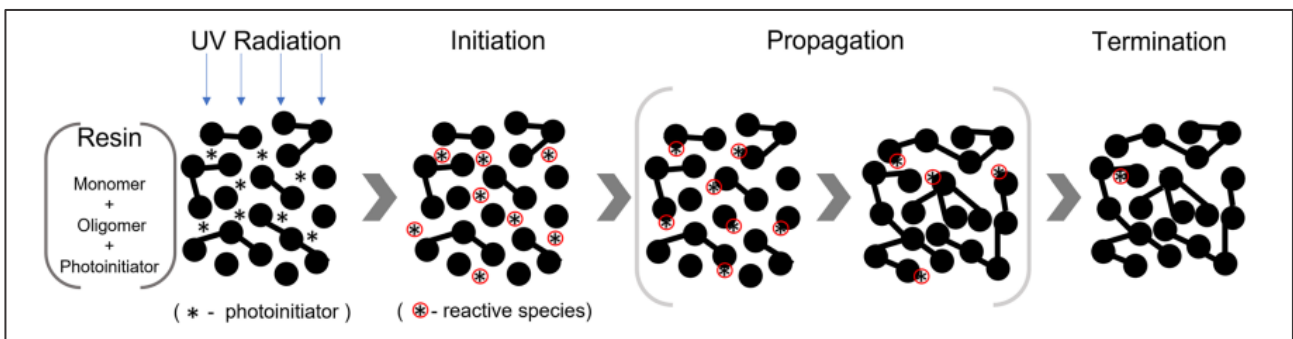

Figure 12 Schematic of a photopolymerization process. (38)

Different light sources exist, such as xenon lamps, mercury arc lamps, LEDs and lasers. Depending on the photoinitator chosen, several light wavelengths can be used, from the ultraviolet range (190-400nm), to the visible range (400-700nm) or even the IR range (700-1000nm). Photoinitator in the UV range are most common.

In vat photopolymerization, the most important parameters are the aforementioned wavelength, as well as the time exposure and the amount of power supply.

The most common 3D photopolymerization techniques are stereolitography (SLA) and digital light processing (DLP). (34,35)

DLP process will be further investigated in chapter 2.4.

1.4.3. PHOTOINITIATORS

In this paragraph, the most common photoinitiator exploited in photopolymerization are briefly presented. They can be classified as Norrish type I, it they are directly activated by light, or Norrish type II if they need for a co-initiator. (40)

As already pointed out, UV-light sensitive photoinitiator are more common. The most common commercial ones are listed in Fig. 13a.

However, photoinitiators responsive to higher wavelength have been studied. These kind of photoinitiator are more advantageous as they permit a higher penetration depth and then an improved photopolymerization rate. Moreover, VIS light is known to be safer: UV light can potentially cause eye damage and may also lead to complications in cell cultures, especially in the context of 3D bioprinting.

Finally, visible LEDs are more eco-friendly compared to the UV light, as they do not release ozone, they have a low thermal effect with long lifetimes. The most common VIS-light sensitive photoinitiator are listed in Fig. 13b.

Figure 13 Chemical Structures of (a) Common UV Light and (b) Common visible light Photoinitiators Used in 3D Photopolymerization Systems. (35)

Because of these advantages, efforts are still done to investigate more on photoinitiators which absorb longer light wavelengths.

1.4.4.3D PRINTING IN THE BIOMEDICAL FIELD

As already pointed out in paragraph 1.1.3.1, 3D printing technology is advantageous in a wide variety of fields, including the biomedical one. In this area, the most common materials are those in liquid state or with low melting point because they are economically accessible, low weight and with processing flexibility. Moreover, these kind of polymers are usually inert and so suited for biomedical requirement. (34)

The difficulty in finding the suitable material is given by the need to balance the properties required by the 3D printing process with the ones that are instead intrinsically required by the biomedical field. (41)

Several studies demonstrated the efficacy of 3D printing in the biomedical field. For instance, it has been used to print 3D skin. The natural structure of the skin can be replicated thanks to 3D printing, improving the reliability of in vitro test and then reducing the number of animals used as test subjects. 3D printing was also used in the pharmaceutical field, by producing drugs with advantages on the efficiency and the reproducibility. Also bone and cartilage have been 3D printed, with the aim of replace bony voids caused by trauma or diseases. (34)

For what concern the regenerative medicine, 3D printing is particularly advantageous, in fact it is possible to tailor some material properties. For example, softer material can be obtained simply adjusting the polymerization process. In this field hydrogel are a cornerstone. (41)

Even cancer research can benefit of 3D printing technologies, as it is possible to print 3D model of cancer used to investigate the tumoral conditions.

3D printing is commonly employed also to produce more accurate, automated and cost-effective orthopaedic aids. (41)

Finally, not to be underestimated the potential of this technique used to print medical models that can be exploited to train surgeons on a 3D model of a real patient's pathological condition. (34,41)

1.4.5.DIGITAL LIGHT PROCESSING (DLP)

Among the 3D photopolymerization techniques, the digital light processing (DLP) is one of the most common. Its main characteristic is the presence of a digital light projector, based on digital micro-mirror device (DMD) technology. The DLP source consecutively projects different 2D layers which are used to locally polymerize the photosensitive resin present in the vat until the complete production of the 3D object. The projected images are composed of light and dark pixels which are created by micrometer mirrors on the DMD. These pixels determine the resolution in the XY plane of the cured layer. At each layer, the building head moves along the Z-axis. DLP has a printing speed rate from 25 to 100mm/min and it the successful outcome relies on the intensity of light power and the sensitivity of the printing material. (38)

Differently from SLA, DLP simultaneously projects the entire layers, allowing for a faster printing process.

DLP can works according to different geometries: the bottom-up (Fig. 14a) or the top-down (Fig. 14b).
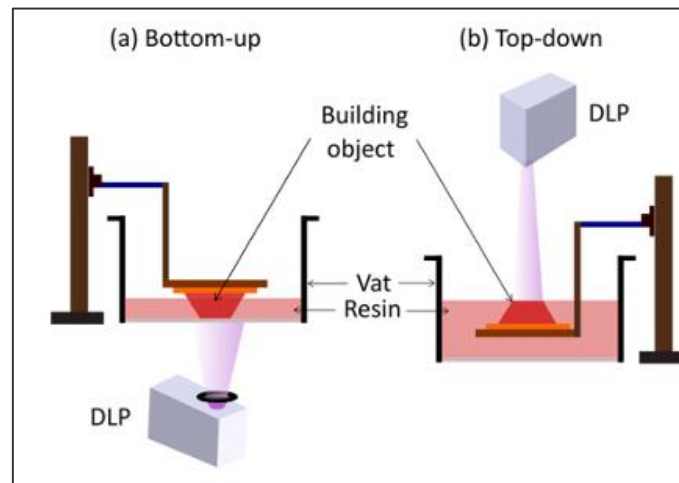

Figure 14 (a) Bottom-up and (b) top-down geometries used in DLP-based printing technology (38)

In the bottom-up configuration, the building head is immersed in the vat containing the photopolymerizable resin. It is positioned at a distance from the bottom of the vat equal to the set value of the layer thickness. Due to the light which passes through the vat, the resin corresponding to that thickness is polymerized. For this reason, in this configuration the vat has to be light permeable. Once the set light exposure is finished, the newly photopolymerized layer will be stuck on the building head. Subsequently, the building head rises to the thickness of the next layer, allowing new resin to be polymerized on the previous layer. The same operation is repeated until the complete 3D object is obtained. (36,38)

The main advantage of this configuration is that it requires little fresh resin in the vat and it allows the printing of very small object. Moreover, during the building head upward movement, vacuum is created and it facilitates the recoating process even for resin with high viscosity. However, with this configuration, there is a risk that the resin does not detach from the vat and therefore does not remain adhered to the building head, causing a printing failure. To minimize this occurrence, the vat is covered with an oxygen-permeable film or perfluorinated film, which helps in reducing the adhesion between the polymerized layer and the printer. (36,38)

In the top down configuration, the building head is completely immersed in the resin. Its depth corresponds to the set layer thickness. Therefore, the quantity of resin corresponding to that thickness is polymerized over the building head thanks to the light coming from the DLP module, which in this configuration is above the vat.

Following polymerization, the building head is lowered of the desired thickness layer and a new layer of resin is positioned on it thanks to a recoating blade. The process repeats until the 3D object is completed. In this configuration, more fresh resin is required, but the presence of the recoating blade allows the use resin with higher viscosity. Moreover, it is no need to concern about the layer adhesion on the building head. The major disadvantage of this configuration is the contact between the resin and the oxygen, which may interfere with the photopolymerization process. (36,38)

1.4.5.1. DLP 3D PRINTING OF HYDROGELS

Considering the advantageous properties both of the hydrogels and of the 3D printing, efforts were made to combine them. In particular, 3D printing of hydrogel is possible using an aqueous solution with photopolymerizable oligomers, a photoinitiator, a photo-inhibitor and/or a cross-linking agent. As already pointed out, the viscosity of the resin could interfere with the 3D printing process, for this reason it should be lower than 100kPa s, even if many DLP precursor solutions possess an apparent viscosity lower than 5 Pa s. This is essential to permit the recovering with fresh resin. If the resin is too viscous, the printing fails as the partially cured formulation cannot be removed from the surface of the printed object.

While printing hydrogel, it is essential to add a photo-absorber in the formulation as it controls the curing depth of the formulation, avoiding that light irradiate all the layer. Moreover, if the hydrogel is over-polymerized, the printing fails. For this reason, also photo-inhibitors are crucial for a good outcome.

Photoinitiators are the key component to initiate the hydrogel polymerization. As already reported in paragraph 2.2.3, they can be responsive both to UV and visible light, even if efforts are made to develop new visible-light sensitive photoinitiators, as their shortage is one of the main challenge of this field.

3D printing of hydrogel is extremely advantageous because of its high printing speed and resolution. These advantages, combined with the well-known unique properties of hydrogels, makes this combination extremely interesting for the tissue engineering field, the soft actuators and flexible electronics. (36)

2.MATERIALS AND METHODS

In the following chapter, materials and methods used for the preparation of the samples and the techniques employed for their characterization will be analysed.

2.1.Materials

In this work thesis, 5 main chemical compounds were used:

- polyethylene glycol methyl ether methacrylate (PEGMEMA) (Chemical formula in Fig. 15a) (42)

- polyethylene glycol diacrylate (PEGDA) (Chemical formula in Fig. 15b) (43)

- poly(ethylene-glycol) substituted Bis(acyl)phosphane oxides (BAPO) derivative (PEG-BAPO) (Chemical formula in Fig. 15c) (44)

- azoPEGMA (Chemical formula in Fig. 15d)

- 9-(Diethylamino)-5H-benzo[α]phenoxazin-5-one (Nile Red). (Chemical formula in Fig. 15e) (45)

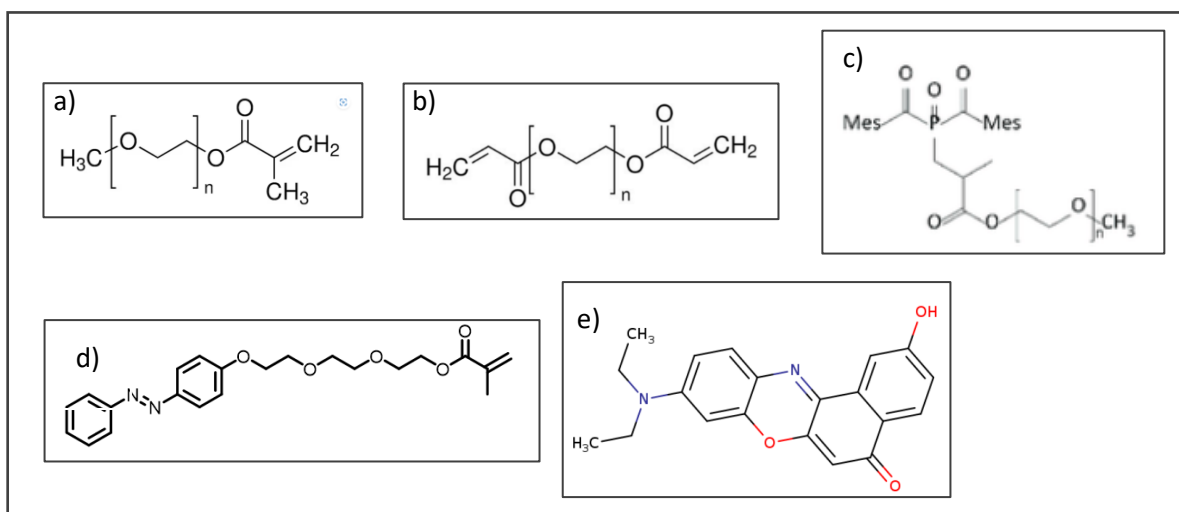Distilled water and dimethyl sulfoxide (DMSO) were employed as solvents.

Figure 15 Chemical formula of (a) PEGMEMA, (b) PEGDA, (c) PEG-BAPO, (d) AzoPEGMA, (e) Nile Red

Among the monomers commonly used for the production of hydrogels,(9,46), the pre-polymers selected for this thesis project were PEGMEMA (MW 950) as the main monomer and PEGDA (MW 700) used as cross linker. They were chosen because both are biocompatible and commonly used in biomedical applications (47,48), when good mechanical properties are necessary. PEGDA (49–52) was chosen also because of its good printability.

Both PEGMEMA and PEGDA were purchased by Merck Italia spa.

As previously mentioned, the hydrogel will be obtained via radical induced polymerization taking advantage of (meth)acrylate functionalities, which was induced by the presence of a suitable photoinitiator (PhI). In this case, the photo-initiator chosen is poly(ethylene glycol) substituted Bis(acyl)phosphane oxides (BAPO) derivative, named PEG-BAPO. It was kindly provided by Grutzamacher group in ETH, which synthesized this compound as reported by Wang et al. (44). It is a Norrish I water soluble photoinitiator with absorption in the visible range, as reported in Fig. 16.
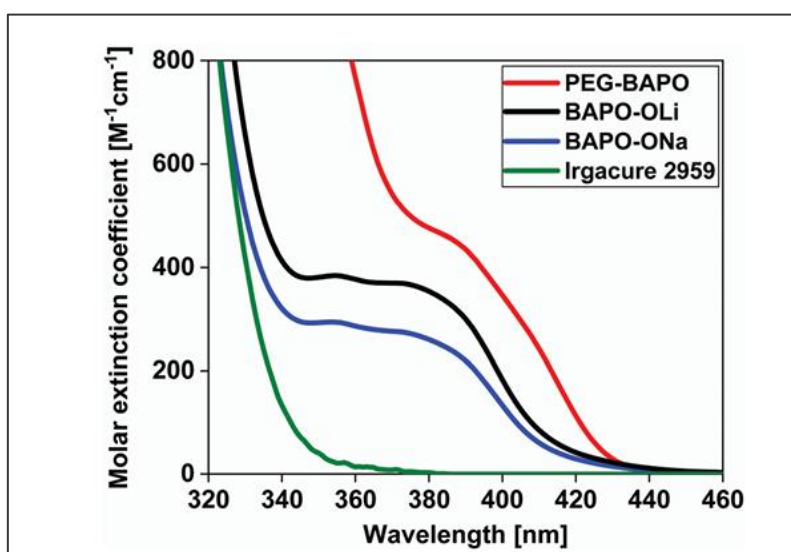

Figure 16 UV-vis absorption spectra of the different PIs recorded at 1mM concentration. (44)

Drawing inspiration from Villa et al. work (33), a modified azobenzene, named azoPEGMA, has been added to the formulation in order to obtain a photo-responsive hydrogel. Differently from the AzoPeg previously described (Chapter 1.3.2) a methacrylate group has been added to the molecule in order to enable a free radical polymerization. It will be further investigated in chapter 3.1. AzoPEGMA has been kindly provided by Istituto ISOF-CNR of Bologna. AzoPEGMA was dissolved in dimethyl sulfoxide, purchased from Merck Italia spa.

Nile Red was used to mimic drug release. It is a fluorescent hydrophobic dye commonly used in biological environment. (53) It was purchased from Merck Italia spa and used as received.

2.2. FORMULATIONS' PREPARATION PROCEDURE

In order to facilitate and expedite the preparation of the hydrogel formulations, multiple stock solutions were prepared.

1. PEGMEMA was dissolved in distilled water at a ratio 2:1 by weight

2. PEGDA was dissolved in distilled water with a ratio 1:1 by weight.

3. PEG-BAPO was solubilized in distilled water at a concentration of 100mg/ml.

4. AzoPEGMA was dissolved in DMSO with three different concentrations: 4mg/ml, 8mg/ml and 9.7 mg/ml. These concentrations were chosen due to the molarity of azoPEGMA and the quantity of DMSO needed. AzoPEGMA solution were kept in fridge after preparation, to avoid thermal isomerization of azobenzene group.

5. NileRed was solubilized in DMSO with two different concentrations: 0.3mg/ml and 35mg/ml.

To prepare the hydrogel formulations, two distinct procedures were followed, contingent upon the presence of Nile Red:

1. When Nile Red wasn't used, the steps were arranged in this order:

    a. placing the required amount of distilled water in a falcon tube,

    b. add PEGMEMA stock solution,

    c. add PEGDA, when needed;

    d. add PEG-BAPO stock solution

    e. add azoPEGMA DMSO solution dropwise.

The composition of the formulation tested will be reported in chapter 3.

2. When NileRed was required, the order changed:

    a. start with NileRed solution in falcon tube

    b. add azoPEGMA stock solution [9.77 mg/ml]

    c. add PEGMEMA solution

    d. add PEGDA if needed

    e. add distilled water to reach the desired concentrations

f.   finally PEG-BAPO solution.

Detailed composition will be given in chapter 3.

The reference hydrogel formulations were prepared following procedure 1 or 2, depending on the request, but without azoPEGMA.

All the stock solutions and the hydrogel formulations were mixed by pipetting and all those containing photosensitive elements, meaning PEG-BAPO, Nile Red and azoPEGMA, were covered with aluminium foil. After preparation, all the formulations were maintained at room temperature.

2.3.HYDROGEL POLYMERIZATION AND AZOPEGMA PHOTOSWITCHING

In this project thesis, the hydrogel was obtained by irradiating the formulation with a 420nm LED purchased from Intelligent LED Solutions (model ILS-XC06-S410-SD111 (54)). 420nm light was chosen as suitable wavelength to activate PEG-BAPO (see Fig. 16) but at the same trying to minimize the E to Z Transition. Thus, efforts were made to employ a low dose: $1.1*10^5$ J/s on 50µl of formulation.

AzoPEGMA photoisomerization was investigated employing two different lights: and 365nm (E-to-Z) and 450nm (Z-to-E). The LEDs were purchased from Amazon (55,56)

In order to better investigate this photoisomerization, two different doses were used. In particular, 450nm had a dose of $1.62*10^5$ J/s and $8.1*10^5$ J/s, while 365nm had a dose of $4.4*10^4$ J/s and $2.2*10^5$ J/s.

All the LEDs were powered using a portable generator (model KPS3010D by EVENTEK).

For convenience, hydrogels were always polymerized and irradiated in a multiwell plate starting from 50 µL of formulation, unless otherwise specified.

2.4.CHARACTERIZATION TECHNIQUES

2.4.1.RHEOLOGY

An ideal elastic material is a material which experiences a proportional deformation in response of a force application, which is then recovered when the force is removed; meanwhile an ideal viscous material is characterized by a strain which changes proportionally with the time in which the stress is given, meaning that the stress is proportional to the strain rate.(12,57)

Polymeric materials, including hydrogels, are typical viscoelastic materials, in which these two characteristics co-exist.(12)

This means that the application of a force produces a viscoelastic response, which can be measured by rheology test. (58)

In this thesis project, these characterizations are used to analyse the kinetics of the sol-to gel Transition, the mechanical properties of the formulations and their photo-polymerization process, using an Anton Paar MCR 302 rheometer along with the software Rheoplus. Concerning the settings of the rheometer, gap was set at 0.2mm and a 25mm parallel-plate geometry was maintained during all the tests.

For this study, the most important parameters followed are viscosity, the storage modulus (G'), which is the elastic component of the complex viscoelastic modulus G*,(59) and the loss modulus (G''), which in turns is the imaginary part, more related to viscous behaviour.

The complex viscoelastic modulus G* is evaluated as the ratio between the shear stress (τ) and shear strain (γ) according to the law of elasticity.

In Fig. 17 is presented the vector diagram showing the relationship between modulus G' and G'' using the phase-shift angle δ. The elastic component of the viscoelastic behaviour is represented on the x-axis, the viscous component on the y-axis (60)
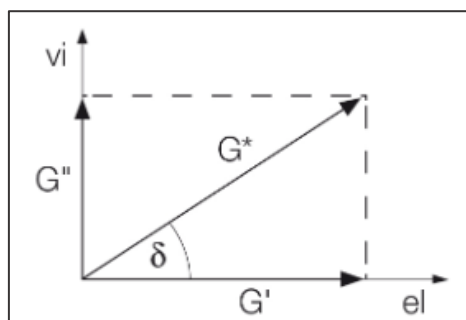

Figure 17 Vector diagram illustrating the relationship between complex shear modulus G, storage modulus G' and loss modulus G'' using the phase-shift angle δ (60)*

Three analyses were conducted: the first was the rotational viscometry, where shear stress is increased step by step to obtain viscosity curve: they show viscosity versus the shear rate. Viscosity is known as the ratio between shear stress [Pa] and shear rate [s^{-1}] according to Newton law (60), reported in Equation 1.

$$\eta = \frac{\tau}{\dot{\gamma}}$$

Equation 1 Viscosity definition

Viscosity curves are also useful to identify the material as shear-thinning, if the viscosity decreases as the shear rate increases or shear thickening if they both increase (Fig. 18).
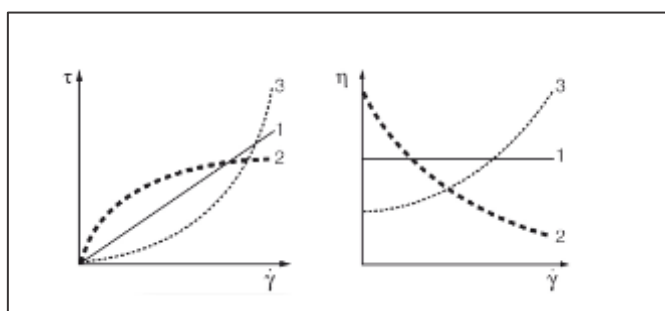

Figure 18 Flow curves (left) and viscosity curves (right) for (1) ideally viscous, (2) shear-thinning, and (3) shear-thickening flow behaviour (60)

In this work, shear rate was set from 0.01 s^{-1} to 1000 s^{-1}.

The second analysis performed was amplitude sweep: this test measures G' and G'' as a function of applied strain. It must be conducted before evaluating the frequency-dependent behaviour of sample (61), which will be measured with photorheology, because it is fundamental to find out the linear viscoelastic region (LVE). The LVE region is a range of strain in which hydrogels are not structurally degraded. In this work, the amplitude gamma was between 1% and 800%, with a frequency of 1Hz.

Photorheology was the third analysis performed. It consists in applying small amplitude, sinusoidal deformation on a sample while also being irradiated. It allows, among other things, the study of storage and loss modulus and the detection of the gel point, that is the point in which G' and G'' intersect. When G'<G'', the sample is liquid, meanwhile when G'>G'' it can be considered a gel. In liquid photopolymerizable

32

formulations G' should be lower than G'' and, once the light is switched on and the photopolymerization reaction occurs, this brings to the hydrogel formation, which in turns leads to an increase of both the storage and the loss modulus. However, G' has a faster growth, meaning that it will cross G'', creating the aforementioned gel point.(62) Moreover, G' is an important value to understand the final rigidity of the hydrogel.

In this project, this analysis was conducted irradiating the samples, starting from after 60s from the start of the measurement, to allow the instrument to stabilize. The light source used was HAMAMTSU lamp (model A9616-09 light source -03) with filter and with an intensity of 36mW/cm^2. In Fig. 19 is reported its visible light spectral distribution.
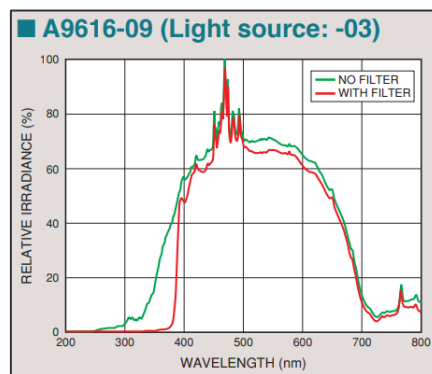

Figure 19 Visible light spectral distribution of HAMAMATSU lamp. (89)

2.4.2.SWELLING

In hydrogels, one of the most common characterization techniques is swelling, as it can affect various properties, such as mechanical ones or drug delivery capacity. It can be measured in different ways, with both dry and wet hydrogel. In biomedical field, it is normally preferable using the wet condition, as drying the hydrogel could damage possible encapsulated cells. (12,13,63)

In this thesis, the formula presented in Equation 2 was applied.

$$SD = \frac{W_t - W_0}{W_0} * 100$$

Equation 2 Swelling formula

SD stands for the swelling degree, W_t is the weight when hydrogel is wet, while W_o is its initial weight.

The procedure from Cafiso et al. (63) was implemented: triplicates of the sample and its reference (with no azoPEGMA) were prepared, polymerized, weighted and then immersed in distilled water. At each timestep (1-2-3-4-5-6-7-24-168-216-264-336-408h), they were removed from the water, dried with filter paper and weighted. They were maintained at room temperature.

Swelling analysis were performed also on a triplicate of polymerized hydrogels with and without azoPEGMA also irradiated with UV light (365nm, $2.2*10^5$ J/s) and then VIS light (450nm, $8.1*10^5$ J/s). Hydrogel were weighted after polymerization and then swelling values were evaluated after 48h from polymerization, immediately after UV irradiation, after 24h from the UV irradiation, immediately after VIS light irradiation and after 24h from this last VIS irradiation.

2.4.3. EVAPORATION

In order to gain a more comprehensive understanding of the hydrogel behaviour, it is necessary to evaluate the evaporation rate, as the quantity of water released could affect other properties. 4 triplicates were prepared: formulation of interest and its reference (with no azoPEGMA), both only polymerized and polymerized + exposed to UV-light ($2.2*10^5$ J/s). They were weighted in the liquid state, after every irradiation, and then at regular intervals. They were maintained at room temperature, covered by aluminium foil.

2.4.4. COMPRESSION TEST

Mechanical properties of hydrogels are crucial properties for different applications. Tensile and compression tests are usually performed. Unfortunately, the hydrogels developed in this thesis were too soft and therefore only compressive tests were performed. (64)

These analyses were carried out at room temperature with an Instron Z5 tensile tester, with load cell of 500N, coupled with the software THSSD, with a preload of 0.025mm and a low speed of 1mm/minute typically suitable for soft tissues.(65,66)

Differently from the standard procedure described for this work (paraghraph 3.3), 7 samples were prepared by polymerization in PDMS molds, starting from 200ul of formulations. Being bigger, the dose of irradiation was proportional to their dimensions.

6 different typologies of samples were analysed, in fact both the formulation of interest and its reference (with no azoPEGMA) were irradiating as following:

- Only polymerized (420nm)

- Polymerized and irradiated with UV light (365 nm)

- Polymerized and irradiated with VIS light (450nm)

Before the compressive test got started, samples were measured with a digital caliper (LinearTools ©).

According to literature the strain was calculated from the resulting data as:

$$\varepsilon = \frac{\Delta L}{l_0}$$

where ΔL stands for the load cell course during the test, starting from zero position.

Meanwhile the compressive stress is considered as:

$$\sigma = \frac{F}{A}$$

where F is the force measured by the load cell and A is the sample area, previously evaluated according to the dimension measured.

Young's Modulus E, commonly calculated as $E = \sigma * \varepsilon$,was estimated as the slope obtained by fitting the elastic deformation region of the stress-strain curve, which has been considered as the initial part up to 6% strain experienced.

Tensile strength was evaluated as the highest stress experienced by the hydrogel before rupture, while elongation at break was taken as the strain corresponding to that point.

2.4.5.FT-IR SPECTROSCOPY

Chemical environment of a sample is investigable due to the vibration modes of its functional groups at different infrared wavenumbers, mainly between 4000 cm^{-1} and 400 cm^{-1}, thanks to Fourier Eform Infrared (FT-IR) spectroscopy. It was suitable for this work's scope since it makes possible to monitor changes due to new interactions, as it happens during photopolymerization. Moreover, this technique is fast and non-destructive.

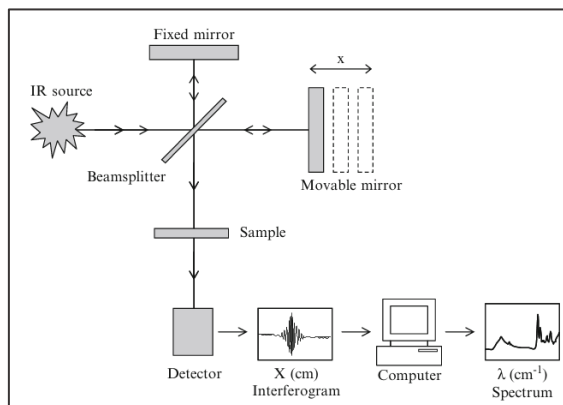In Fig. 20 is represented a schematic sketch of the essential features of FT-IR spectrometer.

Figure 20 Schematic sketch of the essential features of a Fourier transform infrared (FTIR) (67)

To simplify, a polychromatic light source emits radiations that strikes a beam splitter: one beam is reflected towards a fixed mirror, the other beam to a moving one. Once they are both reflected off their respective mirrors, they recombine: this generates a destructive interference. This brings to two beams: one returns to the source, while the other one moves towards the sample for detection. One or more interferograms are produced and processed on a computer and then converted into conventional Emittance or absorbance spectra via Fourier Eform analysis. (67)

In order to carry on with this analysis, a Nicolet™ iS50 FTIR Spectrometer by ThermoFisher spectrometer was used along with Omnic™ software.

Several samples were prepared and dried by simply letting the water evaporate, as it can cover the signal of interest: (67)

1. Formulation of interest and reference of the formulation of interest (without azoPEGMA)

2. 50 µl of formulation and of its reference both polymerized

3. 50 µl of formulation and of its reference both polymerized and UV irradiated

4. 50 µl of formulation with no PEG-BAPO and of its reference (without azoPEGMA and PEG-BAPO)

2.4.6. UV-VIS SPECTROSCOPY

UV-vis spectroscopy is a non-destructive and quick analytical technique commonly used to investigate the absorption in the UV or visible light regions of electromagnetic spectrum. Absorption follows the Beer-Lambert's law, presented in Equation 3:

$$A = \varepsilon L c$$

Equation 3 Lambert-Beer's law

where A stands for the absorbance and it is adimensional, ε for the molar absorptivity expressed in L mol^{-1} cm^1, which is specific to the given material, L for the path length, in cm and finally c in mol L^{-1} for the concentration of the sample. (68)

In this work thesis, this technique was used to monitor E-AzoPEGMA and Z-AzoPEGMA photoisomerization. Samples were polymerized in multiwall plates and then UV-vis spectroscopy was performed using BioTek Synergy HTX Multi-Mode Microplate Reader along with GEN5 software. Spectra were taken in a range of wavelengths from 250nm to 600nm, with 1nm step. In order to analyse azoPEGMA's signal, reference spectrum (composed by all the ingredients except azoPEGMA) was subtracted.

2.4.6.1. DEGRADATION ANALYSIS

Degradation analyses were carried on to investigate if azoPEGMA undergoes photodegradation. Analyses were run in two different ways: in the first one, the hydrogel formulation, made only of H_2O, PEGMEMA, PEGDA and azoPEGMA, was exposed to ultraviolet light (365nm) for 30 minutes and visible light (450nm) for 7 hours with the configuration described in paragraph 3.2, but with different timings. At each timestep (1-2-3-5-30 minutes for UV irradiation, 1-2-3-5-30 minutes, 1h-3h-7h for visible irradiation), 50µl of the irradiated formulation were placed in the well of the multiwell plate and UV-vis spectra were taken as previously explained in paragraph 3.3.3. In the second run of analysis, formulations were exposed to light, alternating UV and visible irradiation for 5 and 10 minutes respectively, up to 10 times each. Every time, 50 µl of the irradiated formulation were placed in the multiwell, in order to assess azoPEGMA ability to maintain its photoisomerization over several cycles of irradiation.

2.4.6.2.KINETIC ANALYSIS

Inspired by Villa et al. work, kinetic analysis was conducted over 168 hours at room temperature. Two samples were prepared with the formulation and its reference made without azoPEGMA as described in paragraph 2.2. Samples were positioned in the multiwall plate, with lid on, surrounded in the nearby wells by salty water, to prevent evaporation as much as possible. The following steps were implemented: firstly, spectra between 250nm and 600nm were recorded prior to irradiation. Secondly, the samples' spectra were measured after visible light irradiation ($1.1*10^5$ J/s) and subsequently after UV irradiation ($2.2*10^5$ J/s). After that, kinetic analysis in microplate reader was initiated for 64 hours, during which absorbance values were recorded once per hour at the wavelengths of 346nm, 355nm and 450nm. Finally, after 64 hours to the 168 hours, complete spectra from 250nm to 600nm were recorded every 24 hours. The reference's signal was then subtracted to the formulation's one in order to obtain azoPEGMA signal.

2.4.6.3.RADICALS-INDUCED DEGRADATION

Based on literature (69), in this work thesis attempts were made to investigate how free radicals react and in particular if radical degradation of azoPEGMA was present. In order to perform this degradation analysis, samples composed by H_2O, azoPEGMA and PEG-BAPO only were irradiated with 420nm, 450nm and 365nm LEDs, following the aforementioned procedures and doses. At each step and then overnight, UV-vis spectra were taken from 250nm to 600nm.

2.4.7.MICELLES ANALYSIS

2.4.7.1.UV-VIS DOUBLE BEAM SPECTROSCOPY

UV-vis has been employed to investigate, at first, the presence of E-azoPEGMA micelles in the formulations. Since they are invisible to the naked eye, the turbidity of the solution was the only immediate way to determine their presence. (70,71)

However, an easy and effective analysis was needed to confirm or deny their presence. UV-VIS double beam spectroscopy was chosen to evaluate the turbidity of the solutions. It works as a standard UV-VIS spectroscopy (Fig. 21a), but it uses two beams of light, one for the sample and the other one for the reference (Fig. 21b).(72)
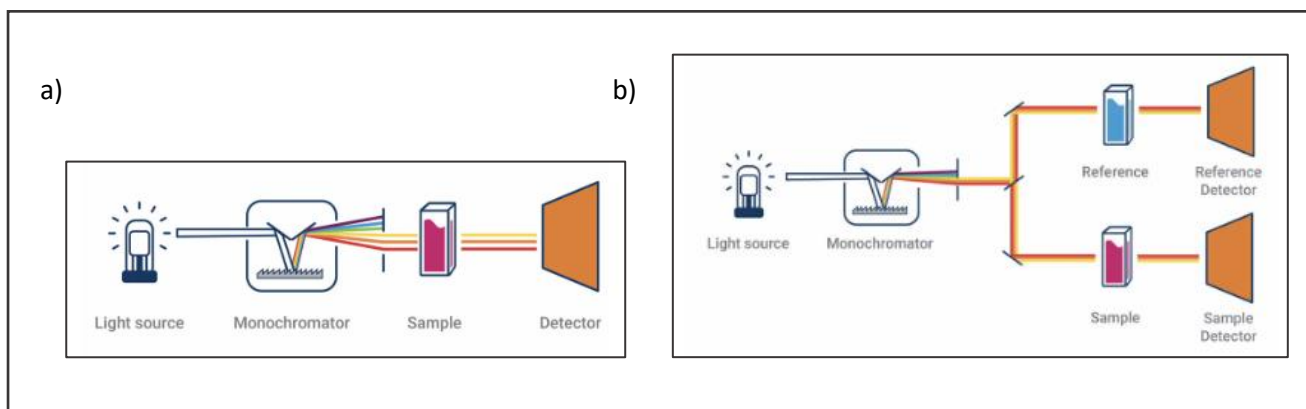
Figure 21 Schematic sketch of the essential features of (a) Single beam and (b) Double beam UV-Vis spectrophotometers. (72)

The beam is split using a rotating wheel with mirrored segments or a beam splitter.

This methodology is more accurate compared with the single beam UV-VIS spectroscopy as the presence of the reference allows a real-time correction which compensate the instrument fluctuations. (72)

Varian Cary 500 Scan UV-Vis NIR Spectrophotometer was used among with SCAN software. Measurements were carried out from 250nm to 800nm in Emittance. Sample were analysed in Emittance mode.

1.6mL of the following samples were analysed:

1. H_2O, PEGMEMA, PEGDA, DMSO

2. H_2O, PEGMEMA, PEGDA, DMSO, PEG-BAPO, both liquid and polymerized

3. Standard formulation without PEG-BAPO, before irradiation, after VIS-irradiation (420nm) after UV-irradiation (365nm) and the after VIS-irradiation (450nm)

4. Standard formulation, before irradiation, after polymerization (420nm), after UV-irradiation (365nm) and then after VIS-irradiation (365nm)

Light doses followed the standard procedure, proportionally to the volume of the formulation.

The reference sample used was a cuvette with H_2O:DMSO in a ratio of 95:5 by volume and it was maintain for all the measurements.

2.4.7.2. SPINNING DISK

According to Villa et al. work, E-azoPEG aggregate should measure around 300-400nm, so efforts were made to directly see them. To observe them, the Nikon CSU-X1 Spinning Disk System was used.

It is a confocal spinning disk, meaning that light can scan a sample through pinholes arranged in spiral on a rotating opaque disk, (73) so it is an optical analysis based on the detection of diffracted light.

50 µl of several formulations were scanned:

1. Standard formulation

2. Standard formulation containing Nile Red

Standard formulation both with and without Nile Red were polymerized.

Exposure was set at 500ms, LUT range was 100-1000 and power 100%.

2.4.7.3.FLUORESCENCE SPECTROSCOPY

Fluorescence spectroscopy is basically the detection of the emission of light deriving from fluorescence, luminescence or phosphorescence phenomena induced in the sample thanks to a specific wavelength of light. (74) It relies on the fact that part of the energy given to a fluorophore is dissipated, creating a difference between its excitation and emission spectra, which means that the absorbed and emitted lights can be distinguished by their appearance as distinct colours or regions within the visible spectra. (75,76) Concerning dissipation, it is obvious that the emission light has a lower energy, thus a longer wavelength.(77)

In Fig. 22 is reported a scheme of a conventional fluorescence spectroscopy system
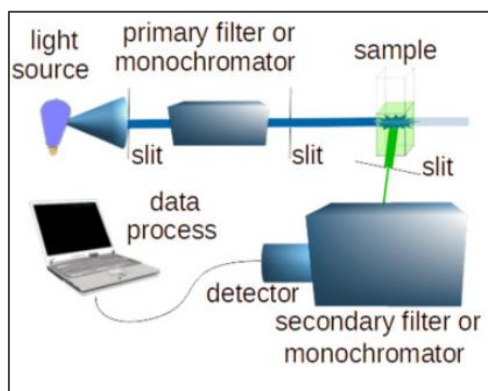

Figure 22 Schematic sketch of the essential features of a fluorescence spectroscopy system (77)

In this work thesis, fluorescence spectroscopy was implemented to verify the encapsulation and release capacity of E-azoPEGMA using NileRed as fluorophore. To carry on this tests, LS 55 perkin elmer fluorometer

was employed along with FL winlab software. The excitation wavelength was 540nm and the wavelengths of the emission was a spectrum from 580nm to 750nm, while scan speed was 200nm/min.

3ml of several samples were prepared and inserted in a cuvette, using a different procedure as the standard described in this work:

1. Formulation composed of H_2O and NileRed

2. Formulation composed of H_2O, DMSO and PEG-BAPO

3. Standard formulation without PEG-BAPO

4. Standard formulation containing NileRed but without PEG-BAPO

5. Standard formulation containing NileRed

6. Formulation as the 4th, but PEGMEMA, PEGDA and H_2O were introduced first, followed by Nile Red and azoPEGMA (procedure 1 of chapter 3.2)

7. Standard formulation containing NileRed, but without azoPEGMA

8. Standard formulation containing NileRed, but without azoPEGMA and PEG-BAPO

Formulation 1,2,3,6 were tested and never irradiated. Formulation 4 was tested before irradiation, after UV irradiation (365nm) and after VIS irradiation (450nm). Formulation 8 was tested in the cuvette before irradiation, after VIS irradiation (420nm), after UV irradiation (365nm) and after VIS irradiation (450nm). All these formulations were tested directly in the cuvette.

For what concerns formulations 5 and 7, 100μL of the formulations were pipetted onto a microscope slide and polymerized to obtain a sample in the form of a film. They were tested before irradiation, after polymerization (420nm), after UV irradiation and finally after VIS irradiation (450nm).

2.4.8.3D PRINTING

In this thesis work, an attempt was made to produce hydrogel through 3D printing. Asiga Pico 2 HD DLP-3D was used for this scope along with Composer software. It is a DLP-type printer and its light source has a wavelength of 405nm, its resolution in the XY plane is of 50μm and the minimum control along z-axis 1μm. As usual, a CAD (STL, SLC, PLY or STM type) was read and sample was built by the printer. (78)

Before printings got started, a simple material test was possible thanks to a specific tool integrated in the Asiga 3D Printer, that irradiates the formulation for a set amount of time (maximum 100 seconds). Material test were accomplished irradiating the formulation with an intensity of 22mW/cm^2 for a decreasing amount of time, from 100s to 10s, with steps of 10s. At each step, it was checked whether the hydrogel had formed or not, and if so, its thickness was measured. Only hydrogels formulations able to produce a manageable sample were considered for 3D printing process.

3D printed samples were obtained varying the intensity of light, the time of irradiation and the width of each layer composing the CAD.

Differences were made between the burn-in layers, which are the initial ones and usually require a higher dose of light to guarantee adhesion of the curing material to the platform, and the Range layers, which are the subsequent ones. They will be further investigated in chapter 3.12.

3.EXPERIMENTAL RESULTS AND DISCUSSION

This thesis project aimed to polymerize photoresponsive hydrogels, taking advantage of the azoPEG characteristics previously reported by Villa et al. Differently from that investigation, in this case an azoPEGMA molecule was employed, in order to enabling the possibility to chemically incorporate the photoresponsive molecule in the gel polymeric network. Therefore, in our view, different scientific questions will be addressed in this Thesis:

1) Do azoPEGMA molecules still form micelles when dispersed in a photocurable formulation?

2) Are those preserving the ability to form light-controllable micelles in liquid solution?

3) Are those micelles maintained when photopolymerization occurs and therefore hydrogel is formed?

4) Do azoPEGMA molecules preserve photoisomerization in the hydrogel?

5) Is it possible to create hydrogels with light-controlled drug release?

6) Is it possible to 3D print those materials?

To answer to these questions a series of experiments were performed, as described in this chapter

3.1.AZOPEGMA CHARACTERIZATION

As reported in Chapter 2.1, azoPEGMA molecules were synthesized in the ISOF-CNR institute of Bologna. For completeness, the basic analysis of those molecules is here provided even if the most of the experiments were performed by the colleagues.

UV-VIS spectroscopies (Fig. 23a) performed on a DMSO solution containing azoPEGMA with a concentration of $2*10^{-5}$M show its photostationary state before and after irradiation at 365nm and 337nm. The outcome represents the spectra of E-azoPEGMA and Z-azoPEGMA. In particular, in the Z configuration, it is possible to notice a decrease of the peak in the UV region, and a corresponding blue shift. At the same time, the appearance of a peak around 430nm is evident.

The nuclear magnetic resonance (NMR) analysis (Fig. 23b) was exploited to analyse the micelles presence in an azoPEGMA aqueous solution with a concentration of 1mM. The ratio between H_2O and DMSO changed as

reported. E-azoPEGMA goes from being in its aggregated form, to be dissolved in solution when DMSO quantity is over 30%, as demonstrated by the appearance of sharp peaks at 8.1 ppm, 7.9 ppm and 7.4 ppm. On the contrary, when the amount of DMSO is under 30%, the Z-azoPEGMA molecules, which should go in solution, are found in their aggregated form, as demonstrated by the appearance of broad peaks at 7.0 ppm, 6.8 ppm, 6.6 ppm and 6.5 ppm.

The dimensions of these aggregates were then studied through a dynamic light scattering (DLS) analysis. It turned out that the micelles have an initial dimension of 150nm, up to 400nm in 24 hours. (Fig. 23c)

Micelles were also investigated through UV-VIS spectroscopy. In this case, their light scattering was followed observing the increase of absorbance between 400nm and 800nm. It results that the presence of scattering is significant when the concentration of azoPEGMA is at least $8*10^{-4}$ M.(Fig. 23d).

At last, FT-IR spectrum of azoPEGMA was analysed. (Fig. 23e, 23f) The most common peak associated with azobenzene (red part in Fig. 23f) are reported (1550 cm^{-1}, 1451 cm^{-1}, 756 cm^{-1}, 690 cm^{-1}). (79) On the other hand, there are some peaks that can be associated to PEGMA moieties (blue part in Fig. 23f) such as 1250 cm^{-1}, 1100 cm^{-1}, and 950 cm^{-1}. (80)
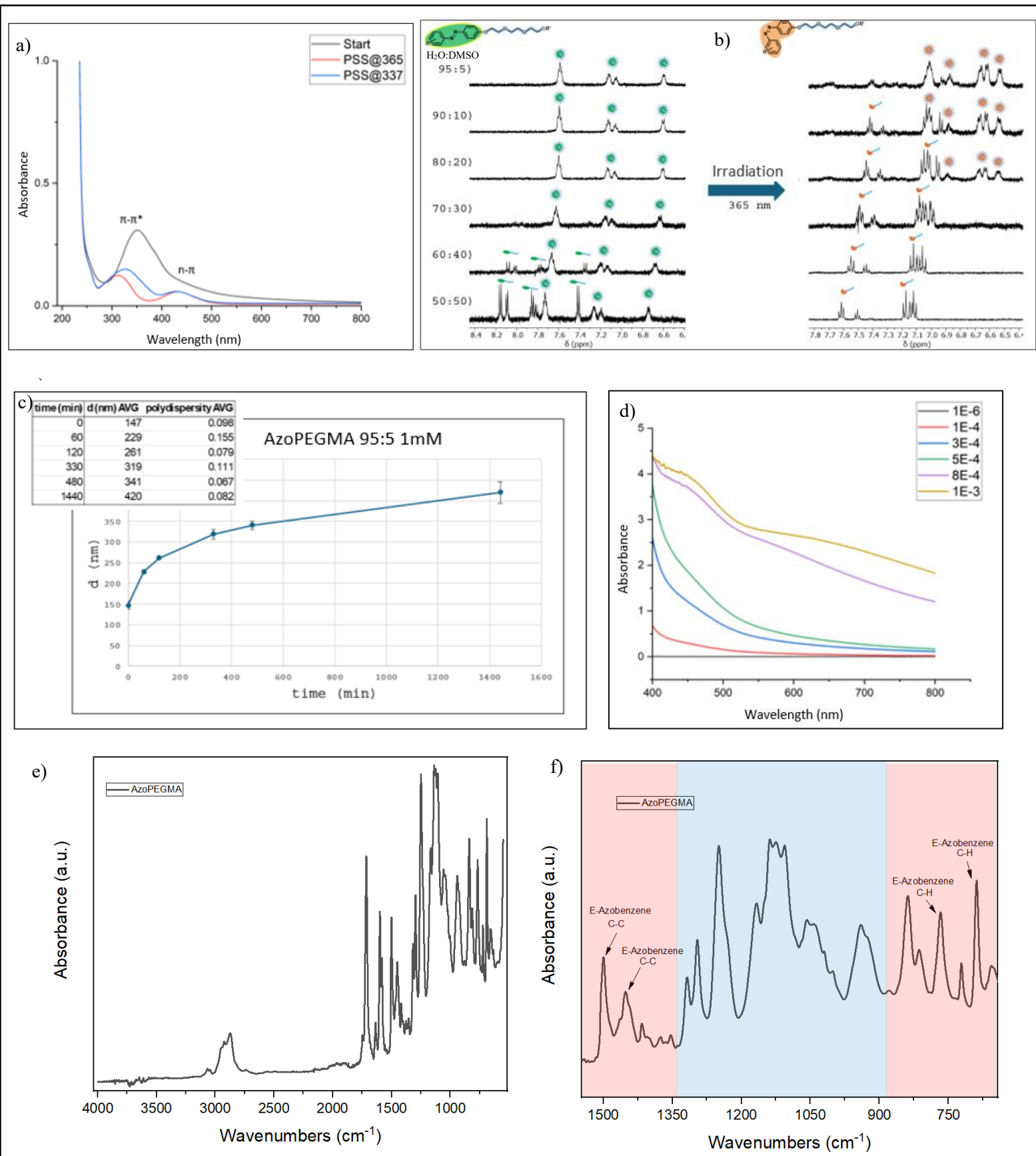
Figure 23 (a) UV-VIS spectroscopy on azoPEGMA 2*10-5M in DMSO. (b) NMR spectroscopy on different H2O:DMSO proportions on E-azoPEGMA and Z-azoPEGMA, (c) DLS analysis on an azoPEGMA solution 1mM. (d) Uv-vis spectroscopy and light scattering associated with the presence of micelles. (e) azoPEGMA FT-IR analysis. (f) azoPEGMA FT-IR analysis between 1500 cm-1 and 700 cm-1

3.2. FORMULATION'S PREPARATION AND POLYMERIZATION

Villa et al. work presented solutions composed of H_2O and DMSO in different ratios. Differently, in this thesis work, the tested formulations will include also the presence of photocurable monomers, namely PEGMEMA, PEGDA and eventually the BAPO-PEG photoinitiator. For simplicity of notation, ratios will always be expressed as H_2O:DMSO throughout this discussion. PEGMEMA and PEGDA will be expressed as %w/w while PEG-BAPO as phr (per hundreds resins).

In a first set of experiments, different H_2O:DMSO ratios were tested. In this context it must be noted that a change in the DMSO quantity was correlated to a change in the azoPEGMA molarity, since an azoPEGMA stock solution at fixed concentration of 4mg/ml was employed. In experiments, all the formulations contained PEGMEMA 33% w/w and PEG-BAPO 3 phr. In Table 1a these initial tested formulations are summarized.

An increase of azoPEGMA quantity might have helped the polymerization due both to its methacrylic group and to its capacity to form micelles (29). However, none of those initial formulation showed evident polymerization, regardless of the irradiation's time. In particular, they were exposed to light up to 1 hour and even left overnight, without showing gelation. For this reason, a different approach was taken, keeping H_2O:DMSO ratio to 95:5 and PEG-BAPO constant at 3 phr, while increasing PEGMEMA quantity. These formulations are outlined in Table 1b.

Table 1 Initial formulations (a) and (b) Formulations with different concentration of PEGMEMA

a)

Formulation's name	H_2O:DMSO ratio [v/v]	AzoPEGMA molarity [mM]
1A	95:5	0,5
2A	90:10	1
3A	85:15	1,5
4A	80:20	2

b)

Formulation's name	PEGMEMA quantity [w/w]
6A	50%
8A	63%
9A	71%

Unfortunately, neither those attempts were successful, and no polymerization was achieved. Therefore, it was hypothesized that the issue does not lie in the amount of PEGMEMA, but possibly in that of PEG-BAPO. In

this context, a higher amount of photoinitiator may result in a higher generation of radicals that possibly initiate more macromolecules. On the other hand, this may lead to lower average molecular weight, and therefore avoid the gelation. Consequently, a formulation with less photoinitiator was prepared and named 10A. It still had 95:5 H_2O:DMSO ratio, and 33% w/w PEGMEMA but only 0.5 phr of PEG-BAPO.

In Fig. 24 the result after irradiation: the irradiated formulation was still very soft and not suitable for manipulations, but it represents certainly an improvement compared to the previous ones, which remained completely liquid.

Figure 24 Formulation 10A after polymerization.

In light of these findings, new formulations were prepared, as listed in Table 2.

Table 2 Formulations after 10A

Formulation's name	H2O:DMSO ratio [v/v]	PEGMEMA quantity [w/w]	PEG-BAPO quantity [phr]	AzoPEGMA molarity [mM]	Polymerization
1B	95:5	50%	0.25%	0.5	Yes
2B	95:5	33%	1%	0.5	No
3B	80:20	33%	0.5%	2	Yes

The 1B and 3B formulation succeeded in creating a hydrogel (Fig. 25a, 25b), while 2B failed. 3B formulation showed a stronger yellow colour due to the greater presence of azoPEGMA.
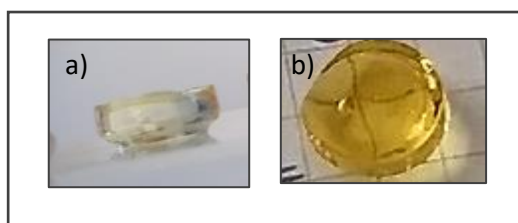

Figure 25 (a) Formulation 1B after polymerization and (b) 3B formulation after polymerization

Considering the good result obtained with the 1B formulation and to better understand the successful formulation, some new ones were prepared keeping 1B as a reference: they are outlined in Table 3. All new formulations contained 50% w/w PEGMEMA and 0.25 phr PEG-BAPO, but with a different H_2O:DMSO ratio.

Table 3 Formulations inspired by 1B one.

Formulation's name	H_2O:DMSO ratio [w/w]	AzoPEGMA molarity [mM]
3B	80:20	2
7B	90:10	1
9B	92.5:7.5	0.75
8B	97.5:2.5	0.25

All these formulations allowed the hydrogel polymerization after irradiation. Thus, it is possible to state that suitable conditions for obtaining photocurable hydrogels were obtained, and then, more tests were carried on.

3.3. RHEOLOGY

Photorheometer was used to determine the viscoelastic behaviour of the formulations both with and without azoPEGMA (DMSO only). Preliminary analyses were performed on formulations listed in Table 4.

Table 4 Formulations analysed with rheology tests.

Formulation's name	H_2O:DMSO ratio [w/w]	AzoPEGMA molarity [mM]
3B	80:20	2
7B	90:10	1
9B	95:5	0.5

Viscosity curves were the first analysis carried on: the results are shown in Fig. 26.
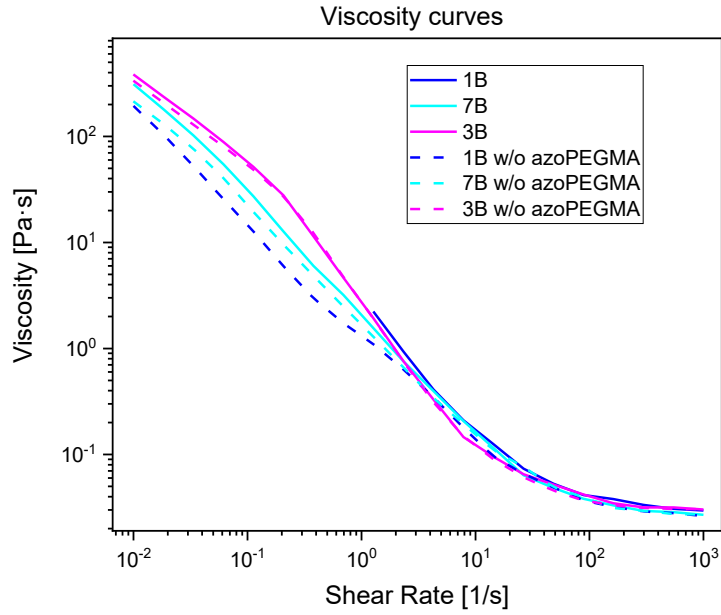
Figure 26 Viscosity curves on formulation 1B, 7B and 3B.

Looking at the obtained curves as a whole, it can be deduced that neither the DMSO nor the azoPEGMA affect the viscosity: all these formulations show shear-thinning behaviour. Subsequently, the photopolymerization behaviour was analysed on the 95:5 and 80:20 H_2O:DMSO ratio formulations, to assess the extreme values behaviours. The amplitude sweep revealed for both of them that a strain of 10% is included in the LVE region (Fig. 27a, 27b), so it was used as the amplitude of photorheology.
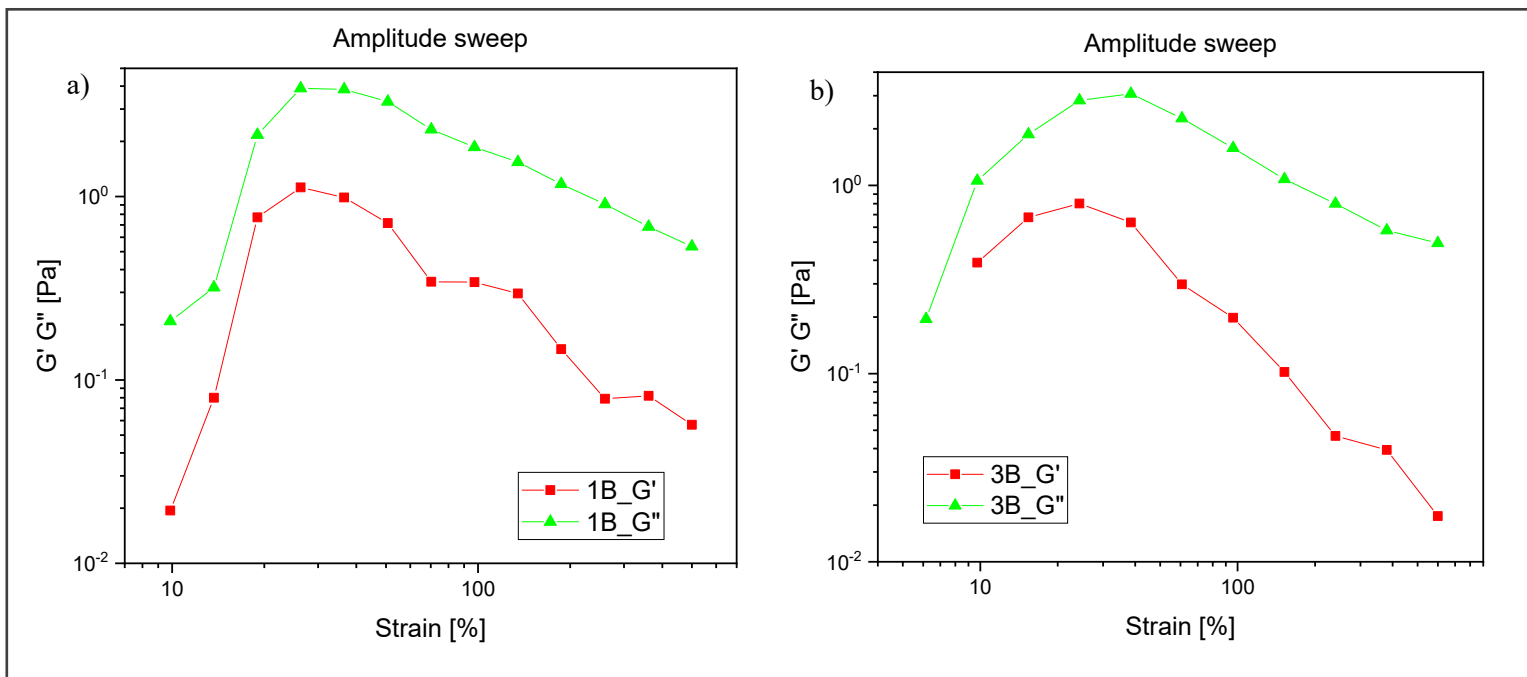
Figure 27 Amplitude sweep on formulation (a) 1B and (b) 3B.

Having determined the suitable parameters, photorheology was carried out and reported in Fig. 28a, 28b. Notably, the presence of a gel point (crossover point between G' and G'') is evident in both the formulations, even if at different timings. Specifically, in formulation 1B the gel point is achieved in about 30s, while in formulation 3B it is reached in about 70s. Furthermore, formulation 1B is more photo-reactive, as evident following G' trend. Interestingly, azoPEGMA/PEG-BAPO ratio seems to affect the final characteristics of the hydrogel. As a matter of fact, with the same quantity of PEG-BAPO, 3B formulation contains much more azoPEGMA, which may compete with the photoinitiator in light absorption, delaying the photocuring. Moreover, formulation 1B has a higher final value of G', which is about 1400 Pa, compared to 3B formulation's one which is just about 640 Pa, meaning that formulation 1B is more rigid after the polymerization process. This may be due both for the same reason as the previous one and for the greater quantity of DMSO present in formulation 3B.
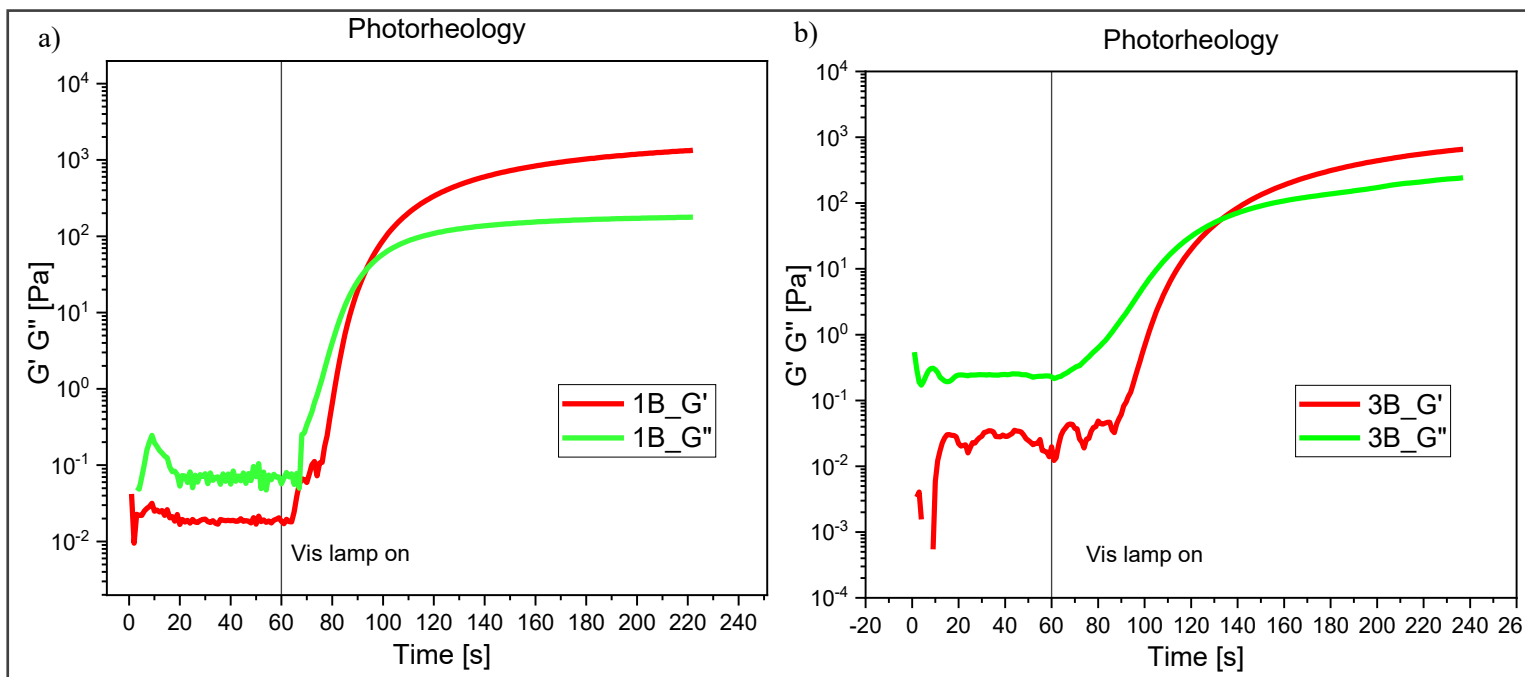
Figure 28 Photorheology on formulation (a) 1B and (b) 3B.

3.4.UV-VIS SPECTROSCOPY

Since the first requirement, namely the polymerization of hydrogels, had been achieved, UV-VIS spectroscopy was carried on, monitoring how every single element of the formulation influence light absorption. Considering photorheology results, the analyses were conducted on formulation 1B.

First of all, PEG-BAPO contribution was analysed (Fig. 29a). According to literature, (44)   the addition of PEG-BAPO leads to the formation of a peak in the absorbance spectrum at the wavelengths of 320nm, 370nm and 420nm.This means that this photoinitiator is suitable for photopolymerization in the visible range. Noteworthy, the spectrum is clearly different after irradiation with 420nm light: this is related to the cleavage of phosphor-benzoyl bond, which generates the radicals that initiate the photopolyerization.

Then, azoPEGMA contribution was investigated (Fig. 29b): the addition of azoPEGMA leads to the formation of a peak in the absorbance spectrum between 300nm and 400nm. Moreover, light scattering is remarkable at higher wavelengths.

PEGMEMA instead doesn't absorb light and it has almost zero contribution to the UV-vis spectrum (Fig 29c). However, it is noteworthy that when PEGMEMA is added to a formulation containing also azoPEGMA, this last element changes its spectrum and in particular the scattering effect is reduced (Fig 29d). This is witnessed by a decrease of absorption at higher wavelengths (>500nm).
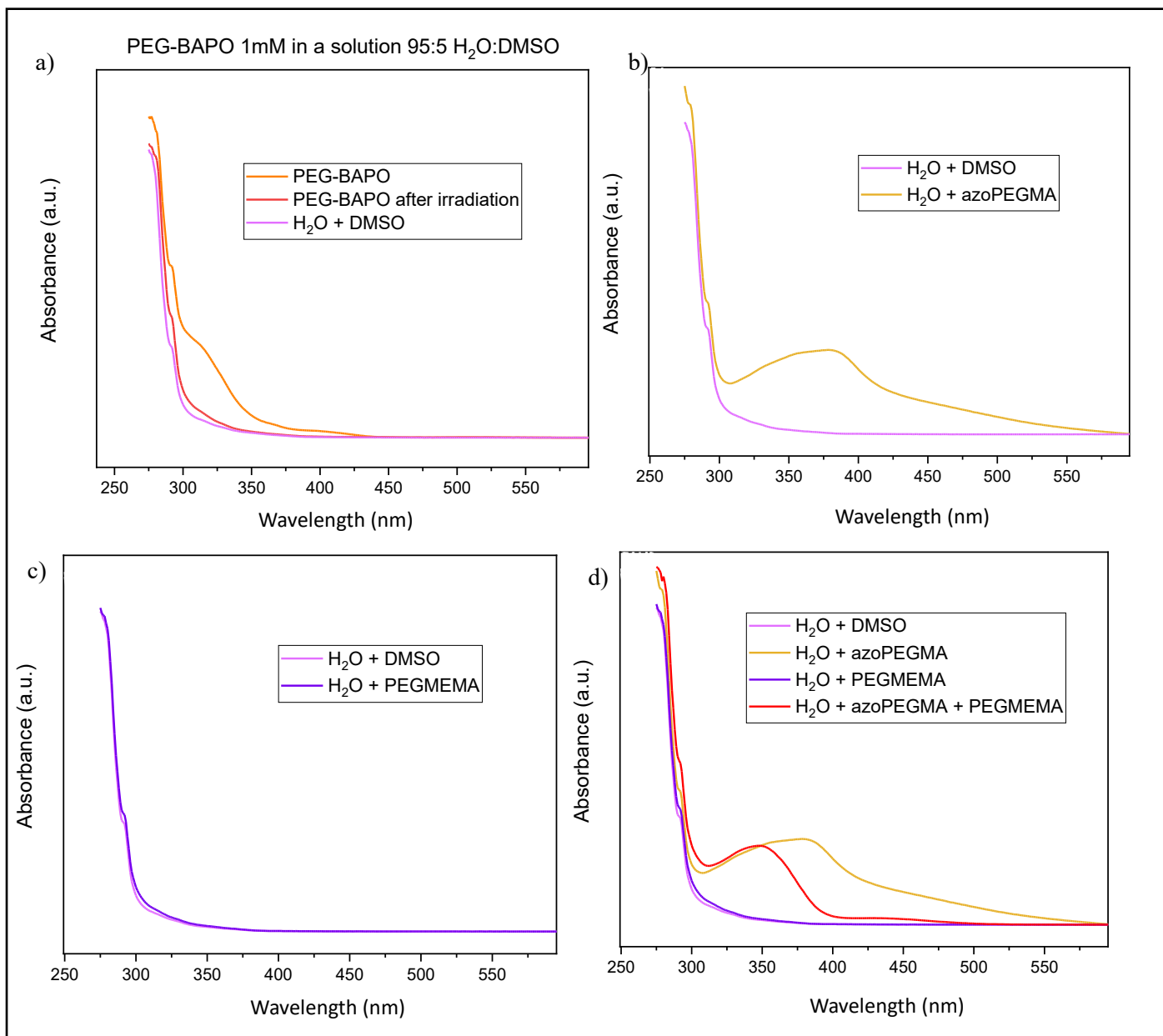
Figure 29 Absorbance spectra of (a) PEG-BAPO (b) azoPEGMA (c) PEGMEMA (d) azoPEGMA and PEGMEMA.

This can be even observed with naked eyes, since when PEGMEMA is added, the solution loses its turbidity. (Fig.30a, 30b)
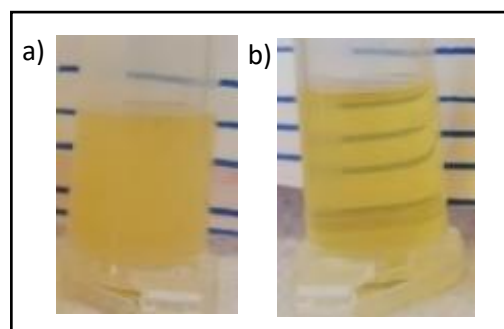

Figure 30 Formulation (a) without PEGMEMA and (b) with PEGMEMA.

Therefore, it can be assumed that the presence of PEGMEMA lead to a loss of micelles (70,81), due to a different interaction between ethylene-glycol tails of azoPEGMA and the surrounding environment.

Therefore, a new design of the formulations was undertaken. In this tested formulation 1B, the CAC (critical aggregation concentration) was respected (33), and so micelles should have been present according to the results reported in chapter 3.1. It was therefore hypothesised that not only the quantity of DMSO could interfere with the spontaneous formation of micelles, but probably also the quantity of PEGMEMA, which could be considered as a "solvent" for azoPEGMA. This is in good agreement with literature. (82)

However, given that a minimum quantity of PEGMEMA was necessary for the formation of the hydrogel, it was decided to proceed for the rest of this thesis work only with formulations that had a 95:5 H_2O:DMSO ratio, in order to keep at least the quantity of DMSO low. Moreover, from now on, azoPEGMA stock solution with fixed concentration of 8mg/ml was used, in order to maintain a higher molarity of 1mM.

Efforts were then made to find a balance between a reduced quantity of PEGMEMA and still having a sufficient quantity to allow polymerization to occur.

3.5. OPTIMIZATION OF THE FORMULATION

Consequently, different formulations have been prepared with a decreasing quantity of PEGMEMA, knowing that 50% w/w was already too much. They are listed in Table 5. Therefore, since the monomer was decreasing, it was decided to preventively increase the quantity of PEG-BAPO, up to 0.75 phr, to achieve polymerization.

Table 5 Formulation with decreasing quantity of PEGMEMA

Formulation's name	PEGMEMA quantity [w/w]
1C	33%
2C	26%
3C	17%
6C	14%
5C	13%
4C	8%

Observing Fig. 31a, it is immediately possible to notice that increasing the amount of PEGMA, turbidity decreases, and the formulation containing 33% of PEGMEMA appears transparent.

This can be also observed monitoring the UV-vis spectra (Fig. 31b), that show an increased scattering decreasing the amount of PEGMEMA. Therefore, among the tested formulations, the one which has the maximum of PEGMEMA and still show turbidity contains 26%. Unfortunately, those formulation didn't show the ability to produce a solid gel via photopolymerization except 2C, which by the way was really soft.
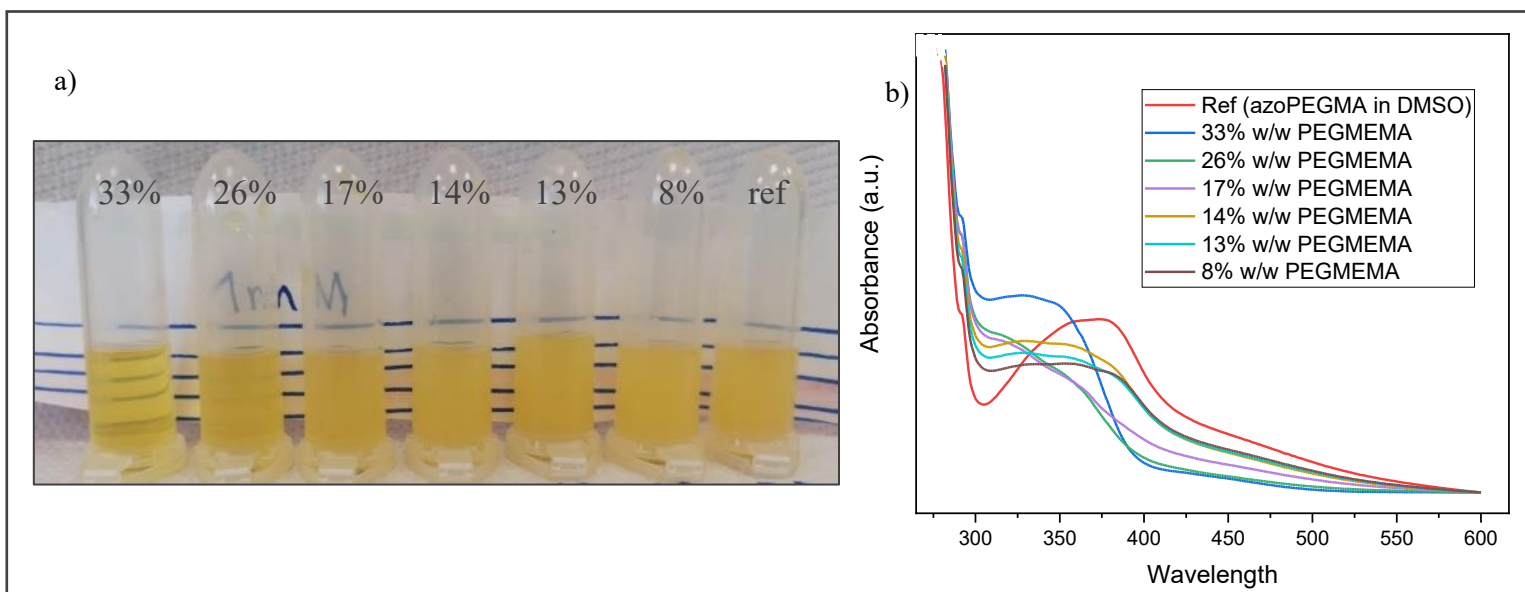
Figure 31 (a) Visible representation of formulation with increasingly lower quantity of PEGMEMA. Ref stands for a reference formulation made of H2O,DMSO and azoPEGMA only. (b) UV-VIS spectra of formulation 1C,2C,3C,4C,5C,6C

Summarizing these tests, 2C formulation contained the maximum acceptable concentration of PEGMEMA, meaning that no additional PEGMEMA could have been added. Therefore, in order to fabricate suitable hydrogel, the amount of PEG-BAPO was modified, reducing it down to 0.25 phr.

At the same time, PEGDA was added as a cross-linker. The presence of PEGDA can allow the synthesis of stiffer hydrogels since those molecules induce the presence of chemical crosslinks. However, to not inhibit the presence of micelles, in the next set of formulation PEGMEMA content was decreased, keeping in this set of new formulations a fixed total amount of monomers (PEGDA+PEGMEMA) of 26% w/w.

The formulations prepared are detailed in Fig. 32.

Formulation's name	PEGMEMA quantity [w/w]	PEGDA quantity [w/w]	PEGDA/ PEGMEMA [w/w]	Monomers quantity [w/w]	PEG-BAPO quantity [phr]
2C	26%	0%	0%	26%	0.75%
4D	26%	0%	0%	26%	0.25%
1E	24%	2%	8%	26%	0.75%
2E	24%	2%	8%	26%	0.25%

Figure 32 Formulation obtained with monomers 26% w/w.

All these ones were turbid and able to polymerize, therefore photorheology was again performed to characterize those new formulations.

3.6. RHEOLOGY ON THE OPTIMISED FORMULATIONS

Viscosity curves shows that the addition of PEGDA (i.e. Formulation 2E) doesn't change the profile of the curves compared to formulation 4D (without PEGDA), as reported in Fig. 33a, maintaining a shear thinning behavior. As expected, the formulations with less monomers (i.e Formulation 2E) have lower viscosity compared with the formulation 1B, as reported in Fig. 33b.
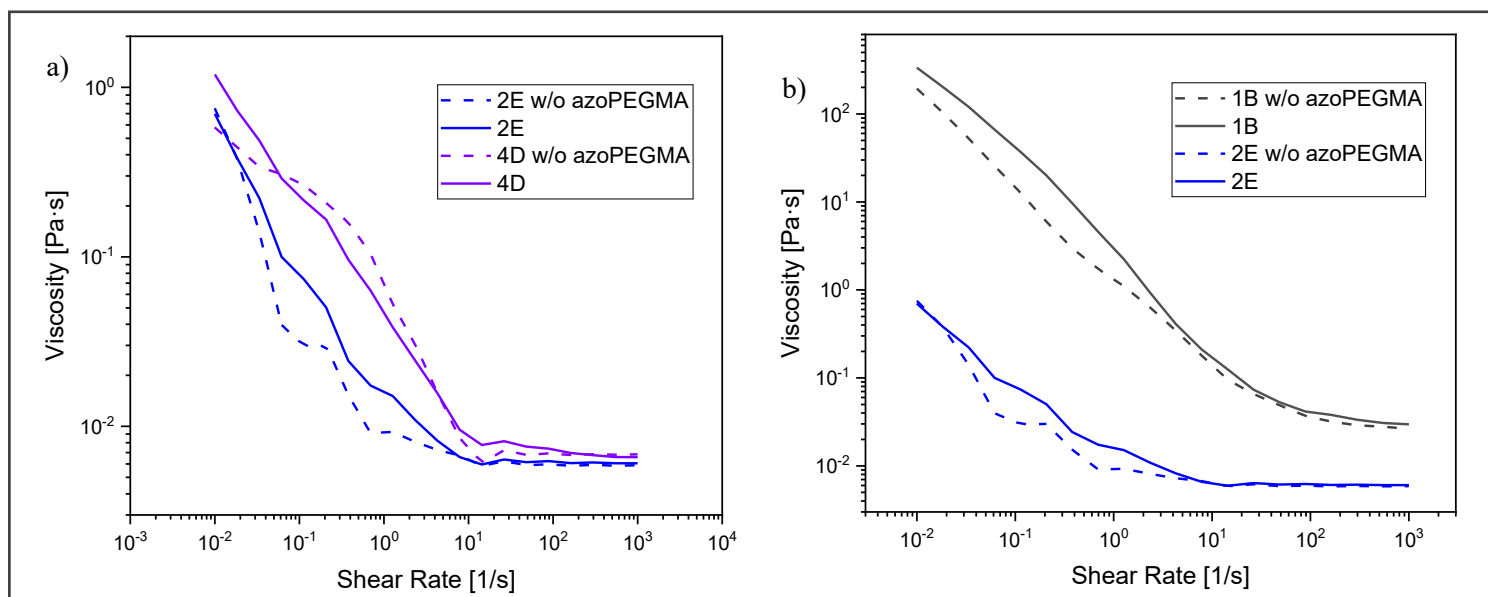
Figure 33 (a) Viscosity curves of formulations on formulations with and without PEGDA. (b) Viscosity comparison between formulation with 26% w/w PEGMEMA (1E) and 50% w/w PEGMEMA (1B). Dotted line represents formulation without azoPEGMA. Solid line represents formulation with azoPEGMA

On the other hand, amplitude sweep tests were less significant, since some points were outside the range of the sensitivity of the rheometer due to low viscosity of those formulations. However, it was still possible to consider a value of 10% of strain as part of the LVE region. (Fig. 34)
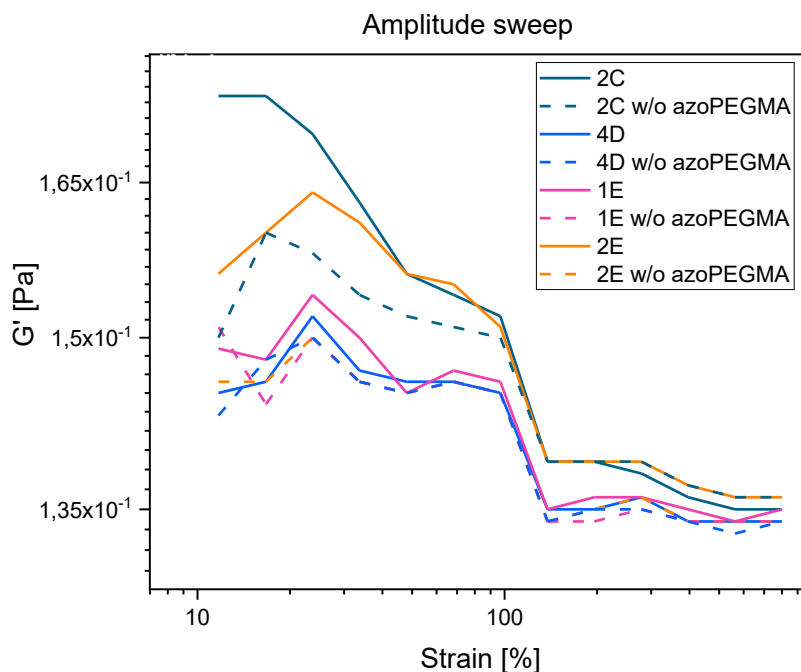

Figure 34 Amplitude sweep on formulations 2C, 4D, 1E, 2E. Solid line represents fomulation with azoPEGMA. Dotted line represents formulation without azoPEGMA

Having assessed the right parameters, photorheology tests were performed (Fig. 35, Fig. 36), the most relevant data are reported in Table 6.

Table 6 Relevant rheological data of formulations.

| Formulation's name	PEGDA [w/w]	PEG-BAPO [phr]	Delay time	Gel point value	Time for reaching gel-point	Final G'
2C_No azoPEGMA	0%	0.75	20 s	X	X	44.2 Pa
4D_No azoPEGMA	0%	0.25	23 s	22.2 Pa	46 s	404.8 Pa
1E_No azoPEGMA	2%	0.75	19 s	13.3 Pa	46 s	3969.7 Pa
2E_No azoPEGMA	2%	0.25	17 s	13 Pa	35 s	4074.5 Pa
2C	0%	0.75	30 s	28.9 Pa	72 s	155.1 Pa
4D	0%	0.25	37 s	2.9 Pa	46 s	637.1 Pa
1E	2%	0.75	27 s	5.9 Pa	41 s	6214.9 Pa
2E	2%	0.25	36 s	1.5 Pa	47 s	3412.3 Pa
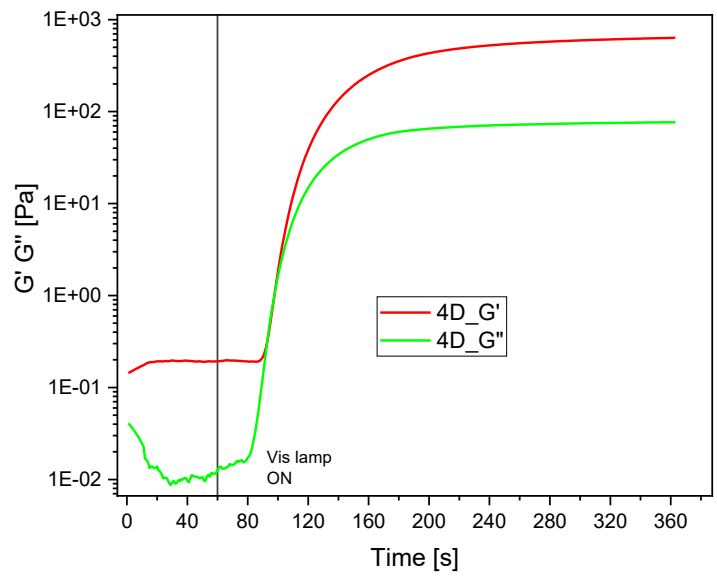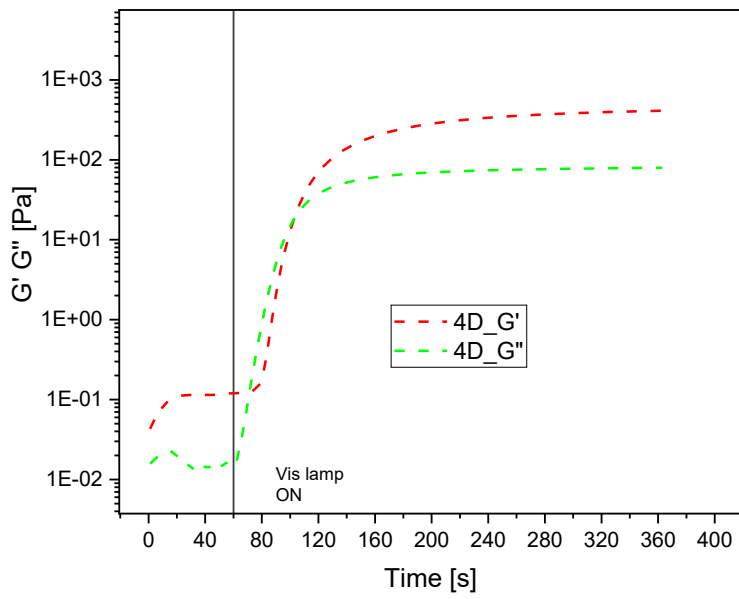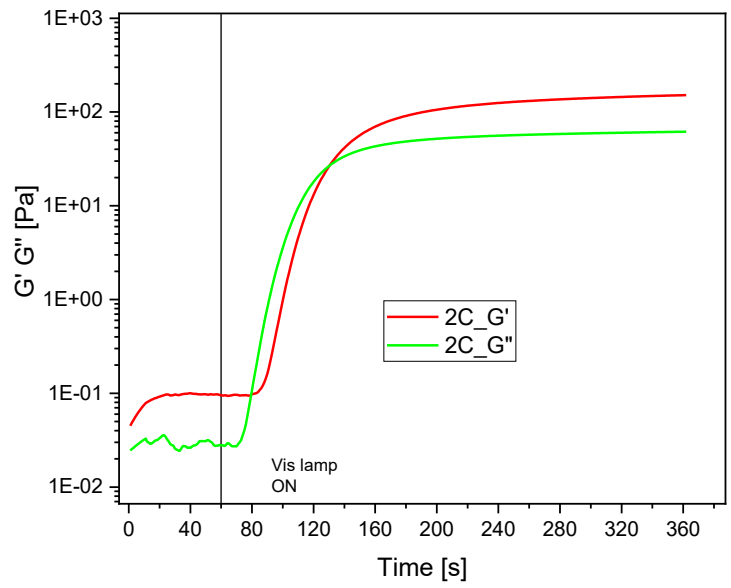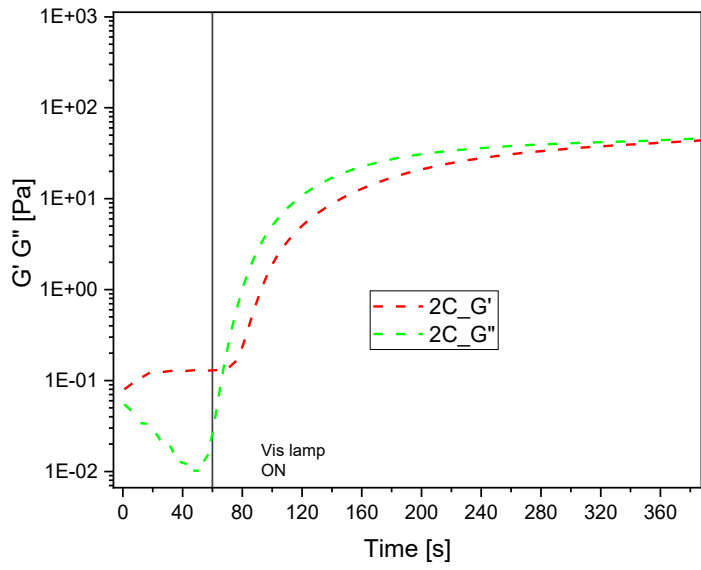
Figure 35 Photorheology of formulation without PEGDA. Solid line represents formulation with azoPEGMA. Dotted line represents formulation without azoPEGMA.
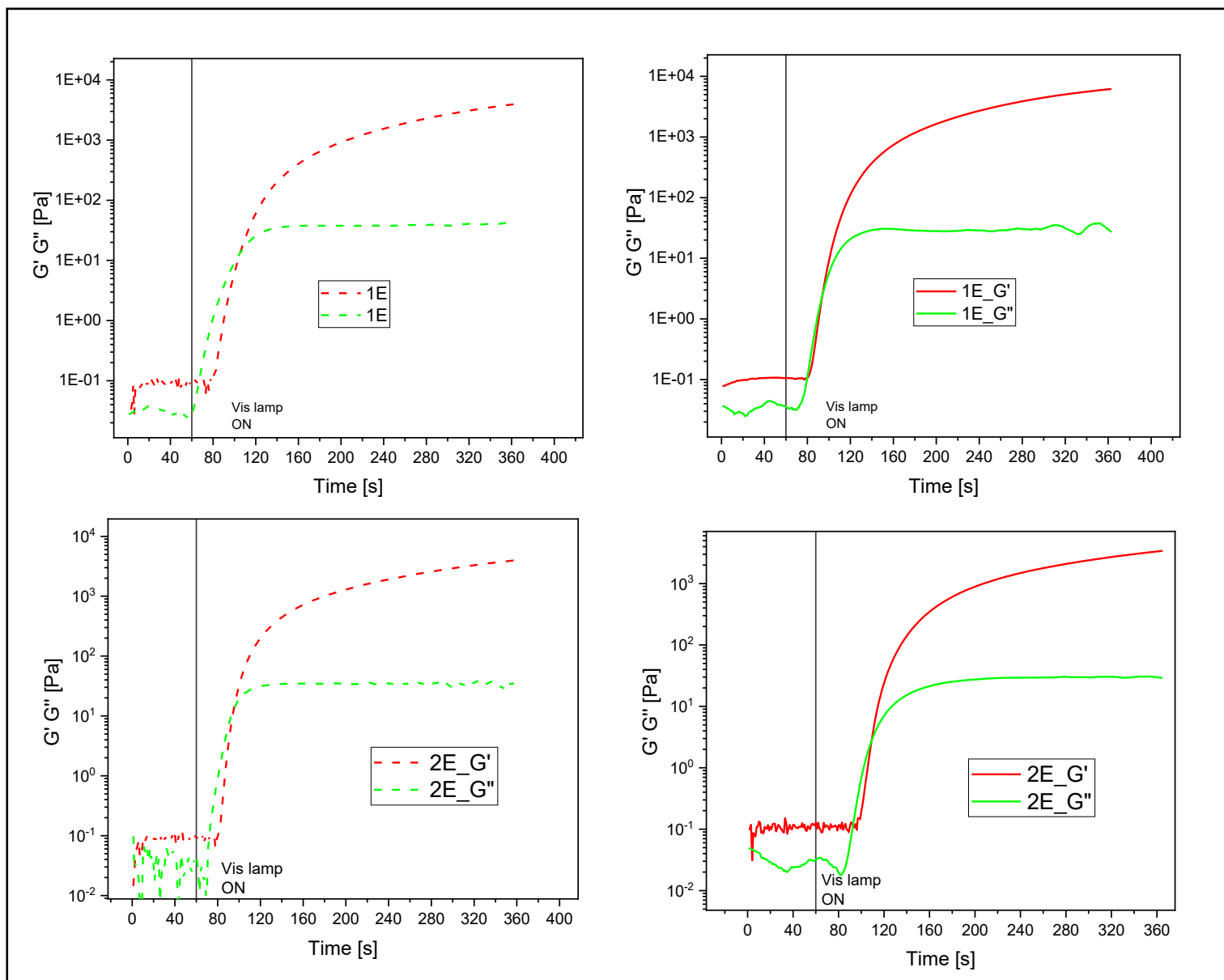
Figure 36 Photorheology of formulation with PEGDA. Solid line represents formulation with azoPEGMA. Dotted line represents formulation without azoPEGMA.

Observing the graphs, it emerges immediately that all the formulations containing PEGDA have plateau value of G' higher than the formulations without it (Fig. 37a); as previously mentioned, this can be related to the formation of chemical cross-links. Then, the effect of PEG-BAPO amount was analysed, comparing formulation without PEGDA and without azoPEGMA (2C, 4D, Fig. 37b). In this case, delay times are comparable, meaning that the quantity of photoinitiator does not influence consistently the kinetics of photopolymerization; on the other hand, the formulation with higher amount of photoinitiator resulted softer. (final G' is lower in 2C formulation). This could be explained considering that a greater quantity of PEG-BAPO led to a higher initiation rate, but also to a higher probability of termination, therefore the average molecular weight of macromolecules may result lower, leading to lower mechanical properties. As previously

mentioned, when PEGDA is present (1E, 2E with no azoPEGMA Fig. 37c), the final G' values increase, maintaining delay times. On the other hand, when adding azoPEGMA, different considerations should be taken, in particular focusing on formulations 1E and 2E (Fig. 37d). In those cases, the effect of the PEG-BAPO content is evident, allowing for a significant increase of G' value. This can be explained considering that azoPEGMA competes in light absorption with the photoinitiator, therefore a higher concentration is required for having effective photopolymerization. Furthermore, it cannot be excluded that the presence of these additional molecules increases the mechanical properties due to some hindering effect on chains mobility. This is immediately evident comparing formulation 2C with and without (Fig. 37e) azoPEGMA: without azoPEGMA, the formulation doesn't photopolymerize, but when azoPEGMA is added, a photopolymerization occurs, even if the gel remains very soft.

This competition effect can be also observed comparing the delay times: all the formulations containing azoPEGMA have a longer delay time (see table 6), meaning that they are generally less photo-reactive. However, also the azoPEGMA/PEG-BAPO ratio can affect this behaviour. 2E formulation, which has less photoinitiator, is less reactive than 2E without azoPEGMA (Fig 37f), while 1E formulation, which contains more PEG-BAPO, has a comparable delay time with 1E without azoPEGMA (Fig. 37g). Finally, 2E formulation, having less photoinitiator, is less reactive than 1E in presence of azoPEGMA (Fig. 37h), while when azoPEGMA isn't present, the delay time is comparable, as already evidenced. (Fig 37i)
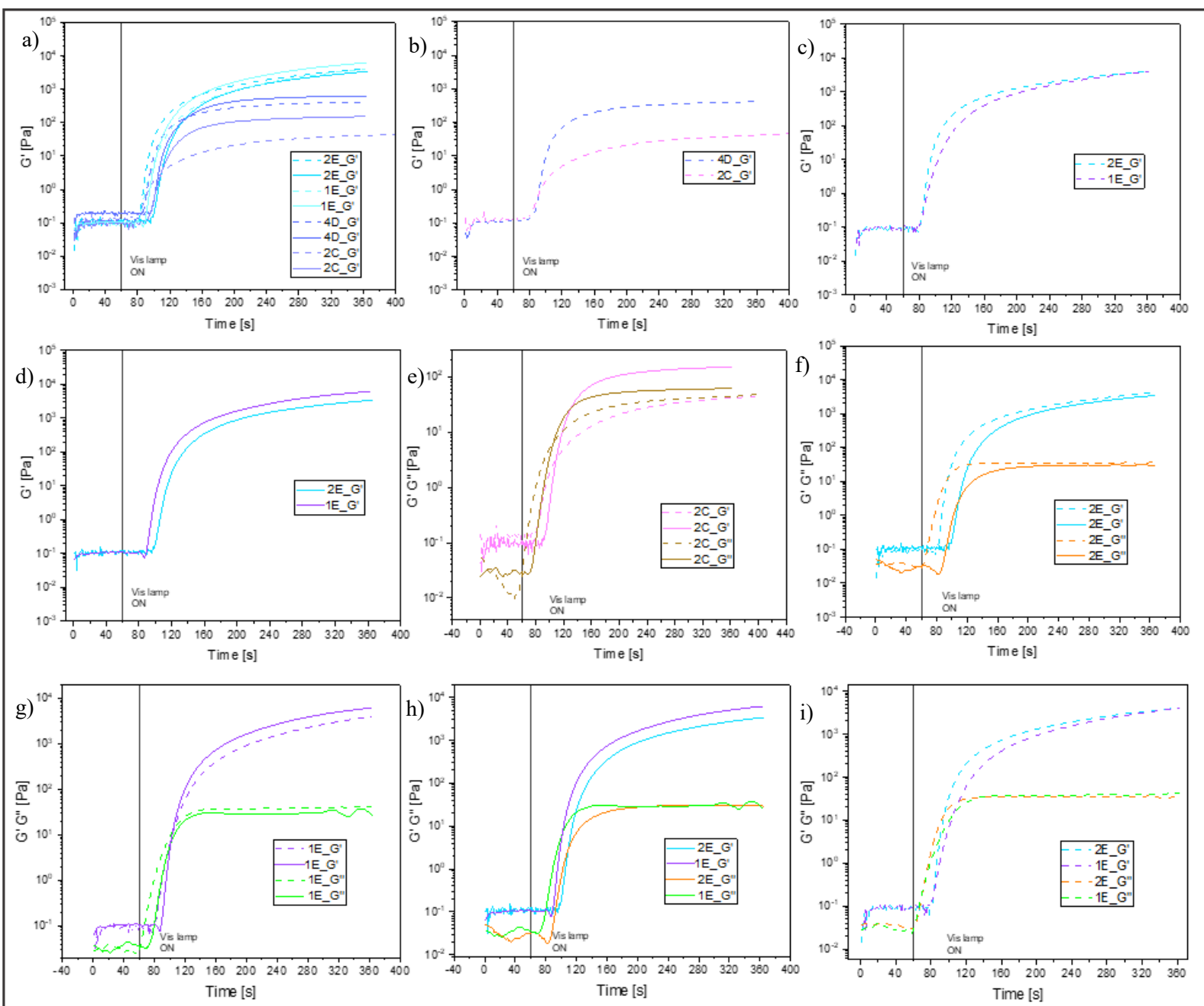
Figure 37 Comparison between: (a) Formulations with PEGDA (blue lines) and without PEGDA (violet lines) (b) Formulation without PEGDA and azoPEGMA (c) Formulation with PEGDA and without azoPEGMA (d) Formulation with PEGDA. (e) Formulation 2C with and without azoPEGMA and difference in polymerization. (f),(g),(h),(i) Comparison between behaviour in photopolymerization with and without azoPEGMA. Solid line represents formulations with azoPEGMA. Dotted line represents formulation without azoPEGMA.

In conclusion, to fabricate hydrogels that can be easily manipulated, it was decided to continue the investigations with the formulations containing PEGDA. This study also demonstrated that in presence of azoPEGMA a higher concentration of PEG-BAPO is advisable: this is the reason why further analyses will be mainly performed on formulation 1E.

3.7.FT-IR SPECTROSCOPY

Polymerization was further investigated through FT-IR Spectroscopy both on formulation 1E (Fig. 38a) and 1E without azoPEGMA (Fig. 38b). To assess the polymerization process, the peak around 810 cm^{-1} was followed as it is correlated with the acrylate group.[83] As reference peak, carbonyl group around 1720 cm-1 was taken. Finally, it must be noted that all those tests were performed on dried samples, since the presence of water affects FT-IR measurements.

Formulations were polymerized and then UV-irradiated to assess the polymerization degree.
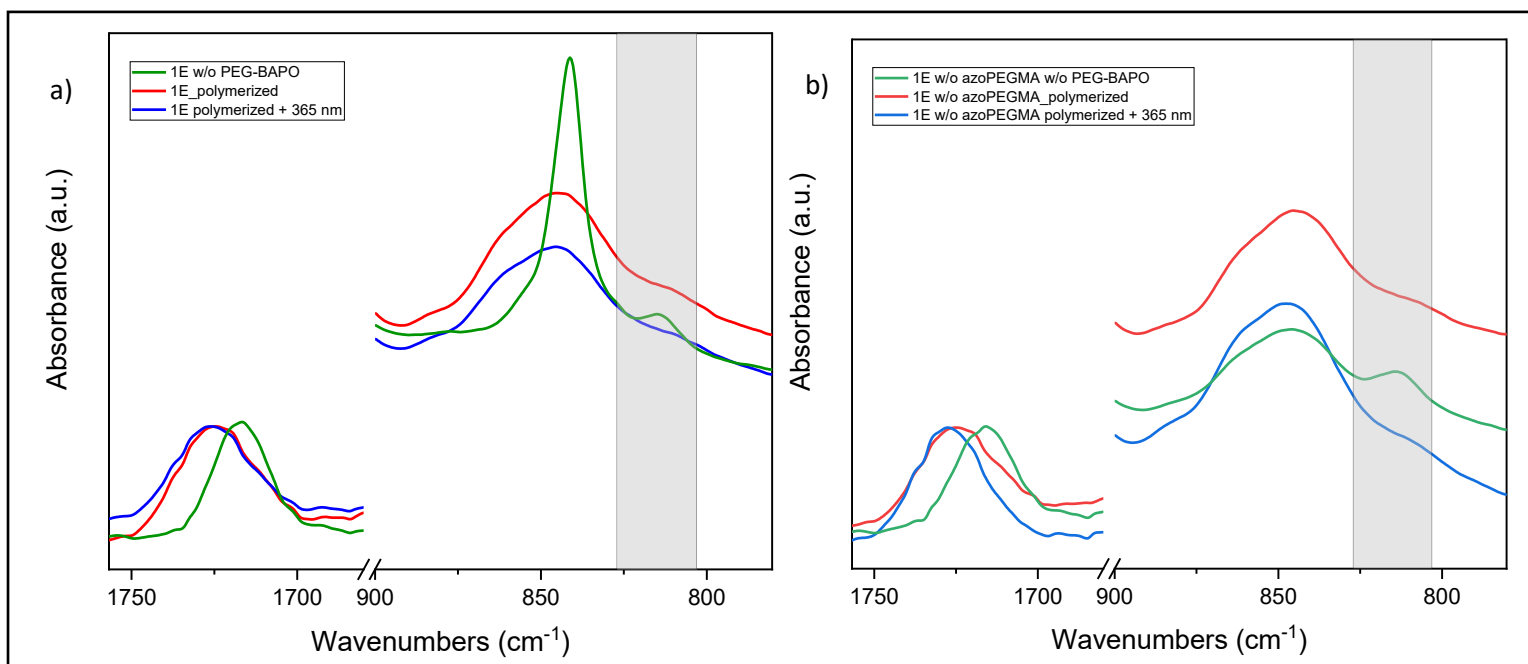

Figure 38 FT-IR spectrum of 1E formulation (a) with and (b) without azoPEGMA

In Table 7, the conversion of acrylates following irradiations compared to samples not irradiated is summarized.

Table 7 Conversion of acrylates following irradiation.

Formulation's name	After irradiation at 420nm	After irradiation at 420nm AND 365nm
1E without azoPEGMA	93%	95%
1E (with azoPEGMA)	65%	76%

It is noteworthy that the formulation without azoPEGMA already shows a good photopolymerization degree after VIS irradiation, and a following UV irradiation does not influence the conversion.

On the contrary, formulation with azoPEGMA reaches only 65% of photopolymerization degree with the 420nm irradiation. Furthermore, UV irradiation, which in the initial idea should just act as a trigger to the isomerization, also increase conversion degree up to 76%.

This outcome is in good agreement with the photorheology results, as the presence of azoPEGMA interferes and slows down the photopolymerization process due to a competition process of light absorption. On the other hand, lower conversion degree somehow highlights the hindering effect related to the presence of the azocompounds. In fact, the hydrogels with those molecules showed higher mechanical properties but with lower conversion, meaning that chain mobility is affected by the same structure of the macromolecule.

Through FT-IR analysis, the presence of azoPEGMA can be also verified. Although azoPEGMA concentration is rather low, a peak at 1175 cm^{-1} was spotted , probably associated to the C=N bond. (84,85)

As shown in Fig.39, this characteristic peak presents in the azoPEGMA spectrum, can also be noticed in 1E formulation, but not in formulation without azoPEGMA.
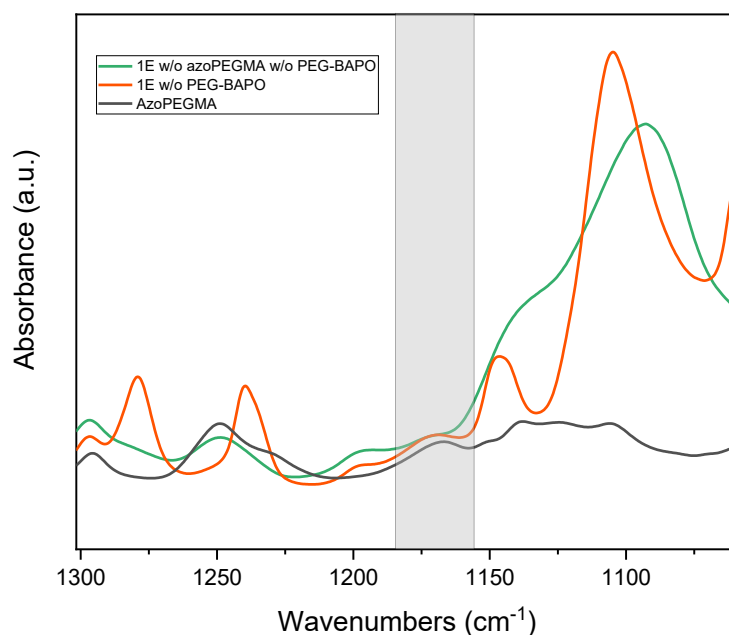
Figure 39 FT-IR spectra of azoPEGMA and 1E formulation, with and without azoPEGMA

3.8. PHOTOISOMERIZATION AND DEGRADATION ANALYSIS

In this paragraph, the analyses performed to investigate whereas azoPEGMA molecules preserve the ability to photoisomerize both in the liquid solution and in the hydrogel are reported.

The UV-VIS spectra of formulation 1E without PEG-BAPO are shown in Fig 40a.

It is possible to notice peaks' variations: when irradiated with UV light (wavelength 365nm), the peak in the UV region (350 nm) disappears, while a peak in the visible region appears (440 nm). The formulation was then exposed to visible light (wavelength 450nm): the peak in the vis region disappears while a peak at 350 nm is present again. This behaviour is consistent with the characteristic features of AzoPeg, that was demonstrated to show light-triggered E-to-Z transition. (33) In this set of experiments, a second UV irradiation was performed to assess the spontaneous reverse photoisomerization overnight, which occurred since final spectrum is totally superimposable to the initial one.

Remarkably, the tested formulation was opaque before irradiation, indicating the presence of micelles; after UV irradiation, and therefore in presence of the Z-azoPEGMA isomers, the formulation becomes clear. After visible irradiation it becomes opaque again. (Fig. 40b) This confirms not only the ability of azoPEGMA

molecules to form micelles when dispersed in a photocurable formulation, but also their capacity to be light-controllable. Light scattering related to micelles formation will be better investigated in chapter 3.12.2.
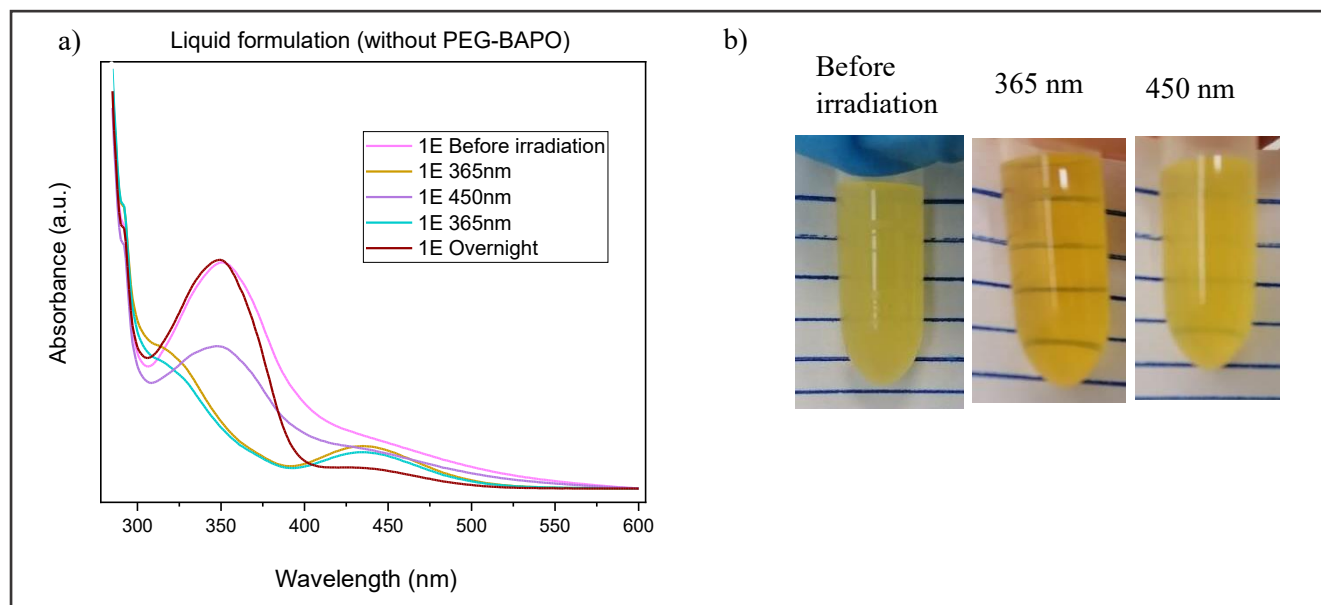

Figure 40 (a) Uv-vis spectroscopy on formulation 1E without PEG-BAPO. (b) Turbidity of 1E liquid formulation following irradiations.

To assess the photostability of azoPEGMA molecule in the photocurable solution, 1E formulation was tested under two different degradation conditions: (i) prolonged exposure to both UV and visible light and (ii) several isomerization cycles.

(i) Experiments were carried on as explained in paragraph (2.4.6.2). Firstly, the formulation was irradiated with UV light up to 30minutes. Results are shown in Fig. 41a.

Isomerization process is presumably completed in the first 3 minutes of light exposure, since no difference can be seen in the spectrum between 3 minutes and 30 minutes of irradiation. These results are in good agreement with previously published studies. (82)

Then, the same test was conducted using visible light. The results are reported in Fig. 41b. A Z-to-E transition occurs in few minutes, as witnessed by UV-vis spectra. This analysis was extended up to 7 hours to ensure that azoPEGMA did not degrade even when subjected to prolonged irradiation. The stability of the peak suggests that degradation doesn't occur.
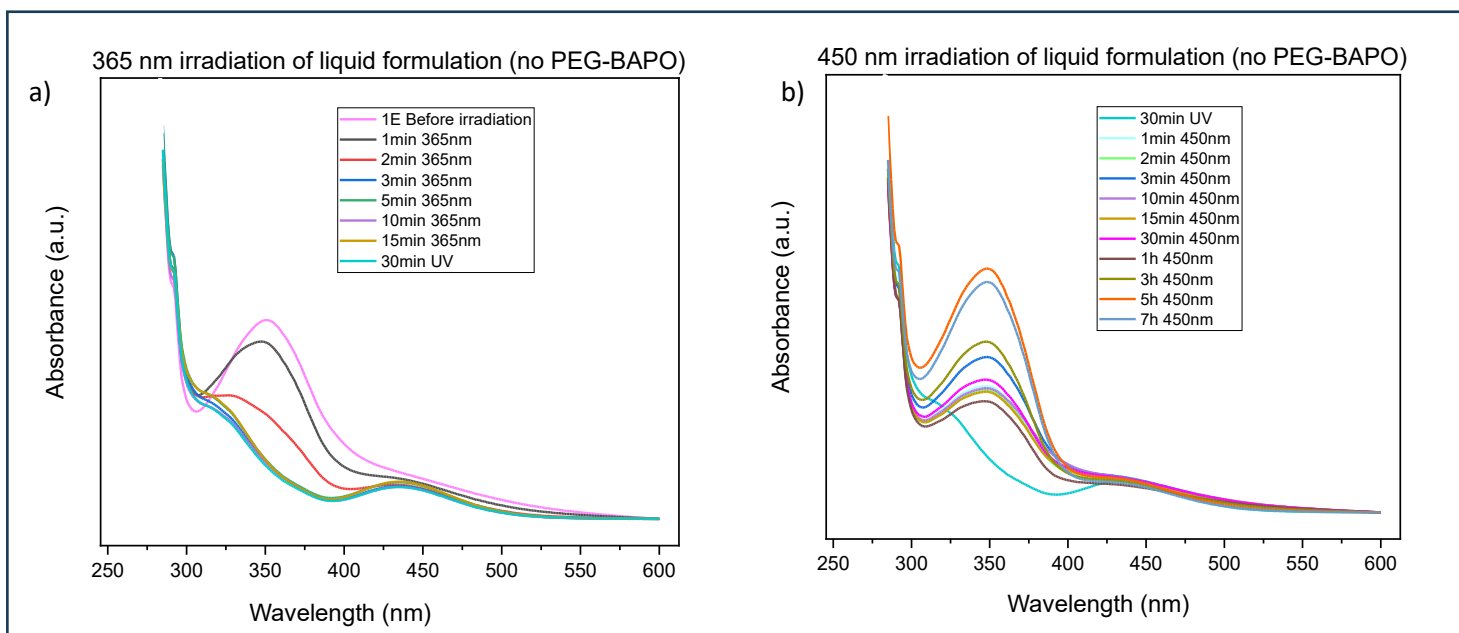
Figure 41 Uv-vis spectroscopy folloqing prolonged (a) UV irradiation (365 nm) and (b) visible irradiation (450 nm)

(ii) Then, several cycles of irradiation were repeated: the spectra obtained are depicted in Fig. 42. Consistently with literature (33), it can be stated that azoPEGMA is able to withstand multiple isomerization cycles without degrading.
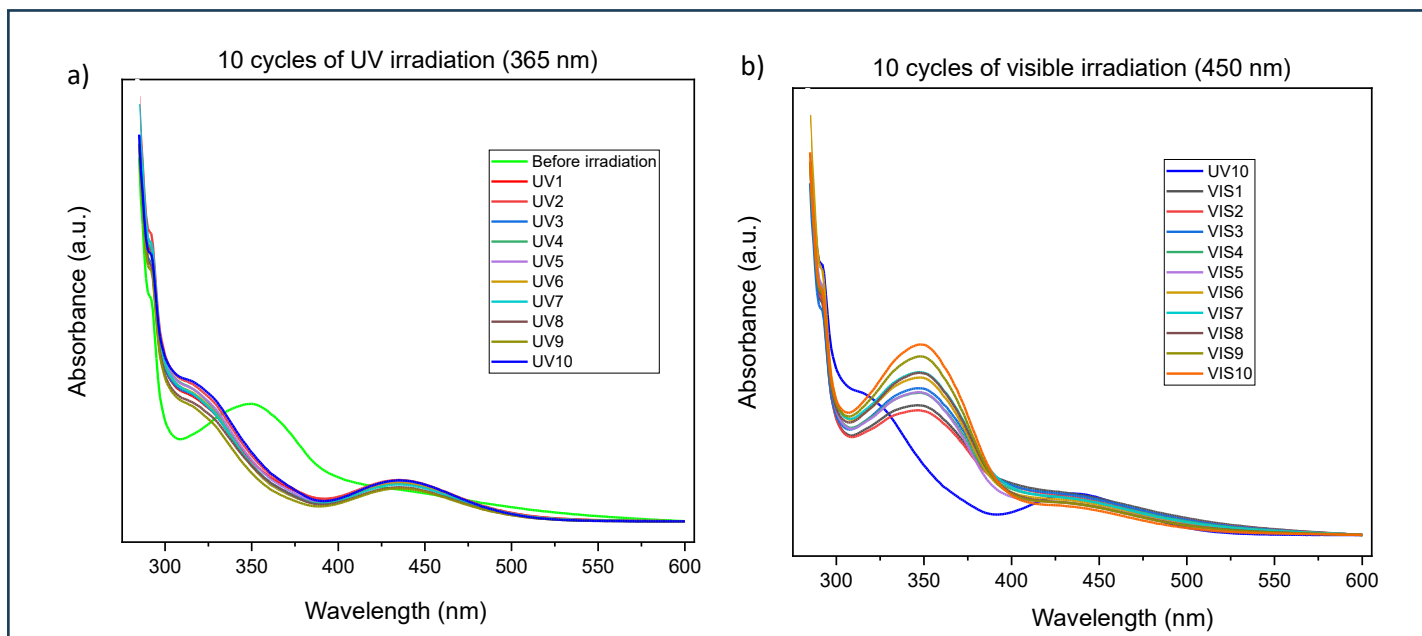

Figure 42 Uv-vis spectroscopy of several cycles of irradiation. (a) Spectra obtained following UV irradiation (365 nm) and (b) VIS irradiation (450 nm)

Ascertained that azoPEGMA effectively maintained its characteristic photoisomerization in liquid formulation, this thesis work focused on verifying that this also occurred in hydrogels.

Formulation 1E has been polymerized and irradiated following the methodology reported in chapter 2.3.

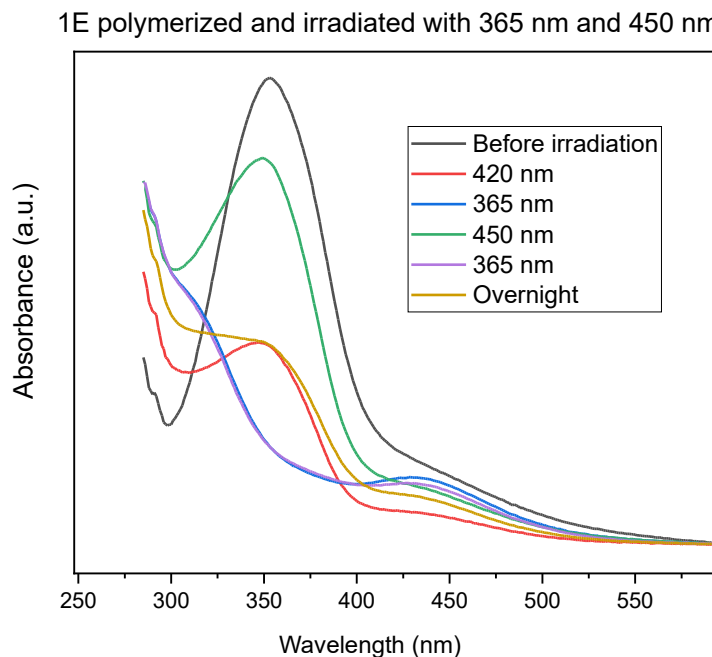The spectra obtained after the subtraction of reference's signal are reported in Fig. 43.

1E polymerized and irradiated with 365 nm and 450 nm

Figure 43 Spectra of formulation 1E polymerized and irradiated. 420nm with a dose of 1.1*10^5 J/s, 365nm with 2.2*10^5 J/s, 450nm with 8.1*10^5

The spectra collected clearly evidence that azoPEGMA photoisomerizes even in the hydrogel, witnessed by the presence of the peaks described above. Interestingly more than one cycle can be done without showing differences. It must be highlighted that in this case the test was not extended longer or for multiple cycles since the tested polymerized hydrogel loss water overtime (see paragraph 3.11.1.1) and therefore robust measurements cannot be performed.

As for the liquid formulation, even in the hydrogel the Z-to-E isomerization occurs simply leaving the sample in dark overnight.

The same analysis was conducted varying the doses of irradiation to investigate whether this would affect the outcome: as shown in Fig. 44, the isomerization was still present.
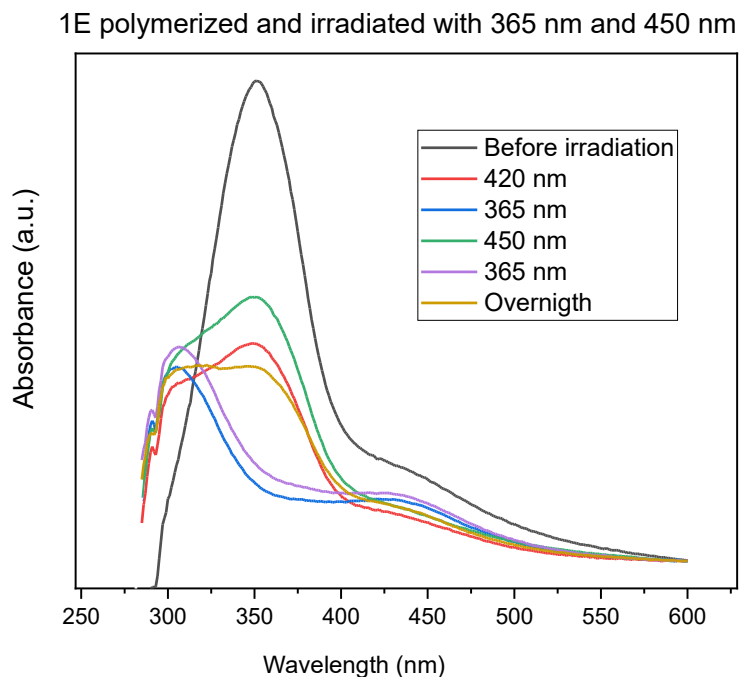
1E polymerized and irradiated with 365 nm and 450 nm

Legend:
- Before irradiation
- 420 nm
- 365 nm
- 450 nm
- 365 nm
- Overnigth

Figure 44 Spectra of formulation 1E polymerized and irradiated. 420nm with a dose of $1.1*10^5$ J/s, 365nm with $4.4*10^4$ J/s, 450nm with $1.6*10^5$. The reference signal in subtracted.

Although these spectra confirmed the azoPEGMA's photoswitching capacity in hydrogels, it must be noted that, after polymerization, the peak in UV region does not reach the pristine values, neither leaving the formulation overnight nor irradiating them with vis light (wavelength 450nm). In this sense it can be hypothesized that this is related to the breaking of micelles, as confirmed later.

3.9.PHOTOISOMERIZATION KINETIC ANALYSIS

From azoPEG's characterization (33) in an aqueous solution, it reported that after the photoinduced E-to-Z isomerization, a reverse transition (Z-to-E) should spontaneously occur in 168 hours, leaving the sample in the dark and at 35°C.The kinetic analysis of this reverse isomerization in the hydrogel was therefore tested.
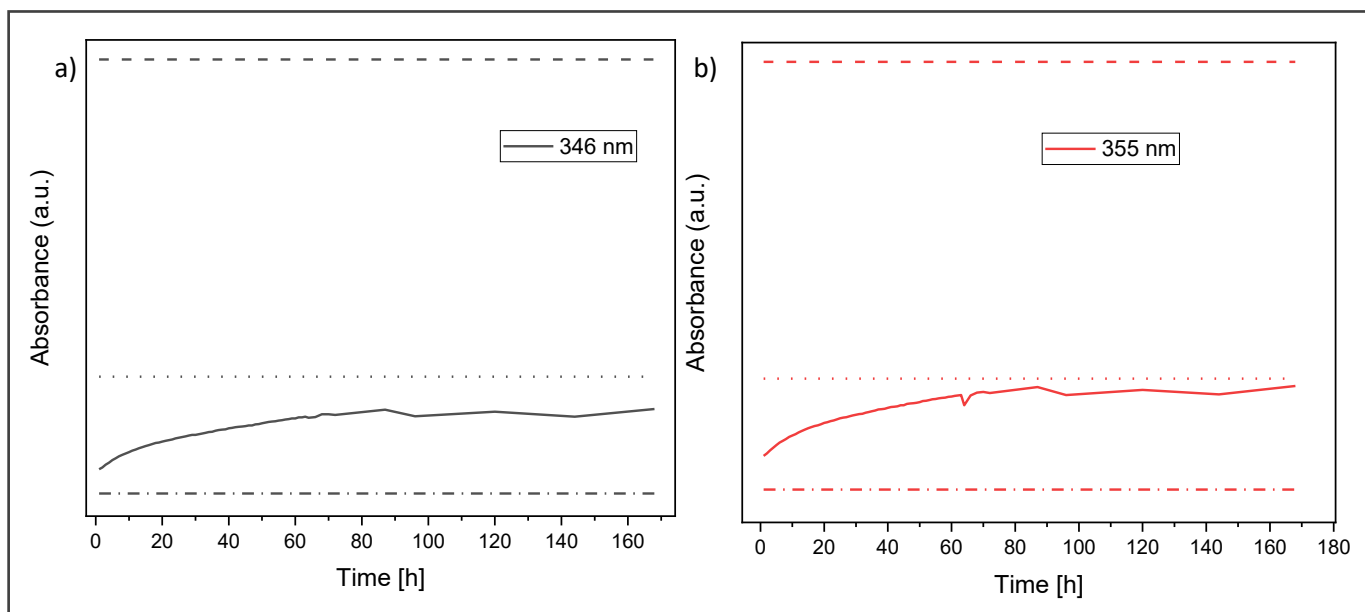
The result is shown in Fig. 45.

Figure 45 Absorbance changes recorded at (a) 346 nm and (b) 355 nm of 1E polymerized formulation at 35°C showing the kinetic of the thermal back reaction to E-azoPEGMA. Solid line represents the absorbance of the sample along the hours, dashed line represents absorbance value before irradiation, dotted line represents the value of absorbance after polymerization (irradiation with 420nm light) and dash-dotted line represents the value of absorbance immediately after UV irradiation. Reference signal is subtracted.

The absorbance value at 346nm and 355nm rises over time, indicating that the peak is forming again after the E-to-Z isomerization, and so that the quantity of E-azoPEGMA is increasing compared to Z-azoPEGMA, as expected. However, differently from neat azoPEG (33), it is evident that this peak is unable to regain either its original value, before irradiation (dashed line), nor its value obtained following polymerization (dotted line). Although it can't be excluded a slight data distortion due to a possible small evaporation, it is reasonable to state that some phenomena occur during the polymerization process, e.g. degradation. These would prevent the azoPEGMA from completing the reverse isomerization (Z-to-E).

3.10. INVESTIGATION ON A POSSIBLE RADICAL DEGRADATION

To investigate these possible phenomena, a formulation of H_2O, azoPEGMA, and PEG-BAPO was irradiated with 420nm light to simulate polymerization. Macroscopically, the formulation loses its typical yellow colour (Fig. 46a) and the presence of intense yellow "agglomerates" can be glimpsed. In Fig. 46b is reported a 25X magnification.
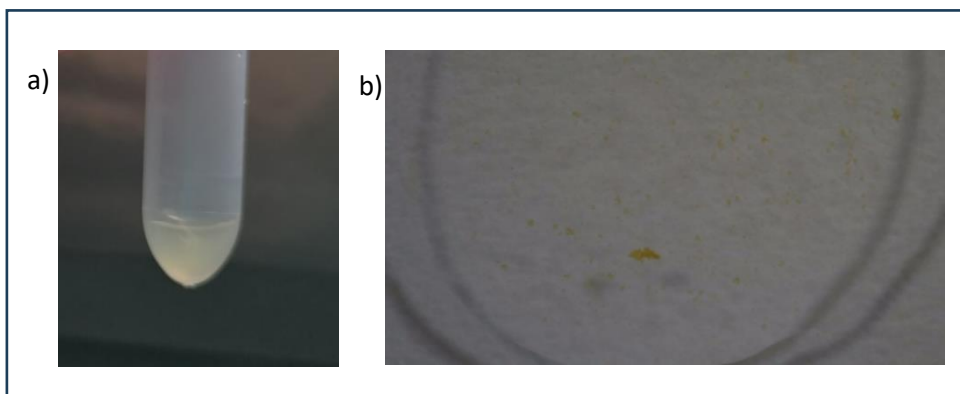
Figure 46 (a) Formulation of H2O, azoPEGMA and PEG-BAPO irradiated with 420nm light and (b) 25X magnification.

UV-VIS spectroscopies were performed on this solution, even after a cycle of irradiation. The results are reported in Fig. 47.
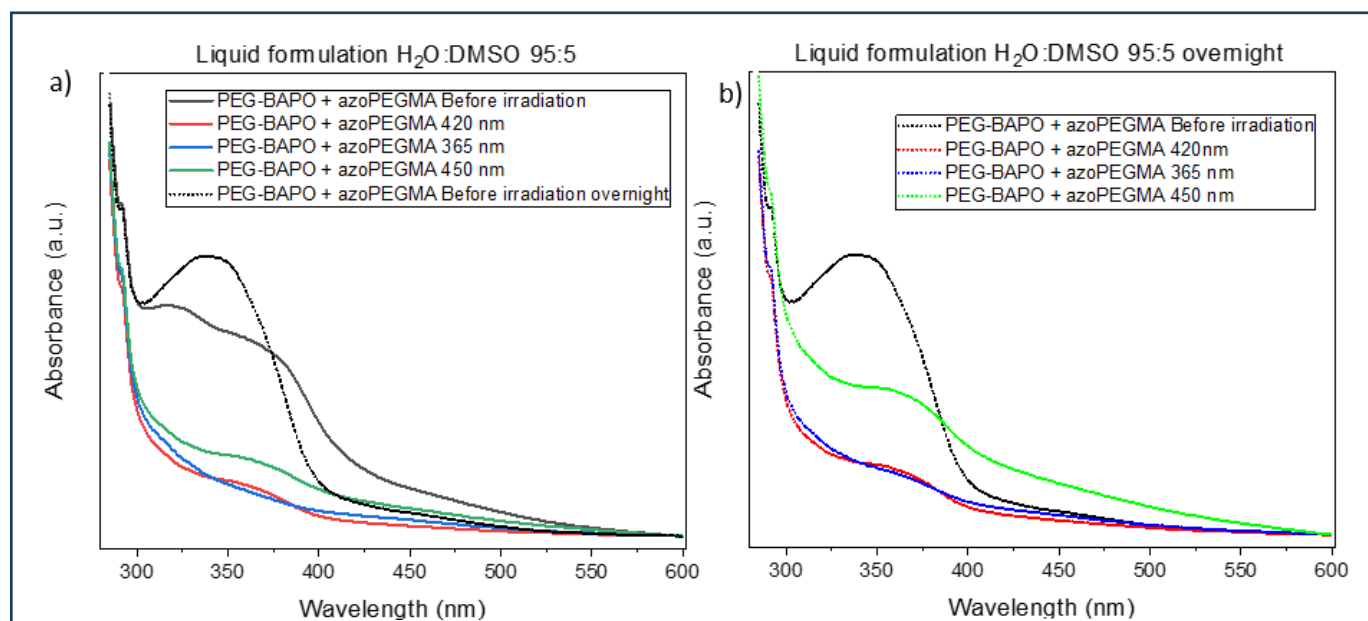

Figure 47 (a) UV-vis spectra of a 95:5 H2O:DMSO formulation composed of PEG-BAPO and azoPEGMA following irradiation and (b) overnight.

After the 420nm irradiation, both E-azoPEGMA and Z-azoPEGMA spectra lose their characteristic peaks, which are not recovered even after the night.

This could probably be due to the fact that azoPEGMA molecules polymerized, forming these aggregates. Consequentially, Uv-vis spectra are not able to collect them due to the inhomogeneity of the solution. These aggregates remain stable even overnight, as demonstrated by the curves collected overnight. The only

exception is the curve related to the formulation not irradiated (black spectrum, Fig. 47b), which loses the typical scattering probably due to solubilization of micelles over time.

Further analysis would be needed, also considering that this behaviour was observed in a liquid formulation and not in the hydrogel environment.

Nevertheless, the aforementioned inability of the peaks to return to their original height during Z-to-E photoisomerization could be consistent with the formation of these aggregates.

3.11. CHARACTERIZATION OF HYDROGEL

Characterizations of the physical properties of the hydrogel obtained were carried out.

3.11.1. WATER UPTAKE

Water uptake was examined through swelling and evaporation rate, both on 1E (PEG-BAPO 0.75 phr) and 2E (PEG-BAPO 0.25 phr) formulations.

3.11.1.1. SWELLING

Looking at the graph as a whole (Fig. 48a), it is noteworthy that hydrogel obtained with the formulation with less photo initiator (2E) has a lower swelling rate, both with and without azoPEGMA.

In hydrogel made of 2E formulation the maximum swelling degree is reached first compared to its respective formulation without azoPEGMA, while in the hydrogel obtained with 1E formulation the opposite behaviour

occurs. (Fig. 48b). Moreover, it can be assumed that both formulations containing azoPEGMA have a higher maximum swelling degree, which is reached in a few hours and remains constant up to 2 weeks.
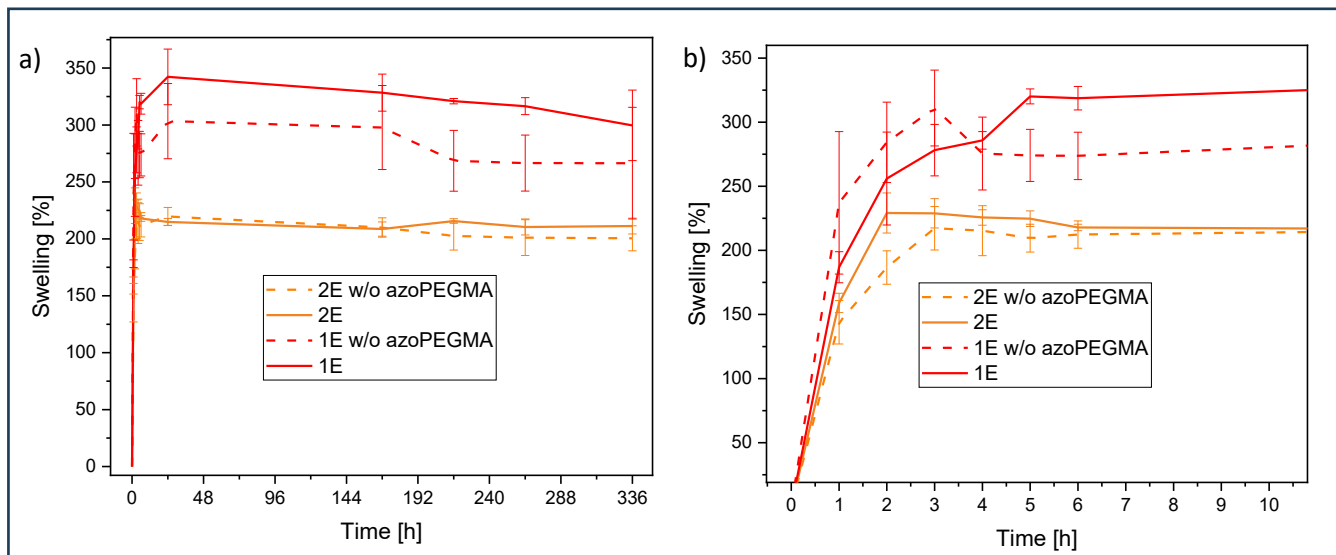

Figure 48 (a) Swelling rate on formulation 1E and 2E. (b) Focus on the first 10 hours of swelling. Solid line represents hydrogel with azoPEGMA. Dotted line represents hydrogel without azoPEGMA

Differently from literature (23), the swelling degree didn't significantly change following the E-to-Z isomerization, as shown in Table 8 and Table 9. As a matter of fact, small variations are evident also in the reference value. It is hypothesized that the presence of methacrylic groups on azoPEGMA molecule may lead to a greater cross-linking density within the hydrogel. This might influence the swelling rate more than the change between hydrophobic and hydrophilic molecule obtained following isomerization.

However, to have a more reliable estimate, it would probably be necessary to evaluate larger samples, (since such small variations are difficult to perceive on small samples.

Table 8 Difference (%) on swelling degree between polymerized hydrogel and polymerized + UV irradiated (365 nm) hydrogel, after different timings from irradiation. The reference is the sample without azoPEGMA

	Polymerized + UV (30min after)	Polymerized + UV (3 hours after)	Polymerized + UV (24 hours after)
1E	1.4 ± 1.2	-10.5 ± 10.1	-13.0 ± 11.4
Reference	-3.1 ± 2.8	2.1 ± 7.8	2.4 ± 4.9

	Polymerized + UV + VIS (30 minutes after)	Polymerized + UV + VIS (3 hours after)	Polymerized + UV + VIS (24 hours after)
1E	-2.9 ± 7.9	-8.3 ± 14.8	-6.5 ± 15.6
Reference	-1.4 ± 1.9	-1.2 ± 1.8	-7.8 ± 1.8

3.11.1.2. EVAPORATION

The hydrogel made of 2E formulation has a lower total evaporation degree compared to 1E formulation, both with and without azoPEGMA. (Fig. 49a) However, the hydrogels obtained with both formulations lose the vast majority of water within 48h. (Fig. 49b)
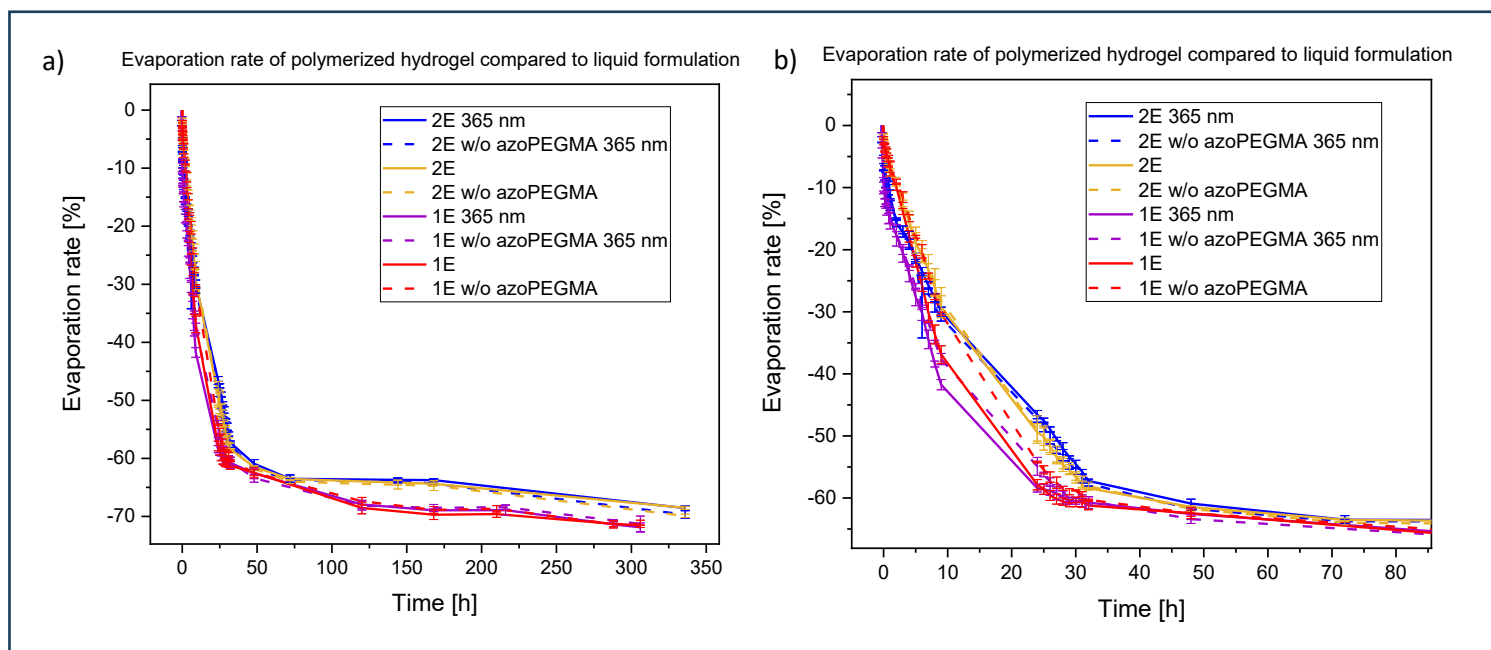

Figure 49 a) Evaporation rate of polymerized hydrogel (eventually further irradiated with 365 nm LED) compared to liquid formulation weight (b) Focus on evaporation rate in the first 80 hours. Solid line represents hydrogel with azoPEGMA. Dotted line represents hydrogel without azoPEGMA.

Furthermore, it is remarkable that the addition of azoPEGMA does not affect the ability of the hydrogel to retain the water (Fig. 50)
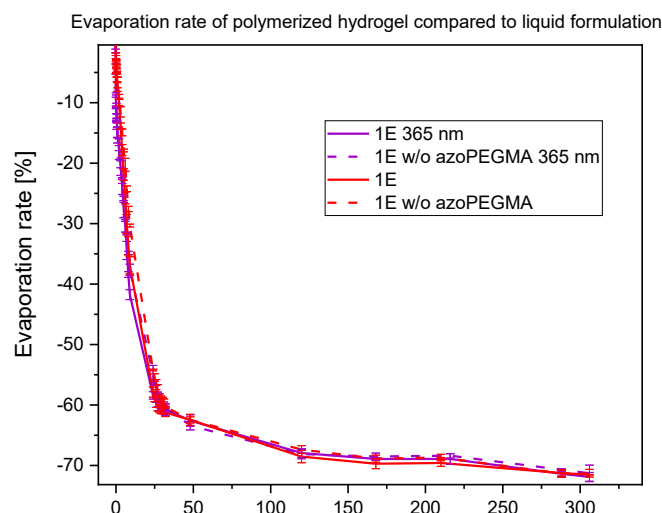
Figure 50 Comparison on the evaporation degree in the absence or presence of azoPEGMA on hydrogel obtained with 1E formulation.

Taking 1E as a reference, it must be highlighted that the evaporation degree, compared to liquid formulations' weight, is initially higher in the formulation with Z-azoPEGMA (Fig. 51a). However, this difference is probably due to the heat produced during the prolonged UV irradiation and not to differences in the hydrogel's network, since this difference is not detectable when evaporation degree is evaluated compared to the last irradiation weight (Fig. 51b).
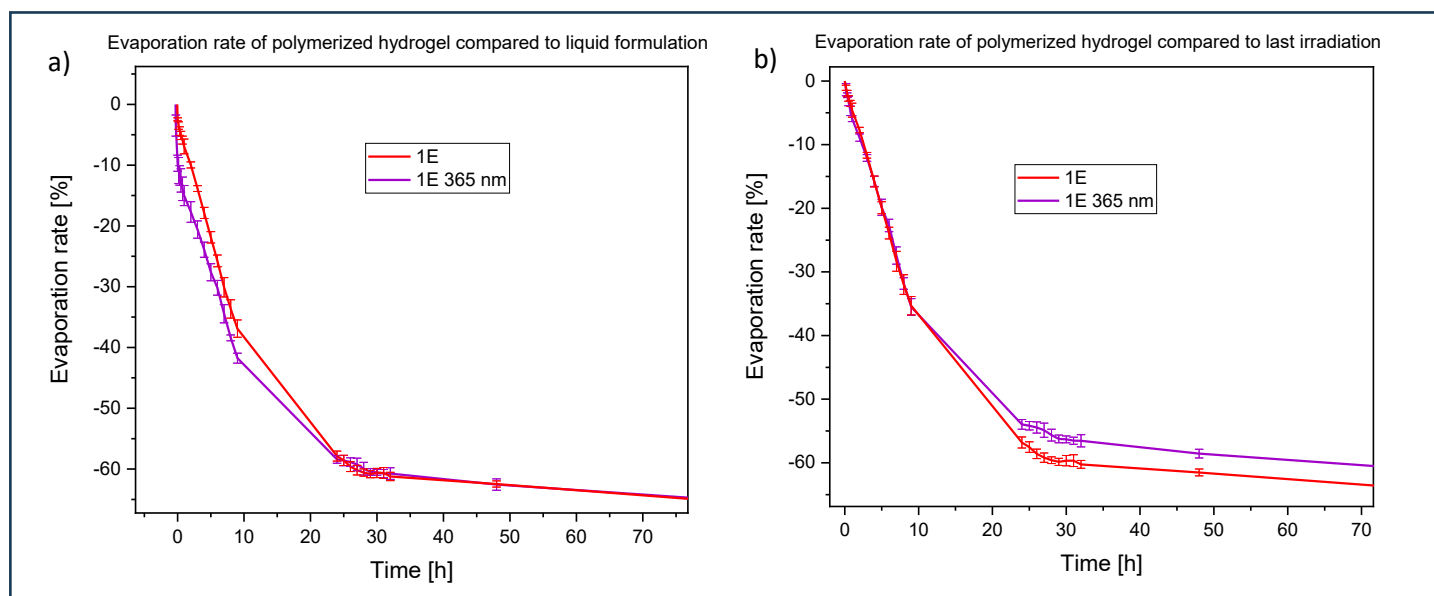

Figure 51 (a) Comparison on evaporation rate compared to last irradiation value or (b) compared to liquid formulation value

3.11.2. COMPRESSION TEST

Mechanical properties were further analysed through compressive stress. In Fig. 52 results on formulation 1E are shown. Both the sigma-epsilon graphs and the medium values are reported. (Fig. 52, Fig. 53)
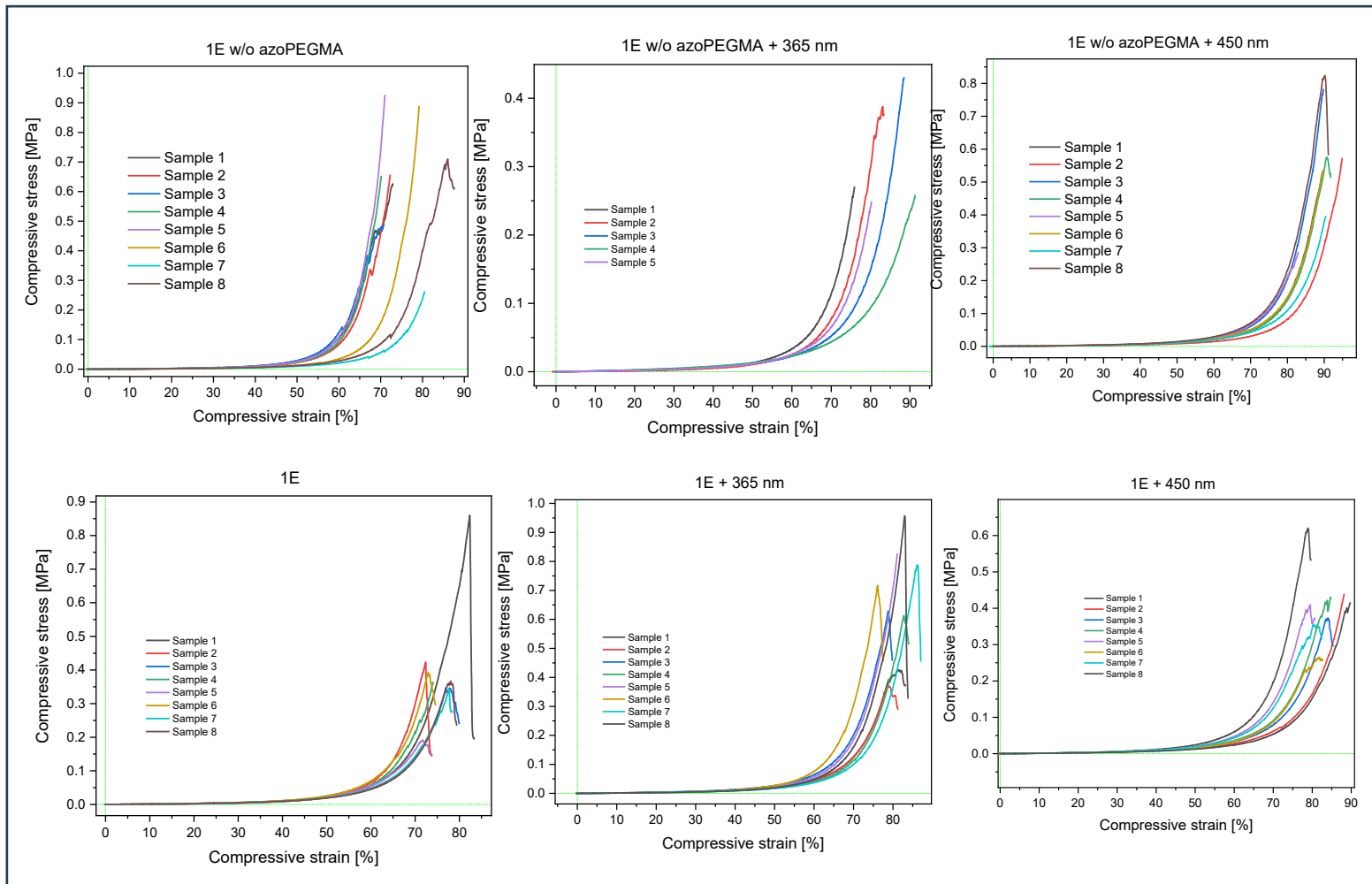

Figure 52 Stress-strain curves on hydrogel obtained with 1E formulation further irradiated with UV (365 nm) or VIS (450 nm) light, both with and without azoPEGMA.
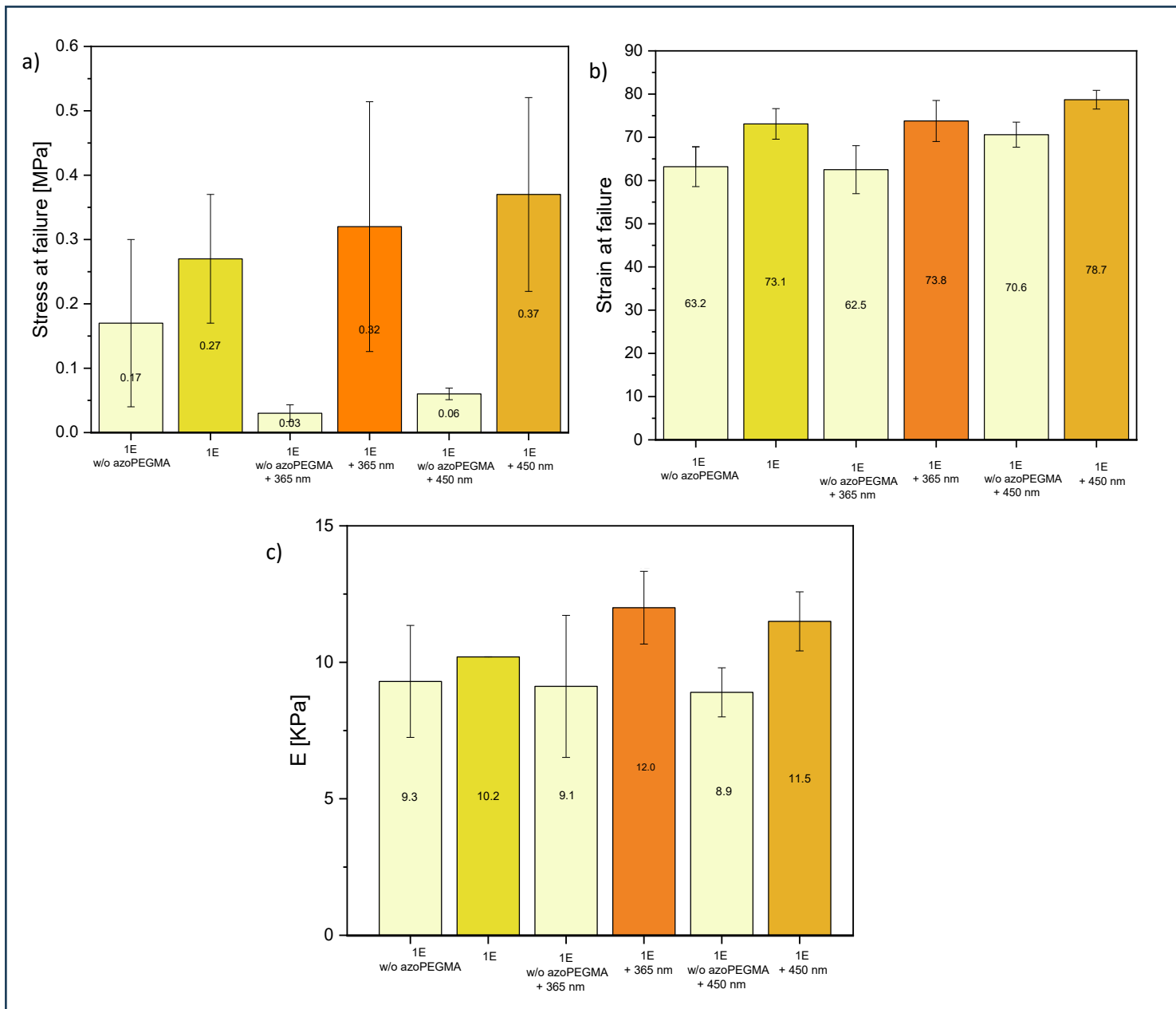
Figure 53 (a) Stress at failure mean value (b) Strain at failure mean value (c) Young Modulus on polymerized hydrogel obtained with formulation 1E with and without azoPEGMA, after UV irradiation and after VIS irradiation.

To evaluate the mean value at failure, the first drop in the compressive stress values was considered (red circle, Fig. 54a) and not the value after which the curve does not increase further (purple circle, Fig. 54a). This choice was made because it was noticed that in some curves this final value was not present, even though the hydrogel was broken at the end of the test.

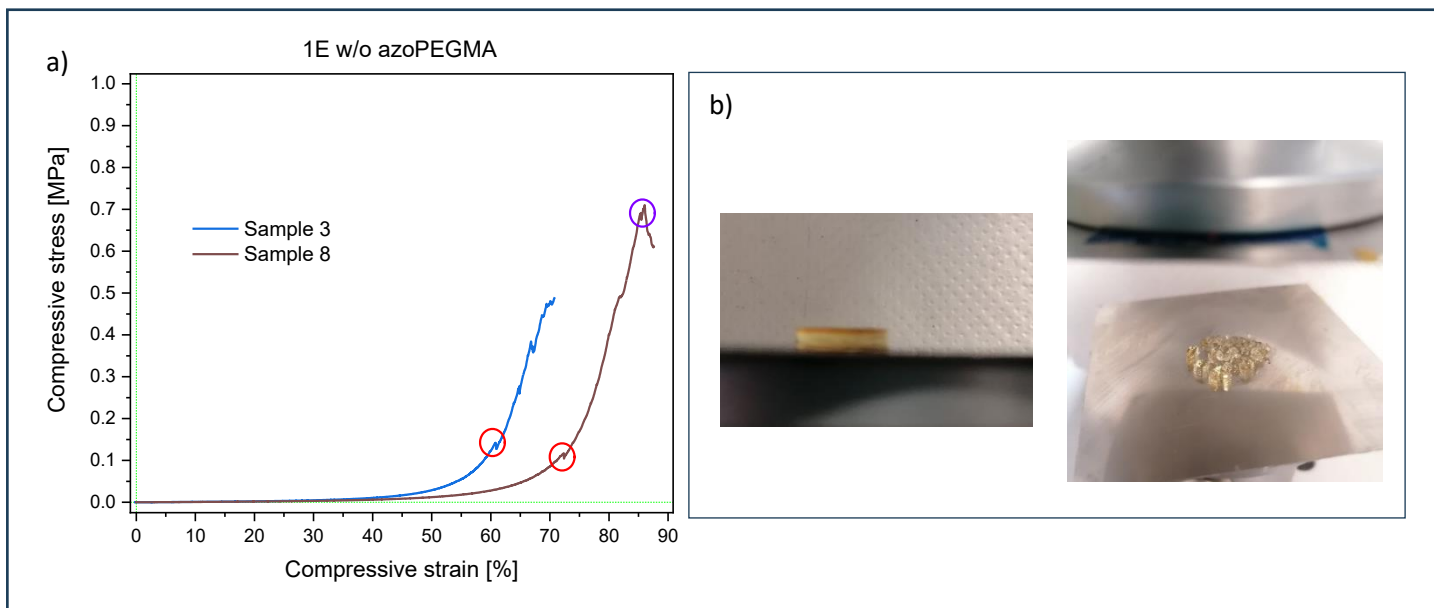*Figure 54 (a) Example of a strain-stress curve. Red circle stands for the considered value at failure. (b) Images of compressive tests.*

The hydrogels obtained, although manageable, are mechanically rather weak. (Fig. 53c, Young modulus)

The rigidity is comparable with cardiac muscle. (86)

No significant differences can be noted analysing both Young's modulus and strain at failure values, neither in the presence/absence of azoPEGMA nor following irradiation. Also stress value at failure in samples containing azoPEGMA remains rather comparable after irradiation, differently from samples without azoPEGMA, whose values following irradiation are significantly lower. (Fig. 53) This may be consistent with the possibility that azoPEGMA forms more entanglements in the hydrogel mesh, and this is in good agreement with photorehology measurements.

3.12. MICELLES ANALYSES

A dye was exploited to simulate the encapsulation and the release of a drug in the liquid formulation, and then in the hydrogel.

In our context, Nile red was selected since its fluorescence emission band changes depending on whether it is encapsulated in micelles (which are a hydrophobic environment, Fig. 55, blue spectrum) or dispersed in the

aqueous environment (Fig. 55, green spectrum). When micelles are photoactively disassembled and thus Nile red is released, its emission band shifts to the red and it is comparable to its emission spectra in water.
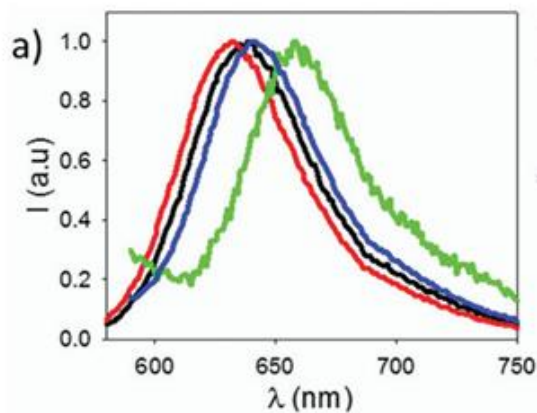
Figure 55 Emission spectra of Nile red following excitation at 540nm (33)

Analyses were effectuated adding Nile red in 1E formulation: the formulation obtained is hereafter named 1EN.

A dye concentration equal to 1mM was chosen to visually investigate the Nile red contribution before and after irradiation. In Fig. 56 the result is reported.

Figure 56 Visual investigation of Nile red contribution to the formulation, before and after irradiation. NR stands for Nile red, PhI stand for photoinitiator (PEG-BAPO), aP stands for azoPEGMA.

The presence of Nile red doesn't affect the azoPEGMA molecule's isomerization properties as demonstrated by UV-vis spectroscopies (Fig. 57). The appearance of a small peak between 550nm and 600nm is characteristic of the dye. (87)

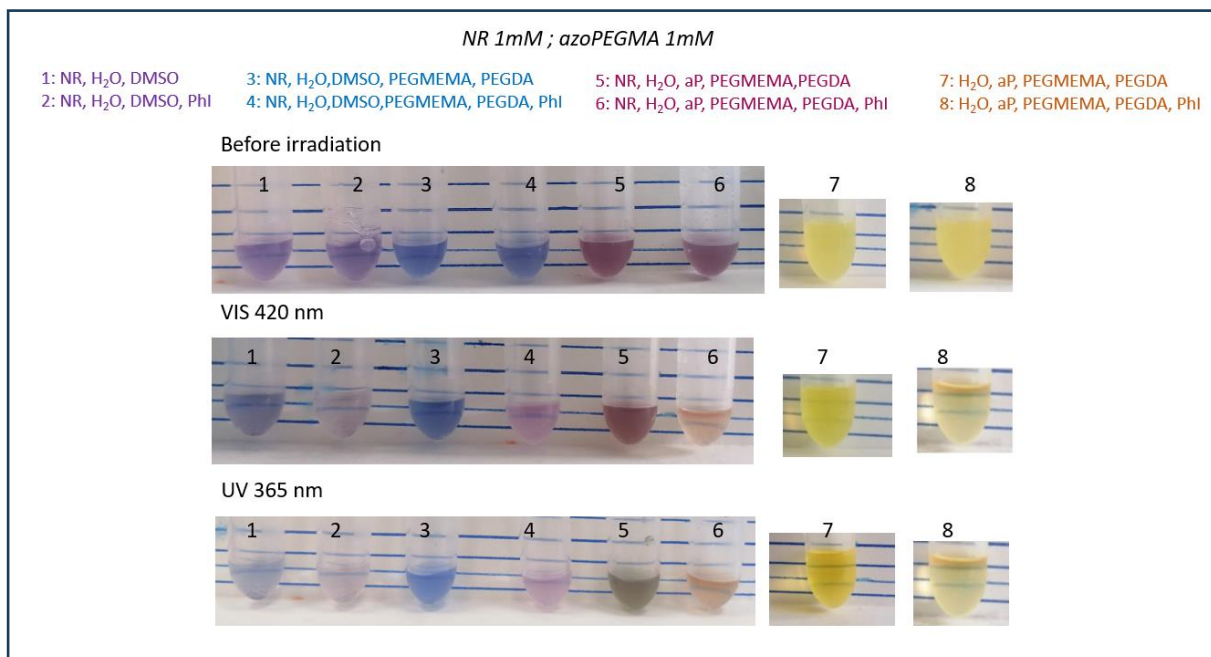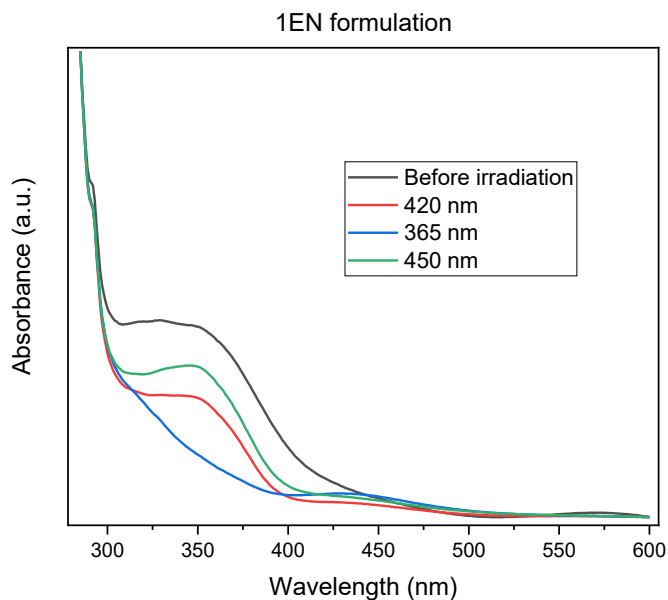*Figure 57 UV-vis spectroscopy on 1EN formulation. Nile red concentration equal to 1mM.*

It is remarkable that if the dye is added after the micelles spontaneous formation (Sample 6, chapter 2.4.7.3), it is not encapsulated. As a matter of facts, a clear phase separation can be seen despite the formulation being pipetted. (Fig. 58a)
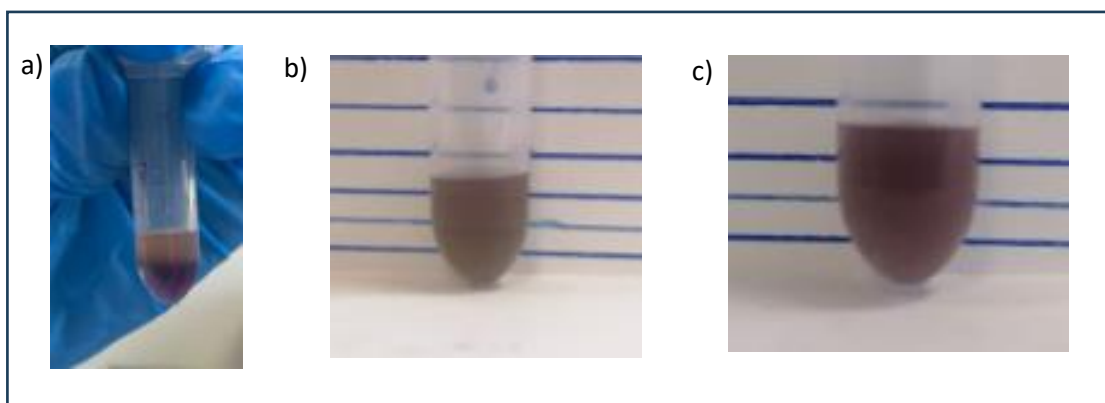
Figure 58 (a) Addition of NileRed in 1E formulation, with an evident phase separation. (b) The same formulation irradiated with 365nm LED. (c) The same formulation further irradiated with 450nm LED.

After UV irradiation at 365nm, the solution becomes homogeneous and remains constant even after the vis irradiation at 450nm (Fig 58b, 58c). This suggests that the Nile red may be encapsulated during the spontaneous rebuilding of the micelles.

3.12.1.FLUORESCENCE SPECTROSCOPY

Fluorescence tests were carried out, both on the sample 6 and on a solution in which Nile red is added while micelles are originally forming (Sample 4, chapter 2.4.7.3). (Fig. 59). The Sample 6 has a spectrum shifted towards the red, as commonly happens when Nile red is dispersed in water (33) (Villa et al.). Even the spectrum of sample 4 (in which Nile red is hopefully encapsulated), undergoes a red shift following UV irradiation, demonstrating the release of Nile red in water.

A subsequential blue shift is instead seen as a consequence of vis 450nm irradiation, with the spectrum overlapping the spectrum obtained before every irradiation. This proves that the micelles have re-formed, re-encapsulating the dye.
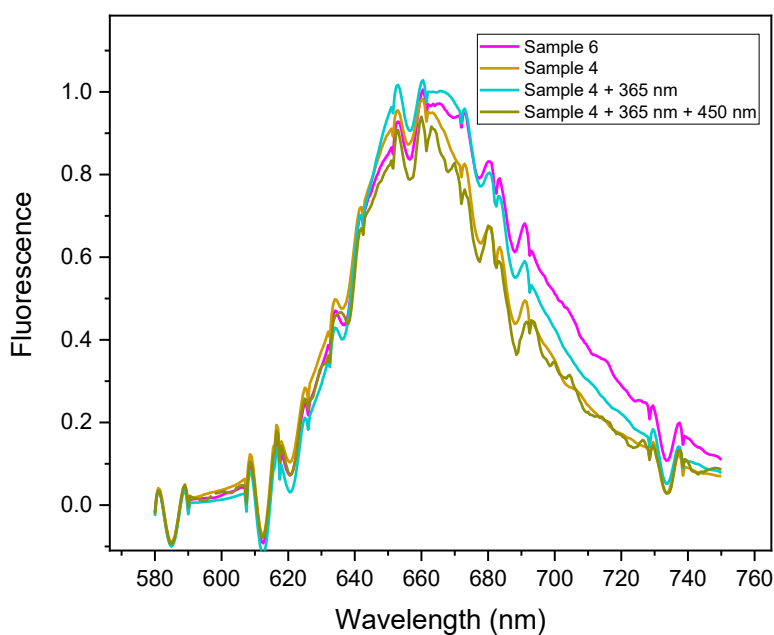
Figure 59 Fluorescence on liquid 1EN solution. Nile red concentration 1mM.

Following analyses were conducted on solution with Nile red concentration of 9.5uM as it was more suitable for representing drug delivery

The same analysis as before was conducted, to ensure the outcome, albeit less appreciable. This is probably due to the lower presence of Nile red. (Fig. 60)
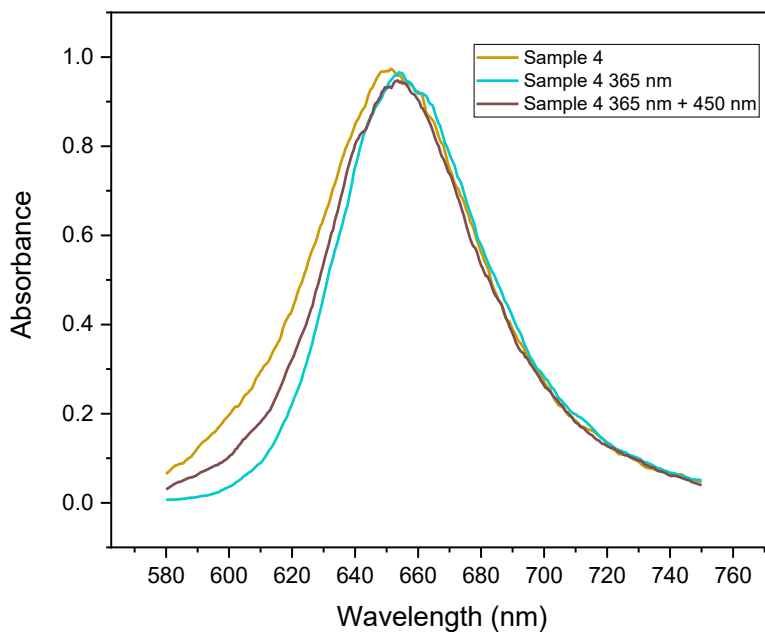
Figure 60 Fluorescence spectroscopy on 1EN solution without PEG-BAPO. Nile red concentration 9.5µM.

As a counterproof, an aqueous solution composed of DMSO, PEGMEMA, PEGDA and Nile red (Sample 8, chapter 2.4.7.3), was analysed. From the outcome (Fig. 61), it is evident that the fluorescence of Nile red alone does not undergo shifts following exposure to different light wavelengths.
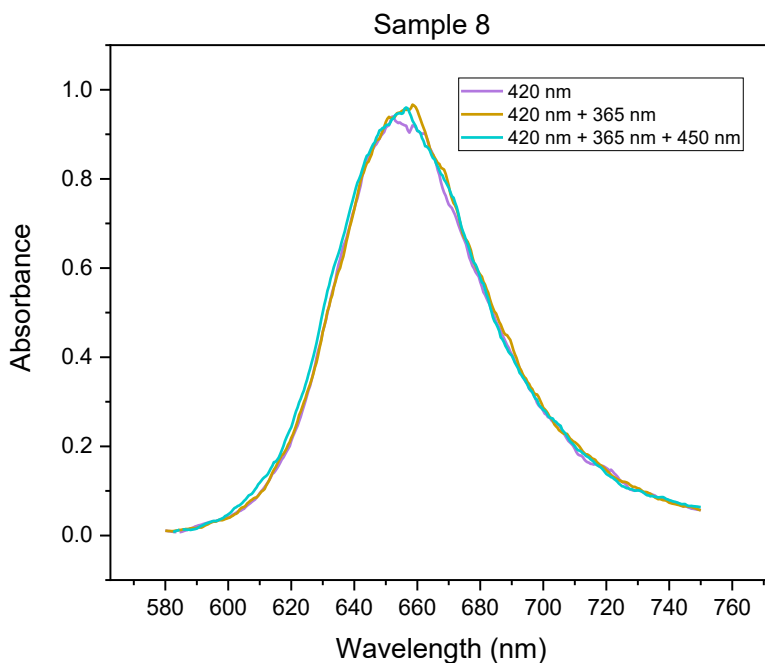
Figure 61 Fluorescence of NileRed aqueous solution.

PEG-BAPO was added to the formulation (Sample 7, chapter 2.4.7.3) and polymerization was achieved. It is noteworthy that Nile red stops fluorescing. (Fig. 62a). Normalizing the graph, an autofluorescence small peak is detected, that could be related to the polymeric matrix (Fig. 62b)
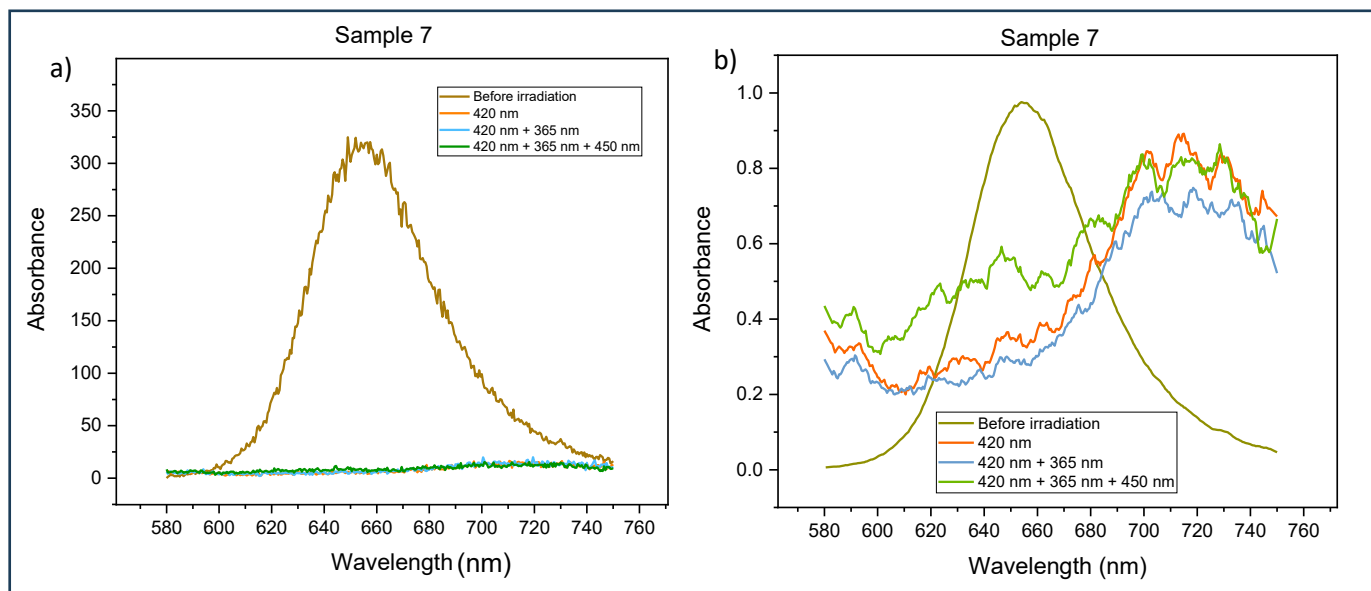
Figure 62 (a) Fluorescence spectroscopy on Sample 7, before irradiation, after polymerization (420 nm), after UV irradiation (365 nm) and after VIS irradiation (450 nm). (b) Normalized data.

1EN formulation (Sample 5, chapter 2.4.7.3), was therefore analysed after irradiation (Fig. 63). By normalizing it, a blue shift is remarkable following polymerization, probably associated with a rigid-chromic factor (88). However, a change in the peaks of the spectra following 365nm and 450nm irradiation is not appreciable.
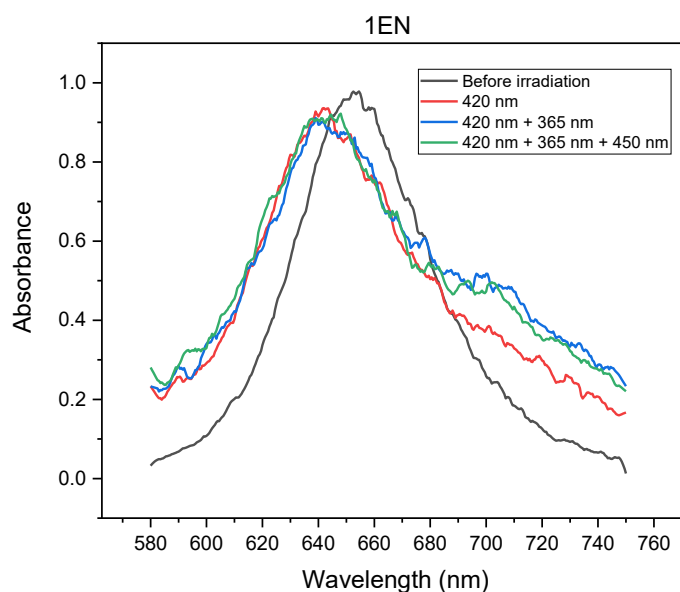
Figure 63 Fluorescence of 1EN formulation following polymerization.

Some hypotheses are possible to explain this outcome. Maybe the dye, although released from the micelles, remains encapsulated in the DMSO inside the hydrogel. Or else, the micelles were opened during photopolymerization and consequently they didn't hold the dye. However, these results together with an evident loss of turbidity following photopolymerization, suggest that the micelles, although present in the liquid formulation, were disrupted during photopolymerization.

3.12.2.UV-VIS DOUBLE BEAM SPECTROSCOPY

The light-triggered assembly/disassembly of nanoaggregates of E-azoPEGMA was investigated by UV-Vis double beam spectroscopies on 1E formulation, following light scattering between 500nm and 800nm.

Initially, a reference sample made of H_2O, PEGMEMA, PEGDA and DMSO was analysed.

Then, PEG-BAPO was added. It is possible to detect the PEG-BAPO typical peak between 320 and 370nm, which disappears once the formulation has been polymerised, as expected. The gel is almost transparent, with a transmittance of around 80%. (Fig. 64a)

Formulation 1E was analysed in the absence of PEG-BAPO, after various irradiations. (Fig. 64b) The black line represents the formulation before irradiation and the E-azoPEGMA peak in the UV region is evident. The solution turbidity is high, as demonstrated by a transmittance of 20% at higher wavelength. Following irradiation with 420nm light. the peak in the UV region decreases and the transmittance also becomes about 50% at higher wavelengths, indicating that part of E-azoPEGMA has isomerized into Z-azoPEGMA. As a result of the UV irradiation, isomerization occurs and the transmittance at higher wavelength reaches almost 80%: in this condition, the micelles are probably completely gone. Finally, following VIS 450nm irradiation, TRANS configuration returns, and transmittance also comes back to 45%.

The same experiment was done on the 1E formulation, also containing PEG-BAPO. (Fig 64c) The initial transmittance of the formulation at high wavelength is equal to 20%. After polymerization, it increases up to 70%, and neither the UV irradiation (365 nm), nor especially the VIS irradiation (450 nm), allow the transmittance value to change, even if photoisomerization happens, as previously demonstrated (Chapter 3.8): micelles probably open during polymerization, and they are unable to reform.
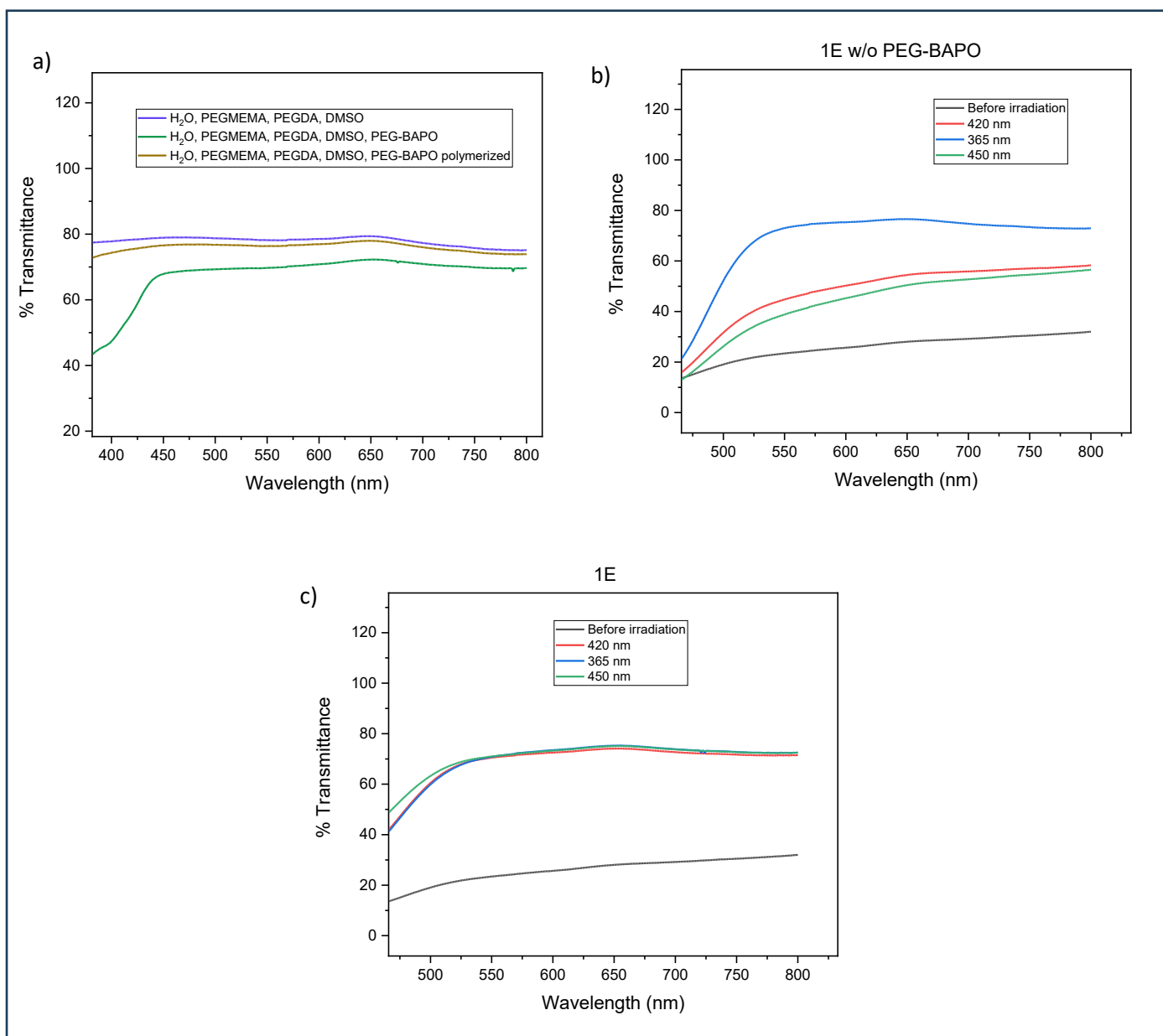
Figure 64 UV-VIS double beam spectroscopies on (a) a solution containing PEGMEMA, PEGDA, DMSO, H2O and eventually PEG-BAPO, (b) formulation 1EN without PEG-BAPO, (c) formulation 1EN.

3.12.3. SPINNING DISK ANALYSIS

The results of fluorescence and UV-VIS double beam spectroscopies were confirmed in parallel by optical analyses performed using spinning disk microscopy.

In Fig. 65 the results on the 1E formulation before irradiation and after polymerization are reported.
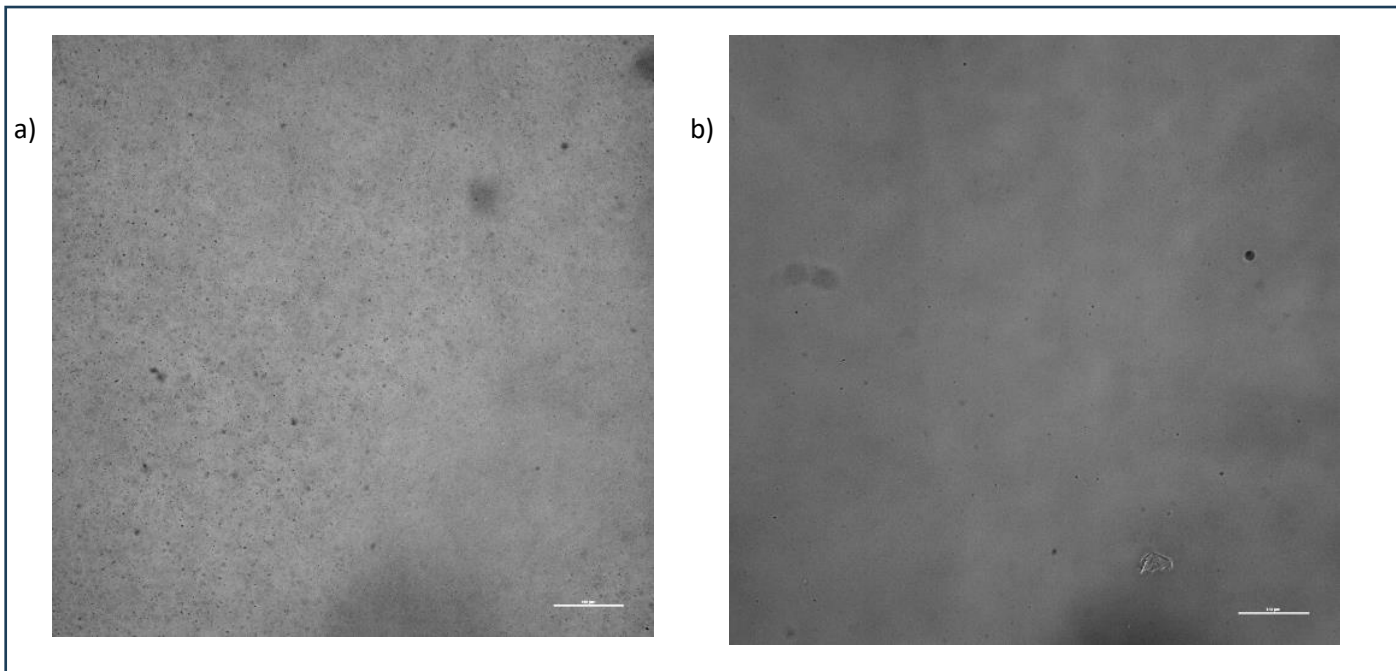
Figure 65 Optical images of (a) 1E formulation before irradiation, (b) 1E formulation polymerized. Scale bar 100µm.

It is noteworthy that the liquid formulation contains many micelles, which however disappear upon polymerization.

Also fluorescence analyses were carried out on formulation 1EN with the same outcome: it is presented in Fig. 66.
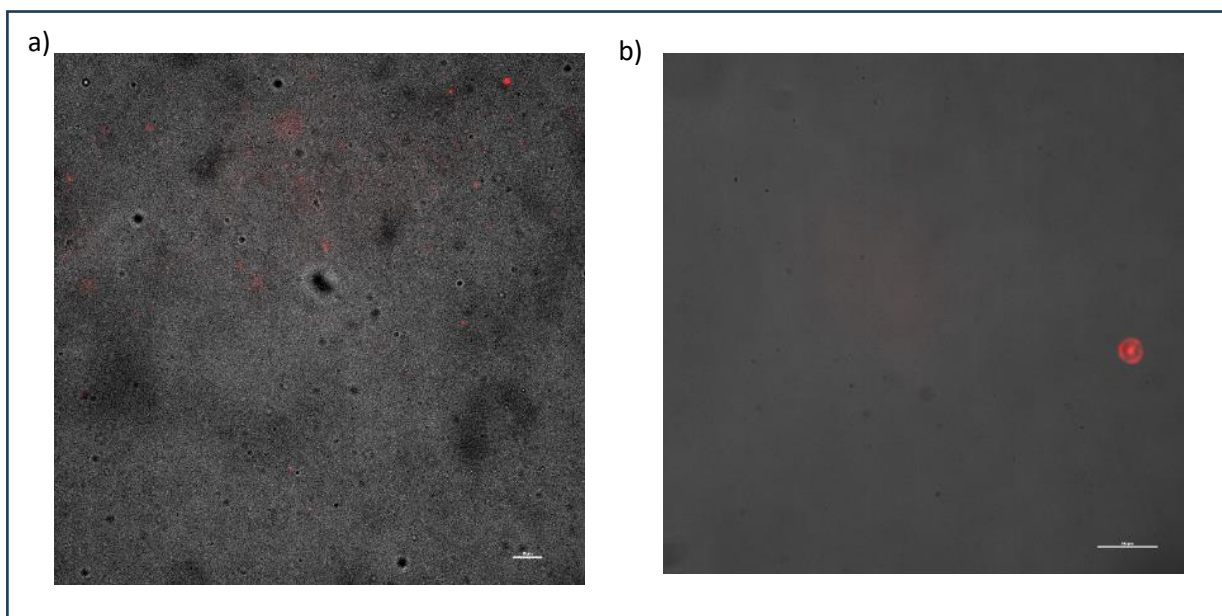
Figure 66 Optical images of (a) 1E formulation before irradiation, (b) 1E formulation polymerized. Excitation wavelength: 540 nm. Scale bar 100µm.

In the image representing 1EN formulation, the presence of micelles is detectable and so it is the fluorescence given by the dye encapsulated in them. After polymerization, micelles are virtually absent, and Nile red doesn't fluorescence anymore.

It is uncertain the reason why micelles are lost over polymerization. Possibly, the cause is a partial E-to-Z isomerization due to irradiation at 420nm. Micelles could not be able to re-form after visible irradiation maybe because azoPEGMA molecules, copolymerizing with growing macromolecules, do not have sufficient mobility to reform micelles. Besides, the methacrylic group of azoPEGMA could interact with monomers during polymerization, drifting apart the molecule and hindering the spontaneous micelles formation. Finally, hydrophilic/ hydrophobic domains could change during the polymerization, leading to the impossibility to form again biphasic system. This aspect is clearly undesired in the view of this work, nevertheless an application can be envisaged, as detailed in the conclusion chapter.

3.13.3D PRINTING

During the development of this thesis project, preliminary study on the 3D-printability of the formulations were performed. Initially, material tests were carried out on all the formulations 2C,4D,1E,2E already analysed with photorheology (Paragraph 3.6), both with and without azoPEGMA. The material tests' results (Table 10, Table 11) were coherent with the aforementioned photorheology. Formulations without PEGDA were not printable and consequently they were abandoned.

Table 10 Material tests on formulation with azoPEGMA. X stands for a formulation which is not polymerized anymore.

FORMULATION 2C		FORMULATION 4D		FORMULATION 1E		FORMULATION 2E	
Irradiation time [s]	Thickness [mm]	Irradiation time [s]	Thickness [mm]	Irradiation time [s]	Thickness [mm]	Irradiation time [s]	Thickness [mm]
100	1.21	100	1.7	100	2.10	100	1.53
90	0.86	90	1.64	80	1.57	90	1.29
80	X	80	1.48	70	1.31	80	1.17
		70	X	60	0.94	70	0.84
				50	0.94	60	X
				40	0.90		
				30	0.85		
				20	X		

Table 11 Material tests on formulation without azoPEGMA. X stands for a formulation which is not polymerized anymore.

FORMULATION 2C without azoPEGMA		FORMULATION 4D without azoPEGMA		FORMULATION 1E without azoPEGMA		FORMULATION 2E without azoPEGMA	
Irradiation time [s]	Thickness [mm]	Irradiation time [s]	Thickness [mm]	Irradiation time [s]	Thickness [mm]	Irradation time [s]	Thickness [mm]
100	1.51	100	2.39	100	2.03	100	2.35
90	1.48	80	1.97	80	1.47	80	2,10
80	X	60	1.23	60	1.89	60	1.64
		40	1.21	40	X	40	1.46
		30	0.77			20	1.32
		20	X			10	X

Since the material test's results were encouraging, hydrogels were printed in a honeycomb geometry using the1E and 2E formulations with a long-needed exposure time to cure. Attempts are listed in Table 12.

TESTED PARAMETERS						
	Thickness [mm]	Formulation	Layer thickness [mm]		Number of layers	Exposure time [s]
1.	1.28	2E without azoPEGMA	0.1	BURN-IN	4	15
				OTHER LAYERS	9	14
2.	1.28	2E without azoPEGMA	0.1	BURN-IN	4	32
				OTHER LAYERS	9	30
3.	1.28	2E without azoPEGMA	0.05	BURN-IN	8	32
				OTHER LAYERS	18	30
4.	2.3	2E without azoPEGMA	0.05	BURN-IN	10	32
				OTHER LAYERS	36	30
5.	2.3	2E without azoPEGMA	0.05	BURN-IN	10	25
				OTHER LAYERS	36	22
6.	2.3	2E	0.05	BURN-IN	10	25
				OTHER LAYERS	36	22
7.	2.3	2E	0.05	BURN-IN	10	32
				OTHER LAYERS	36	30
8.	2.3	2E	0.05	BURN-IN	10	48
				OTHER LAYERS	36	42
9.	2.3	2E	0.05	BURN-IN	10	51
				OTHER LAYERS	36	48
10.	2.3	2E	0.05	BURN-IN	10	62
				OTHER LAYERS	36	60
11.	1.66	2E	0.05	BURN-IN	8	62
				OTHER LAYERS	25	60
12.	1.66	2E	0.05	BURN-IN	8	80
				OTHER LAYERS	25	77
13.	1.66	2E	0.05	BURN-IN	8	85
				OTHER LAYERS	25	80
14.	2.3	2E	0.05	BURN-IN	8	85
				OTHER LAYERS	38	80
15.	2.3	1E	0.05	BURN-IN	8	85
				OTHER LAYERS	38	80
16.	1.66	1E	0.05	BURN-IN	8	62
				OTHER LAYERS	25	60
17.	1.66	1E without azoPEGMA	0.05	BURN-IN	10	32
				OTHER LAYERS	36	30

The third attempt allowed the hydrogel to be printed with formulation 2E without azoPEGMA. However, it was too thin (Fig. 67a) and impossible to detach from the vat. So, the thickness was increased (attempt 4), obtaining good results. (Fig. 67b)
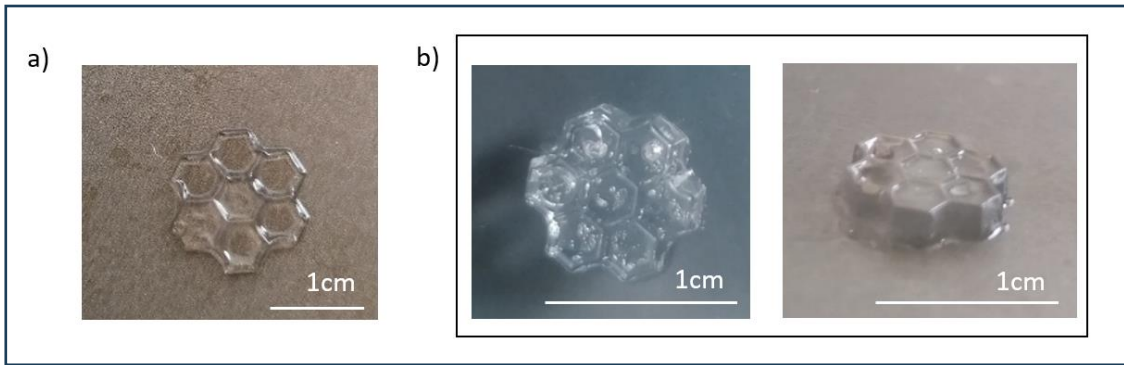
Figure 67 (a) attempt 3; (b) attempt 4

Formulation 2E, was then printed with the parameters exposed in attempt 14: results are shown in Fig. 68.
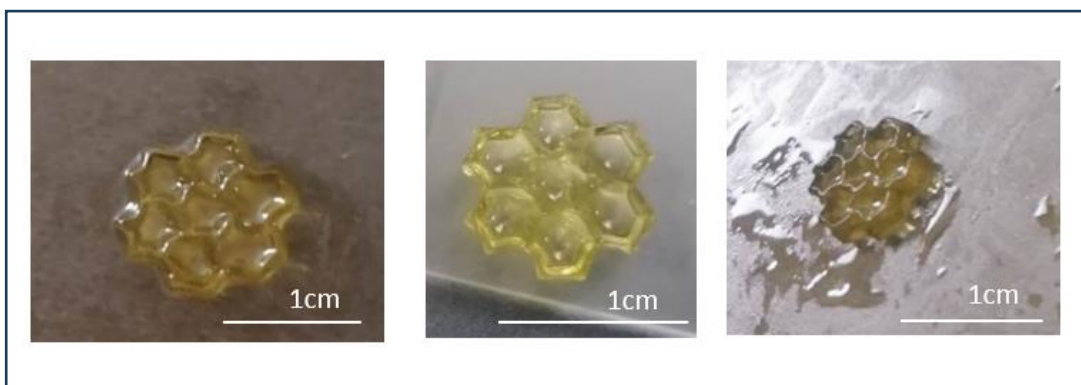

Figure 68 Attempt 14

Formulation 1E was then printed with the same parameters (attempt 15). The result is in Fig.69.
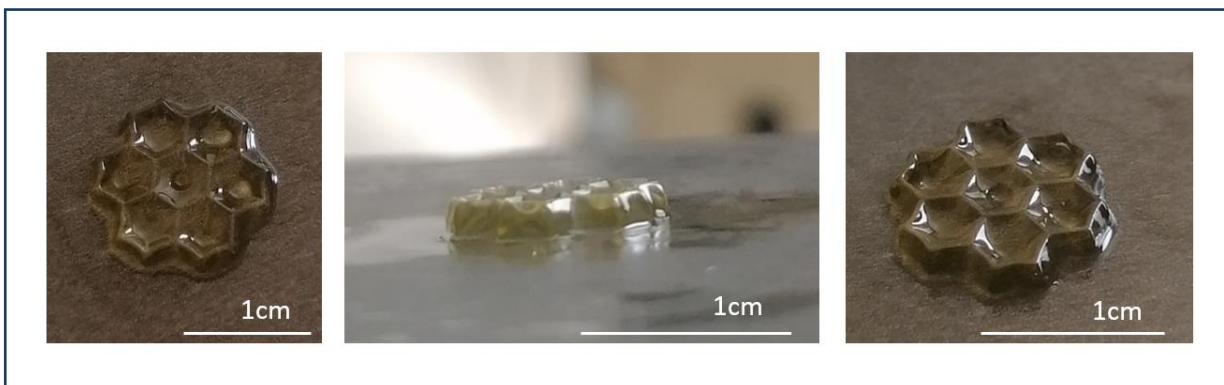
Figure 69 Attempt 15

As already demonstrated with photorheology and material tests, 1E formulation is more polymerizable compared to 2E formulation: reducing exposure time (attempt 11 and 16) 1E formulation is successfully printed, whereas the 2E formulation is not, as shown in Fig. 70.
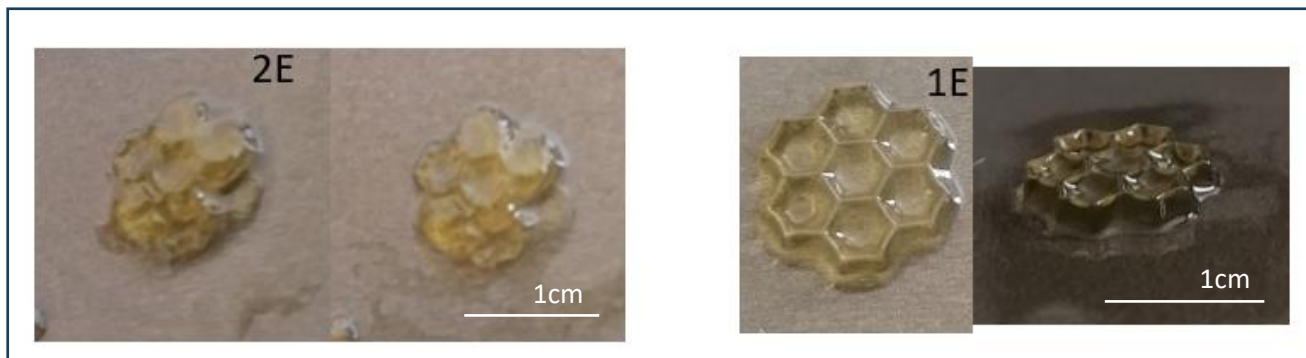
Figure 70 Attempts 11 and 16.

At the same time, trying both the formulations without azoPEGMA (attempt 4 and 17), it is evident that 1E formulation is actually less defined. (Fig. 71)
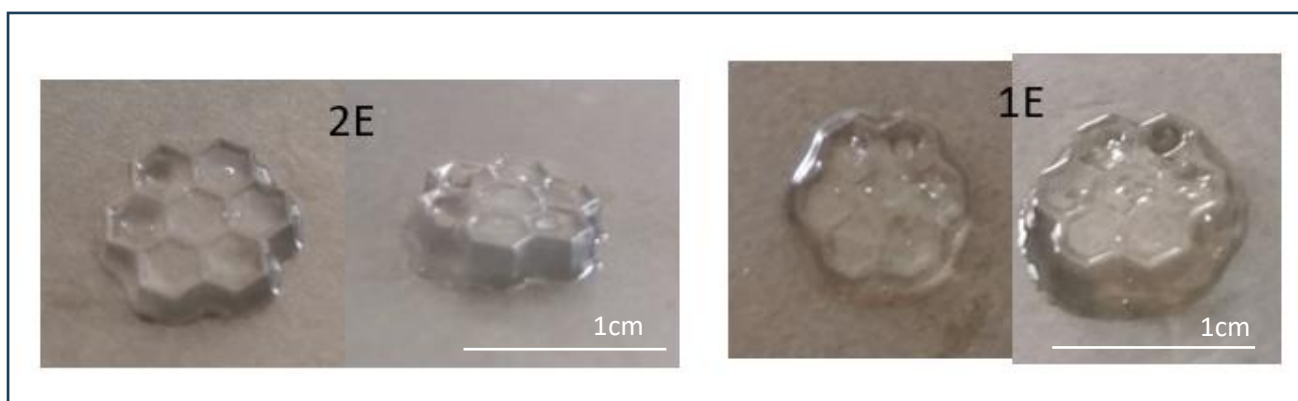
Figure 71 Attempts 4 and 17.

These results offered promising indications that successful printing of more complex geometries may be achievable, though additional studies are required. Moreover, the 3D printer uses a 405nm LED to polymerize. This means that a more relevant E-to-Z isomerization may occurred during the printing process.

4.CONCLUSIONS

With the final goal of developing smart hydrogels and inspired by the reported behaviour of photoresponsive compounds, named azoPEG, this thesis project aimed to investigate the possibility of fabricating hydrogels based on a modified version of this molecule, named azoPEGMA, with light triggered behaviour.

In the first chapter, a brief introduction on the hydrogel field and the 3D printing area has been discussed. In particular, the hydrogels' classification, as well as their properties and applications have been explored. A focus was then made on smart hydrogels, particularly on photoresponsive ones, as they were the central topic of the thesis. The last part of this chapter described the 3D printing field, focusing on the DLP method and generally the photopolymerization process, as one of the objectives of this work was the development of a 3D-printable hydrogel.

In the next chapter, materials and methods employed during this thesis project were presented. In particular, the hydrogel synthesized is composed of PEGMEMA, PEGDA, PEG-BAPO and azoPEGMA. Water and DMSO were used as solvents. To polymerize the formulation, a 420nm LED was employed, while the isomerization of the azo compound was obtained through light irradiation at different wavelength. 365nm LED was employed to achieve the E-to-Z isomerization, while the Z-to-E was reached with 450nm LED. The analyses conducted to investigate the hydrogel properties were rheology, UV-VIS spectroscopy and UV-VIS double beam spectroscopy, as well as FT-IR and compression test. Water uptake was examined through swelling and evaporation tests. Since the amphiphilicity of azoPEGMA should have permit the spontaneous formation of micelles, a well-established dye, named Nile red, was used to mimic its encapsulation and release. Fluorescence spectroscopy and spinning disk analysis were selected to investigate this possibility.

Third chapter was dedicated to experiments and discussion. Approaching the topic of this thesis, 6 scientific questions were posed:

1) Do azoPEGMA molecules still form micelles when dispersed in a photocurable formulation?

2) Are those preserving the ability to form light-controllable micelles in liquid solution?

3) Are those micelles maintained when photopolymerization occurs and therefore hydrogel is formed?

4) Do azoPEGMA molecules preserve photoisomerization in the hydrogel?

5) Is it possible to create hydrogels with light-controlled drug release?

6) Is it possible to 3D print those materials?

The results reported allow now to reply to those questions, even if new scientific doubts emerged.

1) Do azoPEGMA molecules still form micelles when dispersed in a photocurable formulation?

Yes, azoPEGMA can still form micelles in photocurable formulation. Nevertheless, the formulation should be adjusted since the presence of photocurable monomers (in this case PEGMEMA and PEGDA) and photoinitiator (PEG-BAPO) may affect the ability to form those. In particular, it was demonstrated that a formulation containing at most 26% w/w of monomers allows the presence of micelles (as a matter of fact, the formulation is opaque). While at higher concentrations azoPEGMA goes in solution and the formulation becomes transparent.

2) Are those preserving the ability to form light-controllable micelles in liquid solution?

Yes, once set the optima formulation, the micelles are able to form, and then be destroyed by UV-radiation and then form again by Visible irradiation. This was verified by Uv-vis double beam spectroscopy which demonstrated a lower transmittance value in the formulation before irradiation (meaning an opaque formulation) and higher one when irradiated with 365nm LED (meaning a transparent formulation). Transmittance value re-decreases when formulation is irradiated with 450nm LED.

3) Are those micelles maintained when photopolymerization occurs and therefore hydrogel is formed?

No. All the tests performed, both visual and instrumental, converge in the statement that once polymerization occurs, micelles are destroyed. That can be ascribed to a certain isomerization E-to-Z, that could be related to the light used for the polymerization. On the other hand, other tests seem to suggest that this effect is negligible, more likely the azoPEGMA molecules react with the growing macromolecules and are forced to get out of the micelles.

4) Do azoPEGMA molecules preserve photoisomerization in the hydrogel?

Yes, the azoPEGMA molecules are able to undergo photoisomerization even when embedded in the hydrogel. This was demonstrated through UV-vis spectroscopy. In fact, following the irradiation, the spectra change according to the wavelength used, meaning that a E-to-Z or a Z-to-E transformation has occurred. Hower, the behavior of such molecules in the hydrogels change compared to their behavior in liquid. First, as already mentioned, micelles are destroyed and are not able to be formed again, even after multiple light-irradiation cycles. This can be related to the lower mobility of the azoPEGMA molecules when chemically bonded to the polymeric network, but also to a different environment related to hydrophobicity/hydrophilicity. On the other hand, the peaks of Z and E isomers (350 nm and 440 nm respectively) were clearly observed in UV-Vis spectra, indicating that the isomerization occurs. Preliminary observations seems to suggests that isomerization is delayed, which can be again related to different mobility, but more tests should be performed.

5) Is it possible to create hydrogels with light-controlled drug release?

No. For assessing this property, Nile red was used to mimic a drug. Experiments performed in liquid solution demonstrated that micelles are able to encapsulate the dye and to release it once they are opened following 365 nm irradiation (as assesses with a red shift of the fluorescence spectrum). Micelles are also able to re-incapsulate the dye while re-forming following 450 nm irradiation (as assesses with a blue shift of the fluorescence spectrum). On the other hand, unfortunately, this behavior cannot be maintained in hydrogels, due to the dissolution of micelles during the photopolymerization.

6) Is it possible to 3D print those materials?

Yes, optimized formulation resulted 3D printable and relatively solid to be manipulated. Mechanical and photorheology tests determined that although azoPEGMA may lead to a small loss of the formulation photoreactivity, it is able to improve the mechanical properties of the hydrogel obtained. The hydrogel has a stiffness comparable to the cardiac muscle. Also swelling and evaporation tests were performed evidencing that the hydrogel can swell up to 350% and the vast majority of the contained water evaporates within 48 hours.

Some perspectives coming from this work's limitations should be considered.

Since azoPEGMA seemed to support polymerization, it would be great to find the balance between the quantity of azoPEGMA itself and photoinitiator able to guarantee a physical cross-linking, avoiding the requirement of a bifunctional monomer. In this sense, it is envisaged to decouple polymerization and photoisomerization to obtain effective light triggering. On the other hand, it could be foreseen a possible application even for these hydrogels, considering a drug release only during irradiation. It could be used for example in wound healing: after the polymerization and the release of the desired drug, the hydrogel will play only a structural role as it could cover the wound avoiding possible inflammation.

Moreover, this work showcases the presence of azoPEGMA aggregates when the micelles are irradiated within the photoinitiator in an aqueous solution and absence of monomers. These aggregates need to be further characterised. It can be envisaged the synthesis of these aggregates as photocontrolable nanocontainers, which can be used then in a hydrogel or in solution.

Alternatively, since the copolymerization associated to the presence of methacrylic moieties on the tails of azoPEGMA compounds induced the loss of micelles, other solutions should be explored. In particular, to polymerize the hydrogel without the azoPEGMA and then introduce it by swelling might be an option, as well as the use of azoPEG molecules could be an option, since those would not react with growing macromolecules. Also, the addition of azoPEGMA/azoPEG to a physical hydrogel should be investigated.

Summarizing, although this project evidenced promising results, it also highlighted new scientific questions that need to be addressed, paving the way for the development of a photopolymerizable and physically cross-linkable smart hydrogels.

5.REFERENCES

1.   Zhao L, Zhou Y, Zhang J, Liang H, Chen X, Tan H. Natural Polymer-Based Hydrogels: From Polymer to Biomedical Applications. Vol. 15, Pharmaceutics. Multidisciplinary Digital Publishing Institute (MDPI); 2023.

2.   Revete A, Aparicio A, Cisterna BA, Revete J, Luis L, Ibarra E, et al. Advancements in the Use of Hydrogels for Regenerative Medicine: Properties and Biomedical Applications. Vol. 2022, International Journal of Biomaterials. Hindawi Limited; 2022.

3.   Batista RA, Espitia PJP, Vergne DMC, Vicente AA, Pereira PAC, Cerqueira MA, et al. Development and Evaluation of Superabsorbent Hydrogels Based on Natural Polymers. Polymers (Basel) [Internet]. 2020;12(10). Available from: https://www.mdpi.com/2073-4360/12/10/2173

4.   Ho TC, Chang CC, Chan HP, Chung TW, Shu CW, Chuang KP, et al. Hydrogels: Properties and Applications in Biomedicine. Vol. 27, Molecules. MDPI; 2022.

5.   Bashir S, Hina M, Iqbal J, Rajpar AH, Mujtaba MA, Alghamdi NA, et al. Fundamental concepts of hydrogels: Synthesis, properties, and their applications. Vol. 12, Polymers. MDPI AG; 2020. p. 1–60.

6.   Hasan S, Kouzani AZ, Adams S, Long J, Mahmud MAP. Recent progress in hydrogel-based sensors and energy harvesters. Vol. 335, Sensors and Actuators A: Physical. Elsevier B.V.; 2022.

7.   Hoffman AS. Hydrogels for biomedical applications [Internet]. Vol. 43, Advanced Drug Delivery Reviews. 2002. p. 3–12. Available from: www.elsevier.com/locate/drugdeliv

8.   Van Hove AH, Wilson BD, Benoit DSW. Microwave-assisted functionalization of poly(ethylene glycol) and on-resin peptides for use in chain polymerizations and hydrogel formation. J Vis Exp. 2013;(80).

9.   Thang NH, Chien TB, Cuong DX. Polymer-Based Hydrogels Applied in Drug Delivery: An Overview. Vol. 9, Gels. Multidisciplinary Digital Publishing Institute (MDPI); 2023.

10.   Mehta P, Mahadik K, Kadam S, Dhapte-Pawar V. Advanced applications of green hydrogels in drug delivery systems. In: Applications of Advanced Green Materials. Elsevier; 2020. p. 89–130.

11.   Bustamante-Torres M, Romero-Fierro D, Arcentales-Vera B, Palomino K, Magaña H, Bucio E. Hydrogels classification according to the physical or chemical interactions and as stimuli-sensitive materials. Vol. 7, Gels. MDPI; 2021.

12.   Ahmad Z, Salman S, Khan SA, Amin A, Rahman ZU, Al-Ghamdi YO, et al. Versatility of Hydrogels: From Synthetic Strategies, Classification, and Properties to Biomedical Applications. Vol. 8, Gels. MDPI; 2022.

13.   Saini K. Preparation method, Properties and Crosslinking of hydrogel: a review. 5.

14.   Caló E, Khutoryanskiy V V. Biomedical applications of hydrogels: A review of patents and commercial products. Vol. 65, European Polymer Journal. Elsevier Ltd; 2015. p. 252–67.

15.   Lei L, Bai Y, Qin X, Liu J, Huang W, Lv Q. Current Understanding of Hydrogel for Drug Release and Tissue Engineering. Vol. 8, Gels. MDPI; 2022.

16.   Bahram M, Mohseni N, Moghtader M. An Introduction to Hydrogels and Some Recent Applications. In 2016.

17.   Patil S V, Shelake SS, Patil SS. Polymeric materials for targeted delivery of bioactive agents and drugs. In: Fundamental Biomaterials: Polymers. Elsevier Inc.; 2018. p. 249–66.

18. Sobczak M. Enzyme-Responsive Hydrogels as Potential Drug Delivery Systems—State of Knowledge and Future Prospects. Vol. 23, International Journal of Molecular Sciences. MDPI; 2022.

19. Georges Akhras. SMART MATERIALS AND SMART SYSTEMS FOR THE FUTURE. In. Available from: https://api.semanticscholar.org/CorpusID:14125349

20. Kumar S, Sehgal R, Wani MF, Sharma MD. Stabilization and tribological properties of magnetorheological (MR) fluids: A review. J Magn Magn Mater [Internet]. 2021;538:168295. Available from: https://www.sciencedirect.com/science/article/pii/S0304885321005710

21. Ofridam F, Tarhini M, Lebaz N, Gagnière É, Mangin D, Elaissari A. pH-sensitive polymers: Classification and some fine potential applications. Vol. 32, Polymers for Advanced Technologies. John Wiley and Sons Ltd; 2021. p. 1455–84.

22. El-Husseiny HM, Mady EA, Hamabe L, Abugomaa A, Shimada K, Yoshida T, et al. Smart/stimuli-responsive hydrogels: Cutting-edge platforms for tissue engineering and other biomedical applications. Vol. 13, Materials Today Bio. Elsevier B.V.; 2022.

23. Li L, Scheiger JM, Levkin PA. Design and Applications of Photoresponsive Hydrogels. Advanced Materials. 2019 Nov;31(26).

24. Xiong X, del Campo A, Cui J. Photoresponsive Polymers. In: Smart Polymers and Their Applications. Elsevier; 2019. p. 87–153.

25. Bhatt P, Trehan S, Inamdar N, Mourya VK, Misra A. Polymers in Drug Delivery: An Update. In: Applications of Polymers in Drug Delivery. Elsevier; 2020. p. 1–42.

26. Xing Y, Zeng B, Yang W. Light responsive hydrogels for controlled drug delivery. Vol. 10, Frontiers in Bioengineering and Biotechnology. Frontiers Media S.A.; 2022.

27. Zhang S, Zhang Q, Zhang Y, Chen Z, Watanabe M, Deng Y. Beyond solvents and electrolytes: Ionic liquids-based advanced functional materials. Vol. 77, Progress in Materials Science. Elsevier Ltd; 2016. p. 80–124.

28. Li L, Zhao W, Qu Z, Shi L, Tan S, Ha E, et al. Novel phthalocyanine-based micelles/PNIPAM composite hydrogels: spatially/temporally controlled drug release triggered by NIR laser irradiation. New J Chem [Internet]. 2020;44(21):8705–9. Available from: http://dx.doi.org/10.1039/D0NJ01882A

29. Wu J, Li H, Zhang N, Zheng Q. Micelle-Containing Hydrogels and Their Applications in Biomedical Research. Gels [Internet]. 2024;10(7). Available from: https://www.mdpi.com/2310-2861/10/7/471

30. Sinha M, Purkait M, Singh R, Mondal P. Stimuli Responsive Polymeric Membranes. 2018.

31. Cheng HB, Zhang S, Qi J, Liang XJ, Yoon J. Advances in Application of Azobenzene as a Trigger in Biomedicine: Molecular Design and Spontaneous Assembly. Vol. 33, Advanced Materials. John Wiley and Sons Inc; 2021.

32. Colaco R, Appiah C, Staubitz A. Controlling the LCST-Phase Transition in Azobenzene-Functionalized Poly (N-Isopropylacrlyamide) Hydrogels by Light. Gels. 2023 Nov;9(2).

33. Villa M, Bergamini G, Ceroni P, Baroncini M. Photocontrolled self-assembly of azobenzene nanocontainers in water: light-triggered uptake and release of small molecules. 2019.

34. Shahrubudin N, Lee TC, Ramlan R. An overview on 3D printing technology: Technological, materials, and applications. In: Procedia Manufacturing. Elsevier B.V.; 2019. p. 1286–96.

35.	Bagheri A, Jin J. Photopolymerization in 3D Printing. Vol. 1, ACS Applied Polymer Materials. American Chemical Society; 2019. p. 593–611.

36.	Ding H, Dong M, Zheng Q, Wu ZL. Digital light processing 3D printing of hydrogels: a minireview. Vol. 7, Molecular Systems Design and Engineering. Royal Society of Chemistry; 2022. p. 1017–29.

37.	Guessasma S, Zhang W, Zhu J, Belhabib S, Nouri H. Challenges of additive manufacturing technologies from an optimisation perspective. International Journal for Simulation and Multidisciplinary Design Optimization. 2015;6:A9.

38.	Chaudhary R, Fabbri P, Leoni E, Mazzanti F, Akbari R, Antonini C. Additive manufacturing by digital light processing: a review. Vol. 8, Progress in Additive Manufacturing. Springer Science and Business Media Deutschland GmbH; 2023. p. 331–51.

39.	Layani M, Wang X, Magdassi S. Novel Materials for 3D Printing by Photopolymerization. Vol. 30, Advanced Materials. Wiley-VCH Verlag; 2018.

40.	Tomal W, Ortyl J. Water-Soluble Photoinitiators in Biomedical Applications. Polymers (Basel) [Internet]. 2020;12(5). Available from: https://www.mdpi.com/2073-4360/12/5/1073

41.	Nadagouda MN, Rastogi V, Ginn M. A review on 3D printing techniques for medical applications. Vol. 28, Current Opinion in Chemical Engineering. Elsevier Ltd; 2020. p. 152–7.

42.	(Poly(ethylene glycol) methyl ether methacrylate average Mn 950, contains 100 ppm MEHQ as inhibitor, 300 ppm BHT as inhibitor | 26915-72-0 (sigmaaldrich.com)). Update 2024/11/26.

43.	https://www.sigmaaldrich.com/IT/it/product/aldrich/455008. Update 2024/11/26.

44.	Wang J, Stanic S, Altun AA, Schwentenwein M, Dietliker K, Jin L, et al. A highly efficient waterborne photoinitiator for visible-light-induced 3D printing of hydrogels. 2018.

45.	https://www.aablocks.com/prod/188712-75-6 Update 2024/11/26.

46.	Nuttelman CR, Rice MA, Rydholm AE, Salinas CN, Shah DN, Anseth KS. Macromolecular Monomers for the Synthesis of Hydrogel Niches and Their Application in Cell Encapsulation and Tissue Engineering.

47.	Farrag Y, Eldjoudi DA, Farrag M, González-Rodríguez M, Ruiz-Fernández C, Cordero A, et al. Poly(ethylene Glycol) Methyl Ether Methacrylate-Based Injectable Hydrogels: Swelling, Rheological, and In Vitro Biocompatibility Properties with ATDC5 Chondrogenic Lineage. Polymers (Basel). 2023 Nov;15(24).

48.	Rekowska N, Arbeiter D, Brietzke A, Konasch J, Riess A, Mau R, et al. Biocompatibility and thermodynamic properties of PEGDA and two of its copolymer. In: 2019 41st Annual International Conference of the IEEE Engineering in Medicine and Biology Society (EMBC). 2019. p. 1093–6.

49.	Moore E, West JL. Bioactive Poly(ethylene Glycol) Acrylate Hydrogels for Regenerative Engineering. Regen Eng Transl Med [Internet]. 2018;1–13. Available from: https://api.semanticscholar.org/CorpusID:105301617

50.	Rekowska N, Huling J, Brietzke A, Arbeiter D, Eickner T, Konasch J, et al. Thermal, Mechanical and Biocompatibility Analyses of Photochemically Polymerized PEGDA250 for Photopolymerization-Based Manufacturing Processes. Pharmaceutics [Internet]. 2022;14(3). Available from: https://www.mdpi.com/1999-4923/14/3/628

51. Nearingburg B, Elias AL. Photopolymerizable sulfonated poly(ethylene glycol) proton exchange membranes for microfluidic and fuel cell applications. J Memb Sci [Internet]. 2012;389:148–54. Available from: https://www.sciencedirect.com/science/article/pii/S0376738811007745

52. Rekowska N, Arbeiter D, Brietzke A, Konasch J, Riess A, Mau R, et al. Biocompatibility and thermodynamic properties of PEGDA and two of its copolymer. In: 2019 41st Annual International Conference of the IEEE Engineering in Medicine and Biology Society (EMBC). 2019. p. 1093–6.

53. Rumin J, Bonnefond H, Saint-Jean B, Rouxel C, Sciandra A, Bernard O, et al. The use of fluorescent Nile red and BODIPY for lipid measurement in microalgae. Biotechnol Biofuels [Internet]. 2015;8. Available from: https://api.semanticscholar.org/CorpusID:3887054

54. https://docs.rs-online.com/db7a/0900766b816cbca1.pdf Update 2024/11/26.

55. https://www.amazon.it/dp/B0C1KC3DSZ/ref=pe_24968671_487041031_TE_item Update 2024/11/26.

56. https://www.amazon.it/dp/B01DBZIP0C/ref=pe_24968671_487041031_TE_item Update 2024/11/26.

57. Janmey P, Schliwa M. Rheology. Curr Biol. 2008 Nov;18:R639–41.

58. Wilson DI. What is rheology? Eye [Internet]. 2018;32(2):179–83. Available from: https://doi.org/10.1038/eye.2017.267

59. https://chem.libretexts.org/Bookshelves/Organic_Chemistry/Polymer_Chemistry_(Schaller)/04%3A_Polymer_Properties/4.08%3A_Storage_and_Loss_Modulus#:~:text=The%20storage%20modulus%20is%20a,lost%20during%20that%20cycling%20strain Update: 2024/11/26.

60. https://wiki.anton-paar.com/en/basics-of-rheology/#rheology-and-rheometry-related-information Update 2024/11/26.

61. Budai L, Budai M, Fülöpné Pápay ZE, Vilimi Z, Antal I. Rheological Considerations of Pharmaceutical Formulations: Focus on Viscoelasticity. Gels [Internet]. 2023;9(6). Available from: https://www.mdpi.com/2310-2861/9/6/469

62. Szymaszek P, Tomal W, Świergosz T, Kamińska-Borek I, Popielarz R, Ortyl J. Review of quantitative and qualitative methods for monitoring photopolymerization reactions. Vol. 14, Polymer Chemistry. Royal Society of Chemistry; 2023. p. 1690–717.

63. Cafiso D, Septevani AA, Noè C, Schiller T, Pirri CF, Roppolo I, et al. 3D printing of fully cellulose-based hydrogels by digital light processing. Sustainable Materials and Technologies. 2022 Nov;32.

64. Ahearne M. 4 - Mechanical testing of hydrogels. In: Li H, Silberschmidt V, editors. The Mechanics of Hydrogels [Internet]. Woodhead Publishing; 2022. p. 73–90. (Elsevier Series in Mechanics of Advanced Materials). Available from: https://www.sciencedirect.com/science/article/pii/B9780081028629000038

65. Karimi A, Navidbakhsh M, Beigzadeh B. A visco-hyperelastic constitutive approach for modeling polyvinyl alcohol sponge. Tissue Cell [Internet]. 2014;46(1):97–102. Available from: https://www.sciencedirect.com/science/article/pii/S0040816613001092

66. Faturechi R, Karimi A, Hashemi A, Yousefi H, Navidbakhsh M. Influence of Poly(acrylic acid) on the Mechanical Properties of Composite Hydrogels. Advances in Polymer Technology. 2014 Nov;34.

67. Ojeda JJ, Dittrich M. Fourier transform infrared spectroscopy for molecular analysis of microbial cells. Methods in Molecular Biology. 2012;881:187–211.

68. Justin Tom P. UV-Vis Spectroscopy: Principle, Strengths and Limitations and Applications [Internet]. 2021. Available from: https://www.technologynetworks.com/analysis/articles/uv-vis-spectroscopy-principle-strengths-and-limitations-and-applications-349865 Update 2024/11/26.

69. Laboratory GHJ, Zimmermann M, Zimmt W, Nudenberg W. [Contribution from the REACTIONS OF ATOMS AND FREE RADICALS IN SOLUTION. XXXI. REACTIONS OF FREE BENZOYL RADICALS WITH AZO COMPOUNDS (PRELIMINARY PAPER) [Internet]. Vol. 14. UTC; 2024. p. 30. Available from: https://pubs.acs.org/sharingguidelines

70. Orlien V, Boserup L, Olsen K. Casein micelle dissociation in skim milk during high-pressure treatment: Effects of pressure, pH, and temperature. J Dairy Sci [Internet]. 2010;93(1):12–8. Available from: https://www.sciencedirect.com/science/article/pii/S0022030210702599

71. Chiu SJ, Wang SY, Chou HC, Liu YL, Hu TM. Versatile Synthesis of Thiol- and Amine-Bifunctionalized Silica Nanoparticles Based on the Ouzo Effect. Langmuir [Internet]. 2014 Jul 8;30(26):7676–86. Available from: https://doi.org/10.1021/la501571u

72. https://www.agilent.com/en/product/molecular-spectroscopy/uv-vis-uv-vis-nir-spectroscopy/double-beam-spectrophotometers#:~:text=Double%20beam%20UV%2DVis%20spectrophotometers,that%20serves%20as%20a%20reference. Update 2024/11/26.

73. https://www.photometrics.com/learn/spinning-disk-confocal-microscopy/introduction-to-spinning-disk-confocal Update 2024/11/26.

74. Tranter GE. UV-visible fluorescence spectrometers. In: Encyclopedia of Spectroscopy and Spectrometry. Elsevier; 2016. p. 520–3.

75. https://www.thermofisher.com/it/en/home/life-science/cell-analysis/cell-analysis-learning-center/molecular-probes-school-of-fluorescence/fluorescence-basics/fluorescence-fundamentals/light-spectrum-fluorescence.html Update 2024/11/26.

76. https://www.thermofisher.com/it/en/home/life-science/cell-analysis/cell-analysis-learning-center/molecular-probes-school-of-fluorescence/fluorescence-basics/anatomy-fluorescence-spectra.html Update 2024/11/26.

77. Zacharioudaki DE, Fitilis I, Kotti M. Review of Fluorescence Spectroscopy in Environmental Quality Applications. Molecules [Internet]. 2022;27(15). Available from: https://www.mdpi.com/1420-3049/27/15/4801

78. Asiga customer, "Asiga Pico 2 / HD." Available: https://support.asiga.com/pico-2-hd/.

79. Webb JD, Neidlingert HH, Connolly~ JS. An Infrared Study of Azobenzene Photoisomerization in a Polymer Matrix. Vol. 7, Polymer Photochemistry. 1986. p. 503–13.

80. https://webbook.nist.gov/cgi/formula?ID=B6009512&Mask=80 Update 2024/11/26.

81. Xu C, Sun N, Li H, Han X, Zhang A, Sun P. Stimuli-Responsive Vesicles and Hydrogels Formed by a Single-Tailed Dynamic Covalent Surfactant in Aqueous Solutions. Molecules. 2024 Nov;29:4984.

82. Tai HT, Lin YC, Ma JY, Lo CT. Hydrogen bonding-induced assembled structures and photoresponsive behavior of azobenzene molecule/polyethylene glycol complexes. Polymers (Basel). 2019 Nov;11(8).

83. Salih AM, Ahmad M Bin, Ibrahim NA, Dahlan KZHM, Tajau R, Mahmood MH, et al. Synthesis of Radiation Curable Palm Oil–Based Epoxy Acrylate: NMR and FTIR Spectroscopic Investigations. Molecules [Internet]. 2015;20(8):14191–211. Available from: https://www.mdpi.com/1420-3049/20/8/14191

84. https://webbook.nist.gov/cgi/cbook.cgi?ID=C103333&Type=IR-SPEC&Index=1 Update 2024/11/26.

85.
 https://chem.libretexts.org/Bookshelves/Organic_Chemistry/Map%3A_Organic_Chemistry_(Wade)_Complete_and_Semesters_I_and_II/Map%3A_Organic_Chemistry_(Wade)/11%3A_Infrared_Spectroscopy_and_Mass_Spectrometry/11.05%3A_Infrared_Spectra_of_Some_Common_Functional_Groups Update 2024/11/26.

86. Guimarães CF, Gasperini L, Marques AP, Reis RL. The stiffness of living tissues and its implications for their engineering.

87. AAT Bioquest Inc. Absorption [Nile Red]. 2024.

88. Hanna S, Dunn B, Zink J. Rigidochromism as a Probe of Gelation, Aging, and Drying in SOL-GEL Derived Ormosils. MRS Proceedings. 2011 Nov;271.

89. https://www.hamamatsu.com/content/dam/hamamatsu-photonics/sites/documents/99_SALES_LIBRARY/etd/LC8_TLSZ1008E.pdf Update 2024/11/26.